# Analyse de la dynamique de réseaux sociaux animaux: de la collecte de données à la détection d'instabilités

Valeria Gelardi

Aix*Marseille université
Initiative d'excellence

NNT/NL : 2020AIXM0001/001ED000

# THÈSE DE DOCTORAT

A soutenir à Aix-Marseille Université
le 3 Décembre 2020 par

**Valeria GELARDI**

## Analysis of animal social networks dynamics: from data collection to (in)stability detection

**Discipline**
Physique et Sciences de la Matière

**Spécialité**
Physique théorique et mathématique

**École doctorale**
ECOLE DOCTORALE 352

**Laboratoire/Partenaires de recherche**

**Composition du jury**

| | |
|---|---|
| Clément SIRE<br>CNRS | Rapporteur |
| Cédric Sueur<br>Université de Strasbourg | Rapporteur |
| Xavier LEONCINI<br>Aix Marseille Université | Examinateur |
| Laura Ozella<br>ISI Foundation | Examinatrice |
| Jean-François PINTON<br>ENS Lyon | Examinateur |
| Alain BARRAT<br>CNRS | Directeur de thèse |
| Nicolas CLAIDIERE<br>CNRS | Co-Directeur de thèse |

# Résumé

La formation et l'évolution des groupes sociaux, dans les sociétés humaines et animales non humaines, est un processus complexe dicté par une variété de mécanismes locaux. En effet, les individus tentent simultanément de satisfaire leurs objectifs sous des contraintes multiples, éventuellement contradictoires : par exemple, ils peuvent interagir avec d'autres personnes qui leur ressemblent, ils peuvent bénéficier de relations de coopération en essayant d'éviter les relations conflictuelles et "déséquilibrées", ou ils peuvent mettre l'accent sur les liens appartenant à des groupes localement denses, en choisissant de nouvelles connaissances qui sont des amis d'amis dans un processus connu sous le nom de fermeture triadique. En général, les individus créent et désactivent leurs liens sociaux, ce qui a un impact et modifie la structure de l'ensemble du groupe auquel ils participent.

Cette (in)stabilité des groupes sociaux a des conséquences importantes dans un certain nombre de contextes.

Chez les animaux vivant en groupes étroitement liés, par exemple, la stabilité des relations sociales est un aspect important de la structure sociale. Les résultats de diverses études suggèrent que la sélection naturelle peut favoriser la capacité à cultiver et à maintenir des liens sociaux dans une série d'espèces. Dans les sociétés de primates par exemple, des relations stables et durables peuvent améliorer la condition physique des individus via la survie et la reproduction de leur progéniture. De plus, les hiérarchies de dominance sont établies pour promouvoir la stabilité, l'ordre et la cohésion sociale et ainsi réduire les conflits et la concurrence pour les ressources, qui représentent des coûts pour la vie en groupe. Il est également prouvé que la perturbation de la stabilité sociale peut avoir des conséquences négatives : certains travaux de recherche sur les babouins ont montré que l'instabilité causée par l'augmentation de la concurrence entre mâles pour la reproduction peut accroître le stress social, tandis que d'autres études sur les pinsons zébrés captifs ont montré l'effet de changements temporaires dans la composition du groupe, démontrant que l'introduction d'instabilités et de changements temporels dans le groupe peut amener les individus à devoir rétablir leurs relations sociales, ce qui leur fait perdre du temps pour d'autres tâches, comme la recherche de nourriture.

Malgré les avantages de la stabilité des relations, divers processus naturels, comme par exemple la démographie, entraînent inévitablement des changements dans les relations sociales : les individus s'adaptent naturellement et modifient leurs stratégies sociales en fonction du contexte et sur différentes échelles de temps, journalières, saisonnières, ou même sur plusieurs années. En outre, les changements de relations au niveau des individus, qui peuvent être basés par exemple sur des facteurs tels que

la parenté génétique et la personnalité, peuvent à leur tour donner lieu à une stabilité ou une instabilité au niveau du groupe. Une faiblesse fondamentale de la théorie sociologique actuelle est que, dans la plupart des cas, la relation entre ces différentes échelles, c'est-à-dire les interactions au niveau micro et les modèles au niveau macro, fait défaut.

À cet égard, l'analyse des réseaux sociaux représente un cadre puissant pour mieux comprendre la structure d'un groupe social, en utilisant des interactions dyadiques pour déduire et relier plusieurs niveaux de modèles sociaux, depuis les interactions au niveau individuel jusqu'au niveau complexe de la population. La science des réseaux sociaux a en fait joué un rôle pionnier dans l'étude des réseaux : elle est ancrée dans la rencontre de la théorie de la psychologie sociale avec la méthodologie des mathématiques et des statistiques, et depuis la définition de la sociométrie par Moreno en 1934, elle est un domaine d'étude en constante évolution. Dans sa forme la plus simple, un réseau social est constitué d'un ensemble fini de nœuds (sommets), représentant des individus (également appelés acteurs), et de liens (arêtes) représentant des relations sociales dyadiques entre eux. Les nœuds ou les liens peuvent contenir des informations supplémentaires et être complexes : les nœuds peuvent être associés à certaines caractéristiques telles que l'âge, le sexe, la position, etc... et les liens peuvent représenter des amitiés entre camarades de classe, des contacts sexuels entre adultes, l'appartenance à un groupe d'intérêt commun ou la collaboration à un projet commun, ou encore la proximité physique. Pour fournir une représentation plus complète d'une structure en réseau, on peut en outre attribuer un poids à chaque lien, qui codifie la diversité de l'intensité de l'interaction entre les nœuds, trait inhérent à la plupart des systèmes sociaux réels. Le poids des liens peut exprimer, par exemple, la force de la relation entre les individus.

Les réseaux sociaux constituent donc un outil polyvalent pour des études empiriques et théoriques variées sur les modèles d'interactions humaines et non humaines. Les informations sur leurs structures peuvent en outre contribuer à la compréhension de divers phénomènes tels que la diffusion d'informations et de maladies et, la disponibilité des données joue un rôle crucial dans les études correspondantes. Pendant longtemps, la grande majorité des recherches existantes sur les réseaux sociaux humains s'appuient sur des données recueillies par le biais de questionnaires, d'entretiens personnels ou d'observations pour révéler la topologie des liens sociaux entre les individus. La taille du réseau pouvant être cartographié était donc limitée. Ce n'est qu'avec le déploiement croissant des appareils numériques que de nouvelles méthodes de collecte de données, combinées à de nouveaux outils d'analyse des réseaux, ont rendu possibles des études à plus grande échelle et l'élaboration de mesures quantitatives de ces relations et modèles dans les sociétés humaines modernes, ce qui a conduit à l'émergence des sciences sociales computationnelles au cours des dernières décennies.

L'étude des sociétés animales a également adopté les outils de l'analyse des réseaux sociaux depuis longtemps. Grâce à sa capacité à décrire de nombreuses caractéristiques des systèmes sociaux de manière quantitative et à les comparer selon des

critères objectifs, l'analyse des réseaux sociaux est en effet devenue essentielle pour étudier la vie sociale des animaux.

Jusqu'à récemment, ces études des réseaux sociaux animaux se concentraient sur les représentations statiques des sommets et des arêtes, en agrégeant toute la séquence de contacts entre deux sommets en une arête unique. Les recherches en sciences sociales animales et en écologie comportementale concernant une approche des réseaux sociaux ont en fait été principalement axées sur des approches descriptives qui identifient la structure des interactions animales.

Les réseaux sociaux réels, cependant, changent continuellement au fil du temps, et la temporalité des connexions et leurs corrélations a des effets qui vont au-delà de ce qui peut être saisi par les réseaux statiques. Négliger cette temporalité peut avoir de graves conséquences, par exemple lors de la description de phénomènes dynamiques sur des réseaux tels que la propagation de maladies. En outre, pour comprendre les processus écologiques et évolutifs qui sous-tendent la formation et l'organisation des réseaux sociaux, et pour étudier comment les changements dans l'environnement, la composition du groupe ou les relations individuelles influencent l'ensemble de la structure du réseau, nous devons comprendre la dynamique de cette structure. L'étude des réseaux dans leurs aspects temporels nécessite la disponibilité de grands volumes de données à haute résolution temporelle, ainsi que des mesures permettant de quantifier ces changements, afin de distinguer, par exemple, les activités sociales ordinaires ou le simple bruit d'événements plus importants.

Dans le cas des réseaux sociaux humains, l'intérêt croissant récent pour le domaine des réseaux temporels a été rendu possible grâce au déploiement de dispositifs numériques qui ont permis de recueillir une énorme quantité de données à haute résolution, ainsi qu'aux progrès de la modélisation de la science des réseaux. Dans ces réseaux temporels, les moments où les liens sont actifs sont rendus explicites dans la représentation du réseau. En particulier, l'évolution des relations sociales est souvent composée d'instantanés successifs correspondant aux relations observées ou mesurées dans des fenêtres temporelles successives (par exemple, des semaines ou des mois successifs), et les outils permettant de détecter les changements entre ces fenêtres temporelles sont généralement basés sur des mesures de similarité entre les réseaux. Ces mesures peuvent être utilisées pour détecter les multiples échelles de temps sur lesquelles un réseau change ; elles peuvent mettre en évidence les changements brusques de la structure du réseau, ou au contraire les périodes pendant lesquelles la structure reste stable. Elles sont facilement généralisables aux réseaux pondérés et permettent de quantifier l'ampleur des changements de structure et de poids du réseau.

L'utilisation du formalisme et des outils de réseaux temporels est cependant encore limitée pour les animaux non humains. En effet, les progrès dans cette direction ont été limités par la nature des techniques utilisées pour recueillir des informations sociales, car les données sur les interactions entre animaux sont encore largement obtenues à partir de méthodes manuelles traditionnelles. Ce n'est que récemment qu'un certain nombre de développements technologiques ont commencé à être adaptés et mis

en œuvre pour recueillir des données comportementales à haute résolution sur les animaux non humains, depuis les logiciels de suivi basés sur des images jusqu'aux GPS à haute résolution en passant par les technologies d'enregistrement de proximité basées sur des capteurs portables.

Les primates sont particulièrement utiles pour développer des enquêtes basées sur des données concernant les réseaux sociaux dynamiques chez les animaux, car de nombreux primates ont des relations sociales très développées. Par exemple, ils peuvent utiliser des tactiques trompeuses, être prosociaux, comprendre les intentions d'autrui et évaluer l'utilité potentielle des autres. En outre, ces relations sociales sont à la fois structurées et flexibles. L'espèce que nous étudions dans cette thèse, les babouins de Guinée (Papio papio), présente des relations sociales complexes et une organisation sociale à plusieurs niveaux. L'unité centrale de la société du babouin de Guinée est un mâle primaire avec 1 à 4 femelles et leurs descendants ; plusieurs unités centrales forment des partis, qui forment des assemblées plus importantes appelées gangs. Les mâles forment des liens forts principalement au sein des partis ; ces liens ne sont pas corrélés avec la parenté génétique et les mâles sont très tolérants les uns envers les autres. En outre, une étude récente a révélé que la structure sociale était flexible, la moitié des femelles d'un groupe ayant changé de mâle principal au moins une fois en 17 mois, un comportement également observé de manière informelle dans notre groupe d'étude. Globalement, un seul groupe d'individus est donc en fait composé de plusieurs unités centrales avec une certaine diversité de structures sociales, et le réseau social décrivant cette structure sociale change spontanément. Ces caractéristiques font des babouins de Guinée un exemple idéal pour étudier les changements dynamiques dans les relations sociales.

Dans cette thèse, nous avons voulu contribuer à l'étude de la science sociale animale et de son évolution dynamique, en utilisant une approche de réseaux temporels pour étudier la détection de modèles d'(in)stabilité dans un groupe de primates non humains. Nous avons recueilli des données sociales temporelles originales sur un groupe hétérogène de babouins de Guinée (Papio Papio), vivant en captivité au Centre de primates de Rousset-sur-Arc (CNRS-UPS846), en France. Nous avons exploité des données qui avaient été recueillies à la fois par des méthodes d'observation traditionnelles et par de nouvelles méthodes de collecte automatique de données à haute résolution. En ce qui concerne cette dernière, nous avons utilisé à la fois des données horodatées de tests cognitifs collectées par Claidière et al. entre 2014 et 2017 et des données de proximité provenant de capteurs portables collectées dans le cadre de cette thèse en 2019. Dans l'ensemble, les données couvrent une longue période de 2014 à 2019, ce qui permet une exploration dynamique du réseau social des animaux à partir de données.

D'une part, les puissants outils existants de la science des réseaux ont été mis à profit pour étudier spécifiquement la dynamique sociale des animaux, en comparant différentes approches d'analyse des réseaux appliquées aux données collectées par différentes techniques.

D'autre part, nous avons présenté un nouveau cadre général comme alternative aux

approches existantes de représentation des réseaux temporels. Nous avons ensuite étendu notre analyse au-delà des relations sociales animales pour montrer que cette nouvelle représentation des réseaux fournit un outil efficace pour analyser la dynamique d'un système social, en nous concentrant principalement sur la détection des points de changement et des instabilités.

Le manuscrit est organisé comme suit. Dans le chapitre 1, nous introduions le formalisme des réseaux variables dans le temps. Dans le chapitre 2, nous présentons plusieurs données empiriques temporelles d'associations par paires entre des individus de primates non humains, à savoir les observations comportementales, qui représentent la méthode traditionnelle de collecte de données sociales sur les animaux, les données horodatées recueillies automatiquement sur les tests cognitifs et les contacts enregistrés par des capteurs portables entre les individus grâce à un système ad hoc adapté, testé et réalisé au cours de ce doctorat. Afin de mieux comparer les modèles sociaux humains et non humains, nous avons également introduit deux ensembles de données concernant les interactions humaines, c'est-à-dire les contacts enregistrés par des capteurs portables entre les étudiants et les enquêtes sur l'amitié. Nous nous sommes ensuite concentrés sur la comparaison entre la méthode traditionnelle de collecte d'observations comportementales et la technique de collecte automatique par des capteurs de proximité portables, en mettant en évidence les différents avantages et limites des deux méthodes.

Par exemple, les méthodes d'observation fournissent des données de haute qualité, grâce auxquelles nous pouvons distinguer différents comportements et décrire en profondeur les relations sociales entre les individus, mais ces données souffrent de plusieurs problèmes d'échantillonnage et de biais. L'objectif de cette comparaison était à l'origine d'évaluer la fiabilité de notre infrastructure à fournir des informations sociales significatives, et nous avons donc effectué un rapprochement entre les deux ensembles de données au niveau des événements individuels, afin de vérifier dans quelle mesure les comportements observés étaient détectés par les systèmes de capteurs. Le résultat aurait pu sembler décourageant, car le chevauchement entre les événements enregistrés par les deux systèmes était très limité : environ un tiers des interactions observées était également enregistré par les capteurs. Néanmoins, lorsque nous avons examiné les structures sociales globales résultant des réseaux construits à partir des deux ensembles de données, nous avons trouvé des résultats complètement différents.

En effet, dans le chapitre 3, nous nous sommes concentrés sur la construction, l'analyse et la comparaison des réseaux temporels construits à partir des données présentées précédemment. Dans un premier temps, nous représentons les réseaux temporels comme une succession de réseaux statiques pondérés, agrégés sur des fenêtres temporelles fixes.

En particulier, les données sur les tests cognitifs des babouins n'ont pas été recueillies à l'origine pour informer sur les associations sociales entre les individus. Cependant, nous avons pu construire un réseau temporel basé sur la coprésence des individus dans les stations de test qui s'étaient révélées instructives sur les relations

sociales réelles entre les individus, comme le montre la forte corrélation entre les poids du réseau de coprésence et du réseau obtenu par les données d'observation collectées au cours de la même période. De plus, en comparant la coprésence observée à un modèle nul, nous avons pu construire un réseau signé représentant à la fois des relations d'affiliation et d'évitement, en supposant simplement que les individus qui se rencontraient plus que par hasard recherchaient activement la compagnie de l'autre tandis que les individus qui se rencontraient moins que par hasard s'évitaient activement. Nous nous demandons ensuite si des données de nature différente pourraient en principe conduire à des descriptions et à une compréhension différentes des liens sociaux entre les individus et des réseaux sociaux qui en résultent. Nous avons abordé cette question en comparant les images des réseaux issues des observations comportementales et des données de contact enregistrées par des capteurs portables, découvrant que les deux réseaux agrégés sur l'ensemble de la période d'observation étaient remarquablement similaires. Lorsque l'on considère les agrégations sur différentes fenêtres temporelles, la méthode d'observation révèle ses limites pour fournir une image fiable de la structure sociale sur de courtes périodes : alors que le réseau d'observation fluctuait fortement d'un jour à l'autre, le réseau de capteurs semblait très stable, ce qui suggère qu'il est potentiellement adapté pour repérer de manière fiable les changements dans la structure sociale du groupe. Dans cette optique, nous avons analysé la détection des changements et de l'instabilité sociale de la période dans le chapitre suivant.

L'analyse des échelles de temps les plus courtes a toutefois révélé que, lorsque l'on présente les données de réseaux temporels comme une succession de réseaux statiques agrégés sur des fenêtres de temps successives, la longueur est quelque peu arbitraire et ne correspond pas nécessairement à une échelle de temps intrinsèque du système. Dans la dernière partie du chapitre, nous avons donc présenté un nouveau cadre qui génère un réseau pondéré, dirigé et en évolution constante, à partir d'un flux d'interactions dyadiques. Cette approche est basée sur l'idée que chaque individu dispose d'un capital fini en termes d'"attention" ou de temps disponible qui doit être réparti entre ses pairs. La dynamique sociale sous-jacente du système est déclenchée par l'interdépendance entre les décisions stratégiques des individus. En d'autres termes, le poids d'un lien, représentant la force des liens sociaux des individus, augmente si les interactions entre les deux nœuds sont itérées, et diminue si l'un des nœuds interagit avec d'autres. Ainsi, la force d'un lien social ne dépend pas seulement des interactions entre les deux nœuds concernés, mais aussi des interactions entre chaque nœud et ses autres voisins. Un paramètre $\alpha$ dicte la sensibilité des poids à chaque nouvelle interaction.

Un premier test du cadre, effectué sur les données de contact enregistrées par des capteurs portables, a fait ressortir deux aspects principaux.

Premièrement, le modèle génère des poids asymétriques avec différents niveaux de réciprocité, ce qui signifie qu'avec deux nœuds i et j, nous pourrions avoir $w_{ij} \simeq w_{ji}$ (réciprocité élevée) ou $w_{ij}(w_{ji}) >> w_{ji}(w_{ij})$ (réciprocité faible). Nous nous serions attendus à ce que ces différents niveaux de symétrie reflètent un effet non aléatoire

de la dynamique sociale. Nous avons donc calculé le réseau temporel à partir des données sur les contacts entre étudiants et nous avons comparé les différents niveaux de symétrie des poids aux données des enquêtes sur l'amitié, où les individus déclarent qui parmi d'autres individus ils considèrent comme leurs amis. Nous nous attendions à ce que les individus qui ont une déclaration mutuelle entraînent un lien plus symétrique dans le réseau temporel. Cependant cet effet, bien que présent, s'est révélé de faible amplitude. La question de savoir si l'asymétrie des liens a ou non une signification sociale pourrait donc mériter une étude plus approfondie. Deuxièmement, la dynamique du réseau est fortement influencée par la valeur du paramètre : des valeurs de $\alpha$ trop faibles ne permettent pas aux poids de s'actualiser assez vite pour détecter les changements dans le réseau alors que des valeurs élevées de $\alpha$ produisent une dynamique des poids trop sensible à chaque interaction, ce qui entraîne des variations brutales. La possibilité d'avoir des scénarios d'évolution aussi différents a soulevé la question de savoir comment estimer une valeur appropriée du paramètre qui pourrait le mieux refléter la dynamique sociale réelle du système sous-jacent.

Pour résoudre ce problème, nous avons analysé dans le chapitre 4 la dynamique des réseaux présentée dans le chapitre 3, en nous concentrant sur la capacité des différentes représentations des réseaux à détecter les points de changement et les instabilités dans la structure sociale.

Dans la première partie du chapitre, nous avons examiné le réseau de coprésence agrégé mensuel calculé à partir de données de tests cognitifs et nous avons étudié la dynamique du réseau social en utilisant une mesure de similarité entre les réseaux au cours de mois successifs, et en comparant les réseaux à deux échelles différentes, c'est-à-dire à l'échelle des individus et à l'échelle du réseau entier. L'utilisation d'une mesure de similarité s'est avérée être une méthode sensible et polyvalente pour comprendre les changements dans les relations sociales des individus et leurs conséquences au niveau du groupe. En particulier, nous avons montré que la stabilité sociale globale d'un groupe est le résultat de réorganisations dynamiques à l'échelle du réseau personnel de chaque individu, et que les synchronisations de ces changements pouvaient générer un changement visible à l'échelle macro.

Dans la deuxième partie du chapitre, nous avons testé la capacité du cadre présenté précédemment à détecter des états discrets du système, dans un double but : (i) découvrir pour quelles valeurs du paramètre $\alpha$ du modèle la détection était plus efficace et (ii) comparer la performance du modèle par rapport aux approches agrégées traditionnelles. Nous avons présenté une méthode basée sur des algorithmes de clustering qui, à partir d'un flux de données de contacts dyadiques, permet de détecter les méso-états et les points de changement du système et de donner également une estimation de la qualité de cette détection.

Sur la base de cette méthode, nous avons ainsi pu comparer différentes représentations de réseaux, c'est-à-dire le modèle avec différentes valeurs du paramètre $\alpha$ et deux approches différentes de réseaux agrégés, dans deux contextes différents, à savoir les interactions entre les primates humains et non humains. Il est intéressant de noter que pour les deux systèmes, nous avons trouvé une gamme de valeurs de paramètres pour

lesquelles le réseau construit avec le modèle a surpassé les représentations agrégées dans la capacité à détecter les changements dans le système et ces valeurs semblent être des caractéristiques du système. Néanmoins, d'autres ensembles de données et d'autres investigations seraient nécessaires pour confirmer cette hypothèse.

Quoi qu'il en soit, nos conclusions soutiennent l'hypothèse, déjà avancée dans la littérature récente, selon laquelle les réseaux temporels représentés par des approches en temps continu semblent plus adaptés que l'agrégation en fenêtres temporelles pour décrire la dynamique des systèmes sociaux.

Enfin, dans le chapitre 5, nous avons analysé le réseau signé dérivé du réseau d'affiliation et d'évitement pondéré obtenu dans le chapitre 3 en termes de structure interne des sous-groupes, c'est-à-dire des structures triadiques.

Premièrement, nous avons évalué que le réseau respectait les prédictions de la théorie de l'équilibre structural, c'est-à-dire qu'un groupe social a tendance à avoir plus de triangles équilibrés que de triangles déséquilibrés. Nous avons montré que les triangles équilibrés étaient en effet surreprésentés et les triangles déséquilibrés sous-représentés dans nos données, par rapport à une distribution nulle basée sur la permutation aléatoire des signes des liens.

Un objectif plus ambitieux était d'analyser l'évolution temporelle des mesures d'équilibre social (en proportion ou en nombre de triangles équilibrés et déséquilibrés) pour finalement découvrir des précurseurs ou indicateurs d' (in)stabilité similaires à ceux trouvés dans le chapitre 4. Néanmoins, cette analyse n'a pas permis d'obtenir un aperçu clair de l'évolution temporelle de la structure du réseau social. L'analyse de l'évolution des nombres de triangles n'a pas révélé de changements clairs entre les périodes de stabilité et d'instabilité sociales, contrairement à l'analyse des similarités entre réseaux utilisées dans le chapitre 4. La raison pour laquelle ces changements ne sont pas reflétés dans l'analyse des triades peut être structurelle, c'est-à-dire que les changements qui se produisent dans les relations impliquent d'autres échelles du système, par exemple des individus isolés, et non des triades. Par ailleurs, ne considérer que le signe des liens pourrait être une approche trop simpliste car ne prenant pas en compte les poids et donc l'importance relative des différentes relations dans le réseau social.

Cependant, très peu d'études ont testé la théorie de l'équilibre social et, à notre avis, elle mérite un examen plus approfondi, notamment parce qu'elle fournit un cadre théorique clair pour comprendre la structure des réseaux sociaux. En outre, il pourrait être utile de caractériser les changements de dynamique au niveau de description d'un sous-groupe, qui est une échelle intermédiaire entre l'individu et le global, qui sont plus fréquemment pris en considération.

Pour conclure, nous avons montré que de nouvelles infrastructures, qui produisent des données à haute fréquence et à long terme sur les interactions sociales des animaux non humains, peuvent ouvrir des perspectives pour l'étude des dynamiques sociales à des échelles (à la fois dans le temps et au niveau du groupe) qui semblaient inaccessibles il y a encore quelques années.

Cette disponibilité des données, ainsi que les avancées théoriques de l'analyse des

réseaux temporels, pourrait aider à l'avenir à comprendre les processus écologiques et évolutifs qui sous-tendent la formation et l'organisation des réseaux sociaux, et à étudier comment les changements dans l'environnement, la composition du groupe ou les relations individuelles influencent la structure entière du réseau.

Cette thèse visait à représenter un petit pas en avant dans cette direction et un pont entre différentes disciplines, la science des réseaux et la science sociale animale.

Mots clés : réseaux temporels, réseaux sociaux, primates

# Abstract

Social groups formation and evolution, in human and non-human animal societies, is a complex process dictated by a variety of local mechanisms. In general, we assist to individuals creation and deactivation of social ties, thereby impacting and altering the structure of the entire group in which they participate. This (in)stability of social groups has important consequences in a number of contexts. Social network analysis represents a powerful framework to better understand the structure of a social group and a versatile tool for very heterogeneous empirical and theoretical studies on patterns of human and non-human interactions, using dyadic interactions to infer and relate multiple levels of social patterns, from individual-level interactions to complex population-level In modern human societies, the increasing deployment of digital devices, new ways of collecting data, combined with new network analysis tools, have made possible studies at larger scale and the development of quantitative measures of social patterns in their time-varying aspects. Studies of animal social networks instead have until recently focused on static representations of vertices and edges, the use of temporal network formalism has in fact been hampered by the nature of the techniques used to gather social information, which are still largely obtained from traditional hand-operated methods. Real social networks, however, change continuously over time, and the timings of connections and their correlations do have effects that go beyond what can be captured by static networks. In this thesis we contributed to the study of animal social science and its dynamical evolution, using a temporal networks approach to investigate the detection of (in)stability patterns in a group of non-human primates, i.e. Guinea baboons (Papio Papio) , exploiting data that had been collected through both traditional observational methods and through novel methods of automatic high resolution data gathering. Moreover, on the one hand existing powerful tools of network science are leveraged to specifically study animal social dynamics, comparing different network analysis approaches applied to data collected through different techniques. On the other hand, as an alternative to existing temporal networks approaches, we presented a novel general framework that takes as input any time-stamped data stream of discrete dyadic interactions between individuals, and yields a continuously-evolving picture of social relationships. Extending our analysis beyond animal social relations, we showed that this novel network representation provides an effective tool to analyze the dynamics of a social system, referring primarily to the the detection of change points and instabilities.

Keywords: temporal networks, social networks, primates

# Remerciements

I am grateful to my supervisors, Alain Barrat and Nicolas Claidiere, for their continuous support, advice and patience during my PhD : they helped me to be more independent but they never left me alone. I would like to thank Lorenzo Bosi, Catherine Levet and all the people of the CPT with whom I shared my working days, for their great company and their precious help. I would like to thank also Julie Gullstrand, Dany Paleressompoulle and the members of the LPC for their support and kindness. Finally my gratitude goes to my families, the one I was born with and all the ones I found on my path.

# Table des matières

# Table des figures

# Liste des tableaux

# Introduction

This thesis work aims to contribute to the understanding of the dynamic changes that take place in the social relationships of animals living in groups, combining the deployment of several data collection techniques with the use of network analysis, in particular through the lens of temporal networks.

Social groups formation and evolution, in human and non-human animal societies, is a complex process dictated by a variety of local mechanisms. Indeed, individuals simultaneously attempt to satisfy their goals under multiple, possibly conflicting, constraints : for instance they may interact with others similar to themselves (McPherson, Smith-Lovin et Cook 2001), they may benefit from cooperative relationships attempting to avoid conflicting and "unbalanced" relationships (Heider 1958; Davis 1963), or they may emphasize ties belonging to locally dense clusters, choosing new acquaintances who are friends of friends in a process known as triadic closure (Rapoport 1953; Granovetter 1973). In general, we assist to individuals creation and deactivation of social ties, thereby impacting and altering the structure of the entire group in which they participate.

This (in)stability of social groups has important consequences in a number of contexts. In tightly bonded group living animals, for example, stability of social relationships is a significant aspect of social structure (Hinde 1976). Findings suggest that natural selection may favor the ability to cultivate and sustain social bonds in a range of species. In primates societies for instance, stable and long-lasting relationships can enhance individuals fitness (Silk 2007; Silk, Beehner, Bergman et al. 2010; Alberts 2019) through offspring survival (Silk, Alberts et Altmann 2003; Silk, Beehner Jacinta, Bergman Thore et al. 2009) and reproduction (Schülke, Bhagavatula, Vigilant et al. 2010). Moreover, dominance hierarchies are established to promote social stability, order and cohesion and thus reduce conflicts and competition for resources, which are costs of group-living (Kappeler, Fichtel et Schaik 2019). There is also evidence that disruption of social stability can have negative consequences : the works of (Sapolsky 1983; Beaulieu, Mboumba, Willaume et al. 2014) on baboons show that instability caused by the raise of inter-male competition for reproduction, may increase social stress, while Maldonado-Chaparro, Alarcón-Nieto, Klarevas-Irby et al. 2018 studied the effect of temporary changes in group composition in captive zebra finches, demonstrating that they can result in individuals having to re-establish their social relationships, thus taking time away from other tasks, such as foraging. Despite the benefits of stability in relationships, natural processes such as demography naturally bring changes in social relationships (Shizuka et Johnson 2019) : individuals thus adapt and flexibly change their social strategies on different

timescales depending on context, from a daily basis (SICK, CARTER ALECIA, MARSHALL HARRY et al. 2014), to seasonal (HENZI, LUSSEAU, WEINGRILL et al. 2009) to several years (SILK, BEEHNER, BERGMAN et al. 2010). Relationship changes at individuals level, which can be based for instance on factors such as genetic relatedness (BEISNER, JACKSON, CAMERON et al. 2011) and personality (MCCOWAN, BEISNER, CAPITANIO et al. 2011), can in turn give rise to stability or instability at the group level.

A fundamental weakness of current sociological theory is that, in most cases, the relation between these different scales, i.e. micro-level interactions and macro-level patterns, is missing. In this regard, social network analysis represents a powerful framework to better understand the structure of a social group, using dyadic interactions to infer and relate multiple levels of social patterns, from individual-level interactions to complex population-level (GRANOVETTER 1973 ; HINDE 1976). The science of social networks has in fact had a pioneering role in the study of networks : it is rooted in the encouter of the social psychology theory with mathematics and statistics methodology, and since the definition of *sociometry* by MORENO 1934 it has been a constantly growing field of study. In its basic form, a social network consists of a finite set of nodes (vertices), representing individuals (also referred to as *actors*), and links (edges) representing social relations or ties between them.

Additional information and complexity can be put on nodes or links : nodes can be associated with some features such as age, gender, position, etc... and links may represents friendships between classmates, sexual contacts among adults (LILJEROS, EDLING, AMARAL et al. 2001), the belonging to a common group of interest or the collaboration to a common project (NEWMAN 2001), or physical proximity. To provide a more complete representation of a networked structure, a *weight* (BARRAT, BARTHÉLEMY et VESPIGNANI 2004 ; NEWMAN 2004) can moreover be assigned to each link, that encodes the diversity of interaction intensity between nodes, which is an inherent trait of most of real social systems. Weights of links may express, for instance, the strength of the relationship between individuals.

Social networks are thus a versatile tool for very heterogeneous empirical and theoretical studies on patterns of human and non-human interactions. Information on their structures can moreover contribute to the understanding of a variety of phenomena such as the spread of information and diseases (LILJEROS, EDLING, AMARAL et al. 2001 ; STEHLÉ, VOIRIN, BARRAT et al. 2011) and to this aim, data availability play a crucial role.

For a long time, the vast majority of existing research on human social networks has relied on data collected through questionnaires, personal interviews or observations for revealing the topology of the social connections between individuals. The size of the network that could be mapped was therefore limited. Only with the increasing deployment of digital devices, new ways of collecting data, combined with new network analysis tools, have made possible studies at larger scale and the development of quantitative measures of these relationships and patterns in modern human societies, leading to the emergence of computational social science in the last decades (LAZER, PENTLAND, ADAMIC et al. 2009 ; CONTE, GILBERT, BONELLI et al. 2012).

The study of animal societies has also embraced the tools of social network analysis since a long time. Thanks to its capability of describing many characteristics of social systems in a quantitative way and comparing them according to objective criteria, social network analysis has in fact become essential to study animal social life (HINDE 1976; HOBSON, AVERY et WRIGHT 2013; KURVERS, KRAUSE, CROFT et al. 2014; WEY, BLUMSTEIN, SHEN et al. 2008; CROFT, JAMES et KRAUSE 2008; KRAUSE, JAMES, FRANKS et al. 2015; WHITEHEAD 2008; WEBBER et WAL 2019).

Until recently, such studies of animal social networks have focused on static representations of vertices and edges, by aggregating the entire sequence of contacts between two vertices in a unique edge. The research in animal social science and behavioral ecology concerning a social network approach has been in fact predominantly focused on descriptive approaches that identify the structure of animal interactions.

Real social networks, however, change continuously over time, and the timings of connections and their correlations do have effects that go beyond what can be captured by static networks. Neglecting the time ordering can have serious consequences, for instance when describing dynamical phenomena on networks such as spreading of diseases. In addition, to understand the ecological and evolutionary processes underlying social network formation and organization, and to study how changes in the environment, composition of the group or single key-relationships influence the entire network structure, we need to understand the dynamics of this structure (FARINE 2018).

The study of networks in their time-varying aspects requires the availability of large volumes of data with high temporal resolution, as well as metrics to quantify these changes, to distinguish, for instance, ordinary social activities or mere noise from more significant events.

In the case of human social networks, the increasing recent interest towards the field of temporal networks (HOLME et SARAMÄKI 2012; HOLME 2015) has been made possible thanks to the deployment of digital devices that allowed the gathering of tremendous amount of high resolution data (ECKMANN, MOSES et SERGI 2004; ONNELA, SARAMÄKI, HYVONEN et al. 2007; KOSSINETS et WATTS 2006; GOLDER, WILKINSON et HUBERMAN 2007; CATTUTO, BROECK, BARRAT et al. 2010; SALATHÉ, KAZANDJIEVA, LEE et al. 2010; ISELLA, STEHLÉ, BARRAT et al. 2011; FOURNET et BARRAT 2014), together with advances in network science modeling (BARRAT, BARTHELEMY et VESPIGNANI 2008; SONG, KOREN, WANG et al. 2010; ZHAO, STEHLÉ, BIANCONI et al. 2011; STARNINI, BARONCHELLI et PASTOR-SATORRAS 2013).

In these time-dependent graphs, the times when the edges are active are made explicit in the representation of the network. In particular, the evolution of social relationships are often composed of successive snapshots corresponding to the relationships observed or measured in successive time windows (e.g., successive weeks or months), and tools to detect changes between these time windows are typically based on measures of similarity between networks. Such measures can be used to detect the multiple time scales on which a network changes (DARST, GRANELL, ARENAS

et al. 2016; MASUDA et HOLME 2019; SUGISHITA et MASUDA 2020) ; they can highlight abrupt changes of the network structure, or on the contrary periods during which the structure remains stable. They are also easily generalised to weighted networks (FOURNET et BARRAT 2014) and quantify the amount of structural and weights change of the network.

The use of temporal network formalism and tools is however still limited for non-human animals (PINTER-WOLLMAN, HOBSON, SMITH et al. 2014). In many cases progress in this direction has been hampered by the nature of the techniques used to gather social information because the data on animal interactions are still largely obtained from traditional hand-operated methods (KRAUSE, JAMES, FRANKS et al. 2015; FARINE et WHITEHEAD 2015). Only recently, a number of technological developments have started to be adapted and implemented to gather high-resolution behavioral data on non-human animals, from image based tracking software to high resolution GPS (HUGHEY, HEIN, STRANDBURG-PESHKIN et al. 2018; CRALL, GRAVISH, MOUNTCASTLE et al. 2015; ROMERO-FERRERO, BERGOMI, HINZ et al. 2019; MATHIS, MAMIDANNA, CURY et al. 2018; GRAVING, CHAE, NAIK et al. 2019; STRANDBURG-PESHKIN, FARINE, COUZIN et al. 2015) to proximity logging technologies based on wearable sensors (RUTZ, BURNS, JAMES et al. 2012; ST CLAIR, BURNS, BETTANEY et al. 2015; RUTZ, MORRISSEY, BURNS et al. 2015; BETTANEY, JAMES, ST CLAIR et al. 2015; MILWID, O'SULLIVAN, POLJAK et al. 2019; WILSON-AGGARWAL, OZELLA, TIZZONI et al. 2019; OZELLA, LANGFORD, GAUVIN et al. 2020).

Primates are particularly useful to develop data-driven investigations of dynamic social networks in animals, because many non-human primates have highly developed social relationships. For instance, they can use deceptive tactics (WHITEN et BYRNE 1988), be prosocial (CLAIDIÈRE, WHITEN, MARENO et al. 2015), understand other's intentions (TOMASELLO, CARPENTER, CALL et al. 2005) and can evaluate the potential helpfulness of others (ANDERSON, KUROSHIMA, TAKIMOTO et al. 2013). Moreover, these social relationships are both structured and flexible. Our study species for example, Guinea baboons (*Papio papio*) exhibits complex social relationships and a multilevel social organization. The core unit of Guinea baboon's society is one primary male with $1-4$ females and their offsprings; several core-units form parties, which form larger assemblies called gangs (PATZELT, KOPP, NDAO et al. 2014).

Males form strong bonds predominantly within parties; these bonds are not correlated with genetic relatedness and males are highly tolerant of each other (PATZELT, KOPP, NDAO et al. 2014). Moreover, a recent study found that the social structure was flexible, with half of the females of a group having changed primary male at least once in 17 months (GOFFE, ZINNER et FISCHER 2016), a behaviour also observed informally in our study group. Overall, a single group of individuals is thus in fact composed of multiple core units with a certain diversity of social structures, and the social network describing this social structure changes spontaneously. These characteristics make Guinea baboons ideal to study dynamic changes in social relationships.

In this thesis we aim to contribute to the study of animal social science and its dynamical evolution, using a temporal networks approach to investigate the detec-

tion of (in)stability patterns in a group of non-human primates. We provide original temporal social data on a heterogeneous group of Guinea baboons (*Papio Papio*), living in captivity at the Rousset-sur-Arc Primate Center (CNRS- UPS846), France. We exploited data that had been collected through both traditional observational methods and through novel methods of automatic high resolution data gathering. Regarding the latter, we used both time-stamped data of cognitive tests collected by CLAIDIÈRE, GULLSTRAND, LATOUCHE et al. 2017 between 2014 and 2017 and proximity data from wearable sensors collected during this research in 2019. Overall, data span a long period from 2014 to 2019, allowing for a dynamical data-driven exploration of animals social network.

Finally, on the one hand, existing powerful tools of network science are leveraged to specifically study animal social dynamics, comparing different network analysis approaches applied to data collected through different techniques.

On the other hand, we present a novel general framework as an alternative to existing temporal networks approaches. We extend our analysis beyond animal social relations to show that this novel network representation provides an effective tool to analyze the dynamics of a social system, referring primarily to the the detection of change points and instabilities.

This manuscript is organized as follows : in chapter 1 we introduce the time-varying networks formalism. In chapter 2 we present empirical data along with the gathering procedures, one of which was a core component of this PhD thesis. The datasets exploited in this work are of different nature and concern both non-human primates, namely the group of baboons under interest in this study (referring mainly to two different periods, i.e. 2014-2017 and 2019), and humans, i.e. a group a students interacting in a high school. A section of the chapter is moreover dedicated to the comparison of social data collected with different techniques and to a detailed matching procedure at the level of the single event. Chapter 3 describes how different temporal network representations were constructed from the data described previously, using the approach of aggregating data over time-windows. We then raise the question of whether data of different nature could in principle lead to different descriptions and understanding of the social bonds between individuals and of the resulting social networks. To address this issue, we compare social networks computed from different data, using several well-known metrics. The last section of the chapter is dedicated to the presentation of a new temporal network approach, which converts data streams of dyadic interactions into a continuous evolving weighted network (AHMAD, PORTER et BEGUERISSE-DÍAZ 2018; JIN, GIRVAN et NEWMAN 2001). In this framework, we assume that each individual has a finite capital in terms of "attention" or available time that has to be divided among peers. The underlying social dynamics of the system is triggered by the interdependence between individuals strategic decisions. In other words, the weight of a link, representing the strength of individuals' social bonds, can increase or decrease depending not only on the interactions between the two nodes involved, but also on the interactions between each node and its neighbours. In chapter 4, the dynamic of the networks presented in chapter 3 is analysed. Different

methods are defined to detect networks change-points and periods of (in)stability, uncovering thus changes of the underlying social system. Moreover, having established a method to evaluate the ability of a temporal network to detect social system changes, we are able to compare different temporal network approaches and to test the effectiveness of the framework introduced in chapter 3 in describing the social dynamics of different systems, i.e. humans and non-humans. In chapter 5 we focus on the analysis of a temporal signed social network in terms of its particular sub-groups structures, namely triads and triangles. On this network, presented in chapter 3, we test social balance theory and we study the triadic closure dynamics.

Some of the work presented in this thesis is already published in scientific papers (GELARDI, FAGOT, BARRAT et al. 2019; GELARDI, GODARD, PALERESSOMPOULLE et al. 2020). In particular, GELARDI, FAGOT, BARRAT et al. 2019 refers to all analyses carried out on top of data collected between 2014 and 2017 (presented in sections 2.4 and 2.2.1). GELARDI, GODARD, PALERESSOMPOULLE et al. 2020 is mainly referred to sections 2.3, 2.2.2 for all that concerns the data gathering and the implementation of an infrastructure for automatic collection of data on animals social interactions, and to section 3.3.2 where results are described on the comparative analysis of networks obtained from different data. The novel framework introduced in chapters 3 and 4 is the subject of a manuscript currently under preparation.

# 1. Networks

**Basic concepts** A *network*, or a *graph* as it is called in much of the mathematical literature, is basically constituted by a set of entities named *vertices* or *nodes*, connected by *edges* or *links*. In principle, any system with coupled elements can be represented as a network (NEWMAN 2003; DOROGOVTSEV 2010). Systems taking the form of networks abound in the world. Examples include the Internet, the World Wide Web,social networks of acquaintance or other connections between individuals, organizational networks and networks of business relations between companies, neural networks, metabolic networks, food webs, distribution networks such as blood vessels.

Additional information and complexity can be put on nodes or links to describe an enormous variety of systems. A basic property assigned to a node is the *degree*, defined as the number of edges connected to a vertex. The degree is not necessarily equal to the number of vertices adjacent to a vertex, since there may be more than one edge between any two vertices. A directed graph has both an in-degree and an out-degree for each vertex, which is the number of in-coming and out-going edges respectively. Edges can in fact also be directed, pointing in only one direction. Graphs composed at least of a fraction of directed edges are themselves called directed graphs *digraphs, for short*. A graph representing citations in scientific papers, telephone calls or email messages between individuals would be directed, since each message only goes in one direction. A fully connected network (or a complete graph, as it is called in graph theory) is a network in which all nodes are interconnected.

Different types of nodes or links can be defined. To provide a more complete representation of a networked structure, a *weight* $w_{ij}$ can be assigned to each edge $(i, j)$ that encode properties or information on the edge itself. Indeed, weighted graphs (BARRAT, BARTHÉLEMY et VESPIGNANI 2004; NEWMAN 2004) take into account the diversity of interaction intensity between nodes, which is an intrinsic trait of most of real networks. In a social network, for example, nodes represent individuals (which can be associated with some features such as age, gender, position, etc...) and links may represent friendship or space proximity between couples of nodes. Weights of each edge may thus express the closeness of the relationship between individuals or their mutual distance. In case of a directed network, we have thus that $w_{ij} \neq w_{ji}$, and consequently, two nodes can be connected even if $w_{ij}$ or $w_{ji}$ are equal to zero.

**Temporal networks** Until recently, network studies have been focused on static representations of vertices and edges, in which the links do not change over time and the time dimension is projected out by aggregating the entire sequence of connections between two vertices in a unique edge, as if these connections were concurrent. In

real systems however interaction patterns change in time, sometimes requiring the inclusion of the time dimension and thus the use of time-dependent graphs, also known as temporal or time-varying networks (HOLME et SARAMÄKI 2012). In a static network in fact, given a contact between two vertices $i$ and $j$ and a successive contact between $j$ and $l$, $i$ will result connected to $l$, even if in reality the two edges were not active at the same moment. The number of available links at each time is thus overestimated and, therefore, the actual lengths of walks and paths is underestimated. This neglecting of the time ordering can have serious consequences, especially when describing propagation phenomena on networks, such as spreading of diseases (MOODY 2002). Contrarily, in temporal networks edges represent pair-wise interactions that appear and disappear over time and the times when the edges are active are made explicit in the representation of the network. This has required some basic concepts of complex network theory, such as path lengths and distances (PAN et SARAMÄKI 2011), centrality (TANG, MUSOLESI, MASCOLO et al. 2010) and connected components (NICOSIA, TANG, MUSOLESI et al. 2012) to be extended to this new formalism.

We may refer to the basic interaction in a temporal network as a *contact*, which captures information about the pair of nodes interacting and the time of the interaction, and may be considered as the closest extension of a link in static networks. Most empirical temporal network data are presented in the form of lists of contacts, where two nodes involved in the interaction are associated with the time stamp or the interval in which the interaction has occurred (examples are data on email, text messages or phone calls exchanges, or face-to-face contacts data). In general, a great variety of systems whose topology is inherently dynamic can be naturally modeled as temporal graphs. Some examples are human communication networks (SARAMÄKI et MORO 2015), which include a wide class of systems from call-data records of mobile phone operators (KRINGS, KARSAI, BERNHARDSSON et al. 2012; KARSAI, KIVELÄ, PAN et al. 2011; MIRITELLO, LARA et MORO 2013) and e-mails (KOSSINETS et WATTS 2006); brain networks, commonly studied through fMRI scanning time series data (BASSETT, WYMBS, ROMBACH et al. 2013);transportation networks, most notably airline connections (ROSVALL, ESQUIVEL, LANCICHINETTI et al. 2014; SUN, WANDELT et LINKE 2015; SUGISHITA et MASUDA 2020). Finally, a central role in the rising field of temporal networks is played by human proximity networks, in which a contact is registered when two people have been close to each other in time and space. These networks allow to give important insights on the dynamics of social groups formations and disease spreading. Several technologies are available to measure these type of interaction , such as WiFi (SALATHÉ, KAZANDJIEVA, LEE et al. 2010) and Bluetooth sensors (SEKARA, STOPCZYNSKI et LEHMANN 2016) and radio-frequency identification devices (RFID) which provide the highest resolution data in terms of space and time and allow to capture people face-to-face social interaction (BARRAT et CATTUTO 2013; BARRAT, CATTUTO, COLIZZA et al. 2013). Moreover, recently we are witnessing a growing interest in animals temporal social networks. Although data in this field have been collected through written records based on direct observations, proximity devices based on GPS (STRANDBURG-PESHKIN, FARINE, COUZIN et al. 2015) or radio

frequency technology (RUTZ, BURNS, JAMES et al. 2012; ST CLAIR, BURNS, BETTANEY et al. 2015; RUTZ, MORRISSEY, BURNS et al. 2015; BETTANEY, JAMES, ST CLAIR et al. 2015; MILWID, O'SULLIVAN, POLJAK et al. 2019; WILSON-AGGARWAL, OZELLA, TIZZONI et al. 2019) begin to be more frequently used.

There are many ways of representing and visualizing temporal networks (well described in HOLME et SARAMÄKI 2012 and HOLME 2015). In many cases we have a *contacts sequence*, i.e. a set of $N$ vertices $V$ interacting at certain times, in which the duration of the interaction is negligible. The system is thus represented by an ordered set of contacts $C$ in which each element is a triplet $(i, j, t)$ where $i$ and $j \in V$ are the nodes involved and $t$ is the time when interaction occurred. If the contact is associated with a duration and thus the edges activate for a finite time interval, we can represent the system as a series of quadruple $(i, j, t, \delta t)$ (*interval graphs*). However, a common temporal network representation consists in the time-aggregation procedure, i.e. grouping contacts over successive time windows of length $\Delta t$, obtaining a series of static graphs or snapshots $\{G_l^{(\Delta t)}, l = 1, ..., L\}$ with $L$ the number of snapshots, each graph containing all the links appeared in that time interval. The time window can be fixed or non-uniform (e.g. increasing) and the choice of the type and the length of this window presupposes a knowledge of the timescale of the system dynamics since it can impact the structure and the dynamics description of the resulting network (KRINGS, KARSAI, BERNHARDSSON et al. 2012; PSORAKIS, ROBERTS, REZEK et al. 2012). This issue represents a crucial point of our work and we will come back to that in the chapters 3 and 4.

# 2. Datasets

## 2.1. Introduction

The possibility to access or to collect extensive data on social relationships has been the foundation and the prerequisite for the emergence of computational social science in the last decades (LAZER, PENTLAND, ADAMIC et al. 2009). For instance, social patterns have been inferred and studied using various data sources ranging from phone calls (ONNELA, SARAMÄKI, HYVONEN et al. 2007), e-mails (ECKMANN, MOSES et SERGI 2004; KOSSINETS et WATTS 2006), online interactions (GOLDER, WILKINSON et HUBERMAN 2007), to face-to-face interactions measured by wearable sensors (CATTUTO, BROECK, BARRAT et al. 2010; SALATHÉ, KAZANDJIEVA, LEE et al. 2010; ISELLA, STEHLÉ, BARRAT et al. 2011; STOPCZYNSKI, SEKARA, SAPIEZYNSKI et al. 2014; FOURNET et BARRAT 2014; TOTH, LEECASTER, PETTEY et al. 2015).

However, this availability of large volumes of data with high temporal resolution regards mostly human activity and has thus contributed to the rapid expansion of data-driven computational studies of human relationships and human social networks. On the contrary, the data collection remains more challenging in the field of animal studies, because the data on animal interactions are still largely obtained from direct observations (KRAUSE, JAMES, FRANKS et al. 2015; FARINE et WHITEHEAD 2015). On the one hand, data resulting from such observations are extremely valuable as they often include detailed information about the nature, duration and location of the interactions between individuals. They thus allow researchers to grasp and investigate complex social patterns in animal groups. On the other hand, observations are time costly and, if they are not performed for a long enough time per individual, suffer from sampling effects (DAVIS, CROFOOT et FARINE 2018). Errors or biased observations made by the observer are almost a common occurrence and may affect the ability to reconstruct the real underlying social structure (SILK, JACKSON, CROFT et al. 2015; DAVIS, CROFOOT et FARINE 2018). Misidentifications are defined as the erroneous identification of individuals in an animal study group and they may arise randomly if, for instance, an individual has its back to the observer, or systematically, in case of individuals physically similar and thus more likely to be mistaken. Other errors may arise from the incorrect recording of the names of study animals. Missing observations can occur when individuals cannot be identified or are not visible. Finally, some interactions are harder to observe and record than others, since they can be very quick, as in case of some plays between babies or maybe more ambiguous and latent, as an avoidance (for more details on behaviors, see Table 2.1).

Recently, a number of technological developments have started to be adapted and

implemented to gather high-resolution behavioral data on non-human animals, leading to the adoption of the term "reality mining", widely used in computational social sciences for the study of human social behavior and relations (EAGLE et PENTLAND 2006), to the case of non-human animal societies (KRAUSE, KRAUSE, ARLINGHAUS et al. 2013). Machine-sensed data concerning the behaviour of animals can indeed now be collected and, most importantly, analysed. We refer to HUGHEY, HEIN, STRANDBURG-PESHKIN et al. 2018 for an overview of existing and emerging technologies used to collect data on movements, behaviour and interactions within animal groups. In particular, image-based tracking software and machine learning tools can be used to identify and track animals and their trajectories from video data (CRALL, GRAVISH, MOUNTCASTLE et al. 2015; ROMERO-FERRERO, BERGOMI, HINZ et al. 2019; MATHIS, MAMIDANNA, CURY et al. 2018; GRAVING, CHAE, NAIK et al. 2019). High-resolution GPS can also be used to analyze animals' relative movements : for instance, GPS tracking of wild baboons revealed that a process of shared decision-making governs baboon movements (STRANDBURG-PESHKIN, FARINE, COUZIN et al. 2015). Different types of data can also be collected jointly (as in the Sociometers deployed in human groups CHOUDHURY et PENTLAND 2003), such as for instance GPS and audio recordings to investigate the role of vocalisation on the cohesion of a group of animals (O'BRYAN, ABAID, NAKAYAMA et al. 2019).

These recent developments also include proximity logging technologies based on wearable sensors that are able to provide information either on the distance between the sensor and a fixed receiver (RYDER, HORTON, TILLAART et al. 2012), or on the distance between two sensors (RUTZ, BURNS, JAMES et al. 2012; ST CLAIR, BURNS, BETTANEY et al. 2015; RUTZ, MORRISSEY, BURNS et al. 2015; BETTANEY, JAMES, ST CLAIR et al. 2015; MILWID, O'SULLIVAN, POLJAK et al. 2019; WILSON-AGGARWAL, OZELLA, TIZZONI et al. 2019). These efforts have enabled the collection of high-resolution datasets in various contexts. Using these techniques presents a number of advantages. First, wearable sensors afford an objective and reliable definition of contact as a proximity event. Second, all individuals are monitored together, continuously and potentially for a long time without the need for constant human supervision. This enables in principle the collection of large datasets covering long periods of times and, consequently, makes it possible to investigate the evolution and stability of social relationships and social groups on long timescales.

Thus, data obtained with different methods have very different nature and could in principle lead to very different descriptions and understanding of the social bonds between individuals and of the resulting social networks. For instance, the authors of CASTLES, HEINSOHN, MARSHALL et al. 2014 compared social networks constructed using different techniques (two interaction and three proximity) from the same two groups of chacma baboons (*Papio ursinus*), at both the ego network and global network levels. They obtained very different results at both levels, finding that proximity networks, which they define as spatial co-occurrences of pairs of individuals using three range criteria (a 10 m threshold, nearest neighbour and a 5 m chain rule), do not correlate with interaction networks and thus should not be used as a proxy

for social interactions. Conversely, the author of FARINE 2015 reinterpret results of CASTLES, HEINSOHN, MARSHALL et al. 2014 repeating the same tests on a different system (thornbill birds and associated species). He found that proximity in mixed-species bird flocks was generally correlated with interaction rates, demonstrating that CASTLES, HEINSOHN, MARSHALL et al. 2014 conclusions cannot necessarily be generalized across species.

This PhD work stems from these considerations to investigate social networks properties and dynamics and social issues with a data-driven approach. We indeed used data of different types and we examined the different social information that could be extracted from them and their resulting networks. Moreover, we dealt not only with the analysis of existing data, but also with the collection of novel data through the implementation of a new infrastructure.

In this chapter we first present the datasets that have been exploited and analysed during this research thesis, mainly regarding a group of Guinea baboons (*Papio papio*) belonging to a large social group of the CNRS Primate Center in Rousset-sur-Arc (France). Concerning this group, several datasets are presented of three different natures :

1. Data on social interactions collected through traditional methods (behavioral observations),

2. Data on interactions leveraging recent technologies (wearable sensors)

3. Data from participation to automated cognitive test infrastructure. These data don't involve interactions.

We note that different datasets may refer to different periods, and thus to different individuals, because the size and composition of the group varied over the years. In Section 2.2 we present the two datasets belonging to the first type, of which one was collected in 2014 and has been already presented and analysed in CLAIDIÈRE, GULLSTRAND, LATOUCHE et al. 2017 and another was collected in 2019 as a part of this PhD. In Section 2.3 a dataset of the second type is presented : it was entirely collected in 2019 as part of this PhD thanks to an ad-hoc system of wearable devices. It is worth mentioning that the acquisition of these data is the result of a collective process of design, manufacturing, assembling, installing and testing work. The third type of data, showed in Section 2.4, had been collected by CLAIDIÈRE, GULLSTRAND, LATOUCHE et al. 2017.

In Section 2.5, we compare the 2019 observations and the sensors data collected during the same period first at the level of the distributions of the interactions' duration and then at the level of single events : we systematically check whether an interaction noted by a human observer was also registered by the sensors.

In Section 2.6, two other additional datasets are introduced which regard instead human interactions in the context of a high school in Marseille, France. The two datasets were collected by MASTRANDREA, FOURNET et BARRAT 2015 with different

methods, namely surveys and using wearable sensors by the SocioPatterns collaboration (*SocioPatterns website*; CATTUTO, BROECK, BARRAT et al. 2010). These data were useful to assess results obtained with baboons data.

## 2.2. Behavioral Observations

Here we present the two datasets of behavioral observations that have been taken into account. These datasets were collected in two different periods : the first in July 2014 and the second in June-July 2019.

### 2.2.1. July 2014 observations

This dataset, described in detail by CLAIDIÈRE, GULLSTRAND, LATOUCHE et al. 2017, was recorded between July $1^{st}$ and July $29^{th}$, 2014. At the time, the group of baboons included 22 individuals, 7 males (mean age = 62 months, SD = 33) and 15 females (mean age = 124 months, SD = 75) ranging from 24 to 226 months. Observations were carried out by four trained observers using scan-sampling (ALTMANN 1974). Scan sampling is one of the two main approaches to collect observational data on animal behavior, in which observers record a "snapshot" of the behaviors of all visible members of the group at designated points in time. In this case, the group was divided into two subgroups of 11 baboons with approximately balanced numbers of individuals per age–sex classes. Two different MP3 soundtracks were recorded to control the observation timing, each composed of a repeated sequence of 11 baboon names. Each sequence lasted 2 mins, with the names presented every 10 s and with an additional 10 s break at the end. Two trained observers recorded the behavior of the group simultaneously for 2 h, with each observer listening to one soundtrack and recording the behavior of the focal baboon when it heard its name.

The data originally contained 210 behavioural observations per monkey per day during the study period, for a total of 79,380 observations for the 22 individuals. For our study, we decided to focus solely on grooming as it is known to be a bonding activity in primates and therefore to represent affiliative relationships accurately (SEYFARTH 1977). More details on the behavioural observations can be found in CLAIDIÈRE, GULLSTRAND, LATOUCHE et al. 2017.

### 2.2.2. June-July 2019

These observations were recorded during our research work, between June $13^{th}$ and July $10^{th}$ 2019. The entire group consisted of 19 individuals (7 males and 12 females) with age ranging from 1 to 23 years old. Among these, 13 baboons, consisting only of juveniles and adults (all individuals at least 6 years old) were collared with leather collars fitted with wearable proximity sensors (RFID tags) developed by the SocioPatterns collaboration *SocioPatterns website* (see Section 2.3 for the description of

the corresponding data). The focal-sampling method (ALTMANN 1974) was used, which consists in following the actions of a single individual over a set period of time. Observations were carried out for five days a week (from Monday to Friday) for a total of 20 days, with two sessions of ~ 2 hours a day at different hours each day, ranging from 8am to 5pm. During each session, a trained observer focused on each individual for a period of 5 minutes and recorded its behavior. The order in which the different individuals were observed was reshuffled at each session. Thirteen behavioral categories, typically corresponding to social agonistic and social affiliative interactions (see also CLAIDIÈRE, GULLSTRAND, LATOUCHE et al. 2017) were recorded, namely : 'Grooming', 'Presenting' (Greeting),'Playing with', 'Grunting-Lipsmacking', 'Supplanting', 'Threatening', 'Submission', 'Touching', 'Avoiding', 'Attacking', 'Carrying', 'Embracing', 'Mounting', 'Copulating', 'Chasing' (see Table 2.1 for details). Another behavior of interest was 'Resting'. Resting is often considered as a behavior performed in isolation, i.e., does not correspond to an interaction between individuals. In some cases however, when two or more individuals were resting together at less than one meter from each other, this was considered as 'social resting' and also counted as an interaction.

'Resting', 'Grooming' and 'Playing with' include a duration and are called *State* events. The other types of behavior do not have a duration assigned and are called *Point* events. For each observed behavior, the individuals involved were recorded as well as the starting and ending time of each state event, and, for each point event, the time at which it took place.

In addition, two categories were included, namely 'Invisible' and 'Other', to refer to the cases in which the individual was not seen by the observer or the behavior was not included among those listed above.

In the following, we may refer to the observed behaviors corresponding to interactions as 'interactions' or 'observed interactions'.

The total number of behaviors recorded for the entire group of 19 individuals is 5,377. From this full data set of observations we keep just the behaviors involving the 13 individuals that were carrying collars with wearable sensors. Among the 995 observed interactions regarding this juvenile/adult subgroup, 944 (~ 95%) are affiliative social behaviors (Grooming, Resting, Presenting, Grunting-Lipsmacking, Touching, Mounting, Embracing, Playing with) which are the most relevant to this study. Moreover, grooming and (social) resting represent more than 98% of the state events and ~ 65% of the total.

Figure 2.1 represents the distributions of durations for the observed interactions (i.e., with associated duration), both for the subgroup of collared individuals and for the whole group (which includes very young juveniles and babies) and distribution of duration for grooming interactions only, for the subgroup of collared individuals. Durations cover a broad range of values with a cut-off point at 300s (5 minutes) corresponding to the duration of the focal observation (i.e., some interactions lasted more than 300s but their total duration is unknown). We note that the distributions of events concerning the whole group or only the collared individuals have similar

shapes, with however a larger fraction of short interactions when babies are included. Contrarily, grooming behaviors are characterized by longer durations.

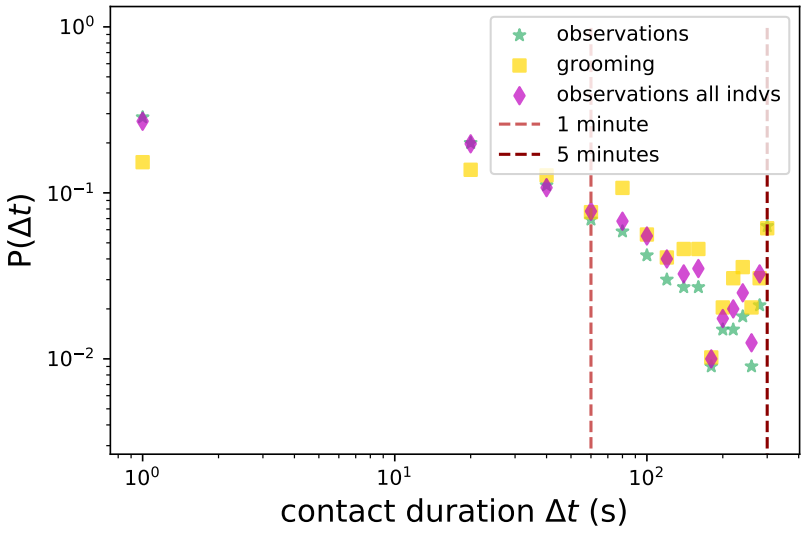


FIGURE 2.1. : **Durations of observed interactions.** Distributions of durations for state events in observed interactions (green stars for interactions involving only the 13 collared individuals; average = 81.3s, std = 90.3s, median = 41.0 s, max = 300s; magenta diamonds for all interactions; average = 43.8s, std = 64.6s, median = 18.0 s, max = 300s; gold squares for only grooming behaviors of the 13 collared individuals; average = 107.4s, std = 93.0s, median = 81.0 s, max = 300s ).

Note that according to the observational method used in this study, individuals are observed for 5 minutes (300 seconds) at a time. The peak value at 300s for the observations data is therefore an artifact of the observation method.

## 2.3. Wearable sensors

These data have been collected on the subgroup of 13 collared individuals already cited in Subsection 2.2.2. Actually, the individuals had been collared since June 2018, when we started a preliminary data collection in order to test the infrastructure and to ensure that the collars would not hurt or bother the individuals. These sensors had already used in many studies involving humans (CATTUTO, BROECK, BARRAT et al. 2010; ISELLA, STEHLÉ, BARRAT et al. 2011; STEHLÉ, VOIRIN, BARRAT et al. 2011; FOURNET et BARRAT 2014; GÉNOIS, VESTERGAARD, CATTUTO et al. 2015; MASTRANDREA, FOURNET et BARRAT 2015; VESTERGAARD, VALDANO, GÉNOIS et al. 2016), and recently also animals (WILSON-AGGARWAL, OZELLA, TIZZONI et al. 2019; OZELLA, LANGFORD, GAUVIN et al. 2020). In our setting, each sensor was secured in a customized box specially

| **Behavior** | **Meaning** |
|---|---|
| Social resting | Staying at the same place without performing other behaviour (e.g. locomotion, social, object-directed) and at less than 1 m from at least one other individual |
| Carrying | Carrying another individual, often a baby. |
| Touching | Gentle contact from one individual to another |
| Presenting (Greeting) | Approaching another individual gently with/without lipsmacks and grunts and presenting the rear. |
| Embracing | Grasping another individual (with one or two arms) |
| Grooming | Fur cleaning |
| Playing with | Playing with another individual |
| Grunting-Lipsmacking | Affiliative mimic and vocalization from one individual to another |
| Threatening | Eyebrow raising and / or slapping the ground with or without vocalization |
| Attacking | Agonistic physical contact (biting, grasping, slapping) |
| Chasing | Threatening by running after another individual |
| Mounting | Social mount |
| Submission/Yak | Teeth bared, body lowered with production of typical yak vocalisation |
| Avoiding | Moving away from an approaching individual |
| Supplanting | Taking the place of another individual |
| Copulating | Sexual mount (generally with copulation call) |

Table 2.1. : **Description of the social behaviours recorded during observation.**

designed with a 3-D printer to contain the sensor and a long-life battery connected to it. The boxes were positioned on the front side of the individuals (Fig 2.2).

The sensors exchanged low-power radio packets in a peer-to-peer fashion. Thanks to the very low power used, the reception by the sensor of an individual A of a radio packet emitted by the sensor of another individual B is a good proxy for a close proximity ($\lesssim$ 1.5 m) of individuals A and B (CATTUTO, BROECK, BARRAT et al. 2010). Moreover, the radio frequency emitted by the RFID tags is absorbed by body water, so that the radio packets tend to propagate mostly towards the front of the individual wearing the device. The packets exchange rate depends thus on the mutual orientation of the individuals and the infrastructure detect mainly face-to-face contacts. The detected spatial proximity relations were relayed from RFID tags to radio receivers (RFID readers), which were installed around the enclosure and connected to a local area network (LAN). A central server received the data, timestamping and storing each event.

Data were finally aggregated with a temporal resolution of 20 seconds (for more details see CATTUTO, BROECK, BARRAT et al. 2010) : we thus defined two individuals to

be in contact during a 20s time window if their sensors exchanged at least one packet during that interval, and the contact event was considered over when the sensors did not exchange packets over a 20s interval.

We will refer to the contacts collected by the sensors as 'contacts' or 'contact events'.

(a) (b)

FIGURE 2.2. : (a) : Individuals in the enclosure, wearing collars with the attached boxes embedding the tags. (b) : Interior of a single box containing the tag (top) and the connected battery (bottom)

For the first ten days of data collection (June $13^{th}$ -$23^{rd}$) only two readers were installed around the enclosure, whereas in the successive days a third reader was added to ensure a better coverage. In this work, a particular relevance was dedicated to data collected between June $13^{th}$ and July $10^{th}$, 2019, i.e., during the period of the observations. These two datasets and, as we will see in the next chapter, the respective resulting networks, were in fact compared. However, the data collection went on for months even after the observation period was over. Here, we consider sensors data collected until November $30^{th}$. Such an extended dataset allows for analyses of the evolution of the network over long time scales.

During the period in which observations were carried out, 31,783 contact events were recorded between the 13 individuals. Of these, 4,823 (15% of the total) were recorded during the periods of behavioral observations. The number of contacts per day was ~ 1,135 on average and ranged from 754 (June $28^{th}$) to 1,768 (June $13^{th}$) for a total duration of 1,259,500 s (349 hours). Contact durations varied on a very broad range : most contacts were short, with an average duration of 39.6s, and 95% of the contacts lasted less than 2 minutes, but contacts as long as 1,520s (~ 25 minutes) were recorded, and the contact durations form a continuous distribution spanning all values in between (see Fig. 2.3), as observed in many different contexts for human and animal groups (CATTUTO, BROECK, BARRAT et al. 2010; SALATHÉ, KAZANDJIEVA, LEE et al. 2010; MASTRANDREA, FOURNET et BARRAT 2015; FOURNET et BARRAT 2014; WILSON-AGGARWAL, OZELLA, TIZZONI et al. 2019). In fact, we report on the same graph the statistics of contact durations measured by wearable sensors between students in

a school, reported in TOTH, LEECASTER, PETTEY et al. 2015 and freely accessible : it turns out that the distributions of contact durations of baboons and of humans are indeed very similar.

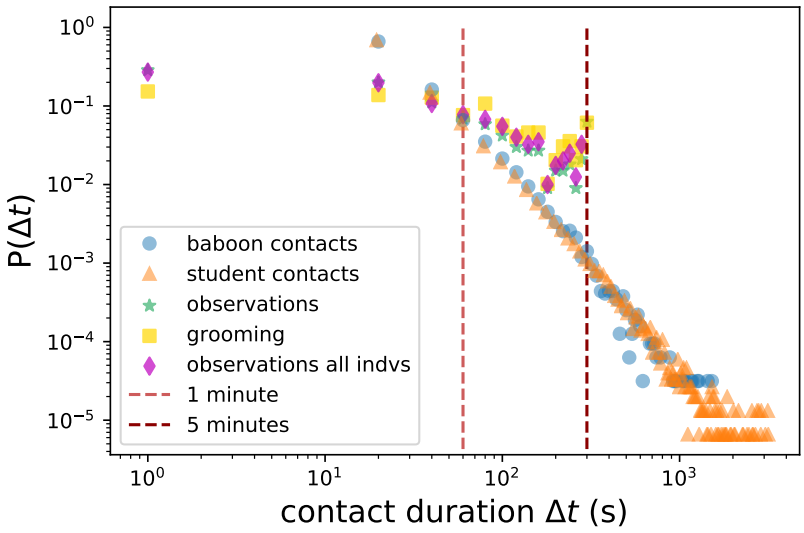


FIGURE 2.3. : **Durations of contacts and observed interactions.** Distributions of durations for : contacts detected by the wearable sensors infrastructure (blue dots; average = 39.6s, std = 52.7s, median = 20.0s, max = 1,520s); contacts between students in a school in Utah (USA) measured by an infrastructure based on wireless ranging enabled nodes (WRENs) TOTH, LEECASTER, PETTEY et al. 2015 (orange triangles; average = 39.6s, std = 72.8s, median = 19.5s, max = 3164s); state events in observed interactions (green stars for interactions involving only the 13 collared individuals; average = 81.3s, std = 90.3s, median = 41.0 s, max = 300s; magenta diamonds for all interactions; average = 43.8s, std = 64.6s, median = 18.0 s, max = 300s; gold squares for only grooming behaviors of the 13 collared individuals; average = 107.4s, std = 93.0s, median = 81.0 s, max = 300s ).

As explained in Figure 2.1, the peak and also cut-off for the observations data at 300 is due to the focal-sampling observation method, which limits the observation of each individual at 5 minutes at a time.

## 2.4. Cognitive tests

Since 2014 a total of 29 individuals of the group of baboons already cited in the previous sections, have been participating in cognitive tests using Automatic Learning Devices for Monkeys (ALDM) in a facility developed by J. Fagot FAGOT et BONTÉ 2010;

FAGOT et PALERESSOMPOULLE 2009. The dataset analysed here, contains all recorded cognitive tests performed by the group of baboons over a period of three years, from 2014 to 2017. During this period, the size of the group varied from 19 to 24 individuals, because of several births and natural deaths during these years. The monthly average size was of 21.8 individuals with 7.3 [7;9] males and 14.4 [12;17] females (mean [min; max]), with age ranging from 0 to 21 years old. The baboons were all marked by two biocompatible $1.2 \times 0.2$ cm RFID microchips injected into each forearm to individually identify each participant.

In the facility, baboons can freely access 10 workstations installed in two trailers (5 workstations in each trailer) connected to their enclosure (see Fig 2.4(b)). Each workstation (Fig 2.4(b)) is constituted of a test chamber with open rear side and transparent sidewalls. The front of the test chamber is fitted with a view port and two hand ports. By looking through the view port, participants can interact with an LCD touch screen installed at eye level and whenever a monkey introduces its forearm through one arm port, its RFID identity is recognized and triggers the presentation of the cognitive task on the touch screen. For each test, the date and time (with millisecond precision), the nature of the task, the name, age, sex and maternal family of the individual performing the test, and the identification number of the workstation in which the individual performed the test, are recorded. The system provides rewards in grains of dry wheat, delivered through a food dispenser, whenever the baboons succeed at the task.

The data covers the period from January 2014 to May 2017. The facility was however closed in the months of August 2014 and 2015, which are thus missing from the data. Furthermore, two individuals were born in May 2017 so they do not appear in some of the analysis (e.g., in the measures of stability from one month to the next).

The data analysed here include a total of 16,403,680 cognitive tests, representing an average of 13,186 records a day over 1,244 days, and an average of 565,640 records per individual. The duration of a single bout of trials (i.e. a succession of trials of a given individual separated by less than 5 seconds) was on average 60 seconds.

Contrarily to other datasets, here there is no direct information about social interactions between individuals. In fact, in the ALDM system the monkeys cannot see each other's screen (observational learning is thus impossible). However, they have visual access to each other in neighbouring workstations through their transparent sides : they can thus approach booths together and see each other during the tests, meaning that co-presence may be interpreted as association. In support of this hypothesis, CLAIDIÈRE, GULLSTRAND, LATOUCHE et al. 2017 recently showed that the timings of cognitive tests could be used to construct a social network of baboons highly similar to the one obtained from behavioral observations.

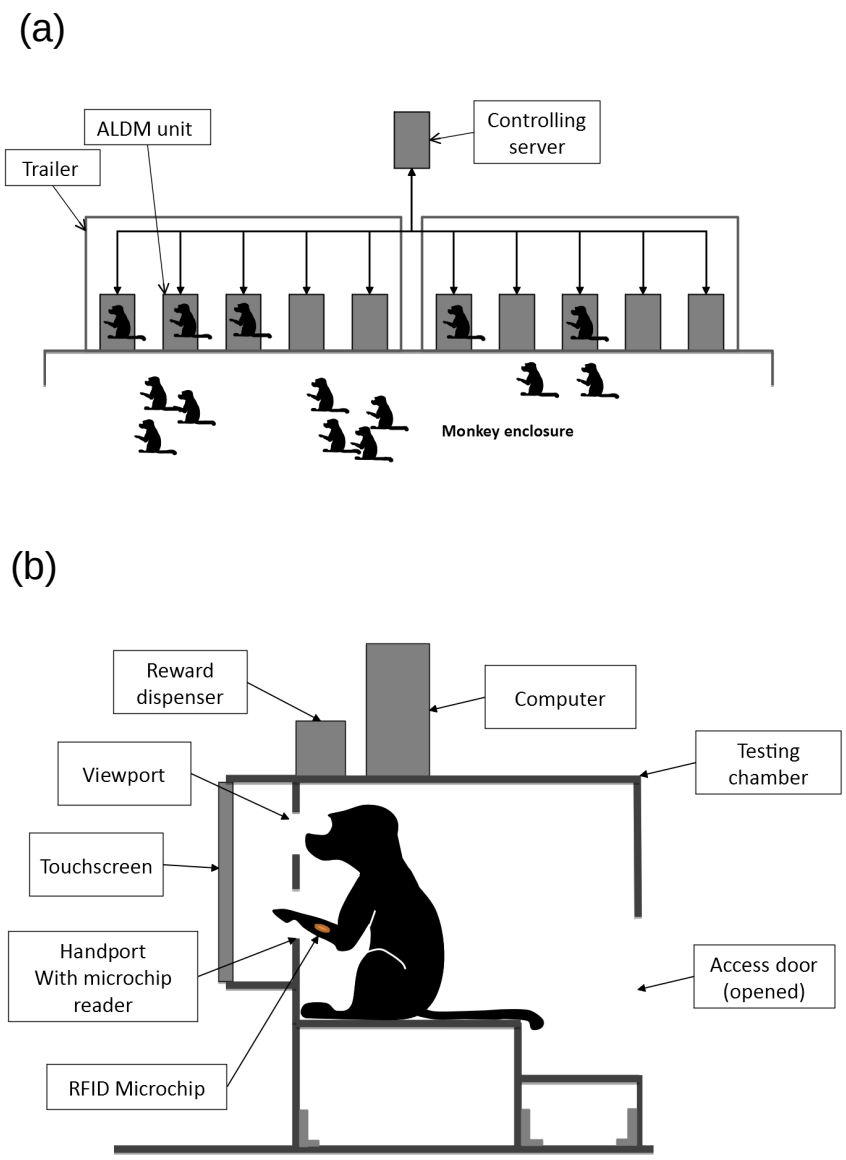


FIGURE 2.4. : **ALDM self-testing system.** (a) Schematic of the ALDM system's organization. (b) Details of the ALDM testing unit

## 2.5. Comparing observed interactions and sensors contacts data

**Distributions** Figure 2.3 shows distributions of durations of the observed interactions and of the contacts registered by the sensors infrastructure. Although they differ, with much larger values for the sensors contacts, they are both broad and spanning

a large range of values. The limited range of the observed interactions durations is due to the observational protocol, since all durations above 300 seconds are cut-off at that value. In addition, the duration of an interaction is necessarily underestimated if it starts before the beginning of a given 5-minutes observation time-window, or if it terminates after the end of the time-window : this biases the resulting distribution of durations in a complex way. Overall, it seems possible that the two distributions would have similar slopes at large durations if this cut-off were not enforced.

**Single Events** To go beyond this statistical comparison, we perform a detailed matching procedure between each single observed interaction (in the behavioral data) and the contact events (obtained from the sensors data).

We computed the fraction of observed interactions that were also detected by the wearable sensors infrastructure as follows. Each observed interaction event involves two individuals $i$ and $j$ and is assigned a time $t$ (for point events) or an interval $[t_{start}, t_{stop}]$ (for state events), with $t_{start}$ and $t_{stop}$ the moments of beginning and end of the interaction, respectively. Note that the observed interactions are often directed, with an actor individual and a recipient individual. However, since the proximity events registered by the wearable sensors are not directed, we consider undirected versions of the behavioral data (i.e., the direction of the interaction is not taken into account).

An observed interaction event is then considered as *tracked* if at least one RFID packet was exchanged between the sensors of individuals $i$ and $j$ within the time window $[t-\Delta t, t+\Delta t]$ or $[t_{start}-\Delta t, t_{end}+\Delta t]$, for point and state events respectively, where $\Delta t$ is a tolerance interval. This tolerance is introduced to take into account three elements : (i) the potential delay of the observer in reporting the interaction with respect to its actual occurrence ; (ii) the 20s time aggregation of the RFID sensors data (iii) the possible asynchrony between the observer's tablet computer in which observed interactions were registered and the time of the computer storing the sensors' data.

Obviously, to compute the fraction of tracked interaction events, we only consider observed events involving two individuals wearing sensors.

Table 2.2 gives the results of this matching, for different categories of interactions and different values of the tolerance $\Delta t$. The fraction of observed interactions finding a match in the sensors data is quite low, with a slightly better performance when the tolerance is increased. For $\Delta t = 20s$, on average only one third of the observed interactions appear in the data obtained from the sensors infrastructure. The fraction is lower for very short events such as greetings but notably larger if we consider only grooming events, which are known to be very important socially (SEYFARTH 1977). We note that in this case the fraction of tracked observed interactions is about 50%, a value very close to the one recently obtained in ELMER, CHAITANYA, PURWAR et al. 2019 in a comparison between the contacts between human individuals as observed in an annotated video and as registered by wearable sensors.

Reference DAI, BOUCHET, NARDY et al. 2020 shows the complexity of this issue : first, the authors analyse the dependencies of the strength of sensors transmitted radio

signals on environmental parameters, as distance and mutual orientation between individuals; then, they explore several supervised learning methods to distinguish between packets indicating real and false social interactions and reconstruct a reliable temporal network.

We finally note that we can consider the reverse procedure, considering the contacts registered by the sensors as ground truth. To this aim, we restrict the sensors' contact data to the time windows corresponding to the behavioral observation periods : only 6.63% of these contacts were recorded by the observer as interactions. Note that this small number is not surprising, as the observer focuses on one individual at a time, while the sensors' infrastructure registers contacts between all collared individuals during the same time window.

| | **All Interactions** | | | **State Events** | | | **Grooming** | | | **Presenting (Greeting)** | | |
|---|---|---|---|---|---|---|---|---|---|---|---|---|
| $\Delta t$ | 20s | 40s | 60s | 20s | 40s | 60s | 20s | 40s | 60s | 20s | 40s | 60s |
| Tot. | 0.32 | 0.36 | 0.39 | 0.36 | 0.4 | 0.43 | 0.48 | 0.53 | 0.56 | 0.23 | 0.27 | 0.29 |
| Avg. | 0.32 | 0.36 | 0.38 | 0.37 | 0.4 | 0.42 | 0.49 | 0.53 | 0.55 | 0.2 | 0.24 | 0.27 |
| Std. | 0.12 | 0.13 | 0.13 | 0.12 | 0.13 | 0.14 | 0.19 | 0.21 | 0.22 | 0.2 | 0.2 | 0.21 |
| Min. | 0.1 | 0.1 | 0.12 | 0.11 | 0.11 | 0.14 | 0.17 | 0.17 | 0.17 | 0.0 | 0.0 | 0.0 |
| Max. | 0.54 | 0.63 | 0.63 | 0.61 | 0.64 | 0.64 | 0.83 | 0.83 | 0.89 | 0.67 | 0.67 | 0.83 |

Table 2.2. : **Fractions of observed interactions with a corresponding match in the sensors data.** We consider an interaction to have a match in the contacts data if the pair of individuals involved in the interaction appears in the sensors data in the same time window $\pm\Delta t$. We report the overall fraction of matched interactions (first row), the average fraction over the days (second row) with the corresponding standard deviation (third row), and the minimum and the maximum (fourth and fifth row) fractions of tracked interactions over the different days. The values were computed for different delay parameters $\Delta t$, and considering either all interactions, only state events (i.e., interactions with duration), only grooming events and only greeting events.

## 2.6. Other Datasets

In order to assess whether results obtained from the analysis of the baboons social network (see Chapters 3 and 4) were species or group-specific or, on the contrary, they could be generalizable also for human social networks, we used additional datasets on human interactions as a benchmark. In particular, we took advantage of SocioPatterns collaboration platform (*SocioPatterns website*) data, which are freely downloadable from the dedicated webpage
http ://www.sociopatterns.org/datasets/. The data concern a group of students in a high school in Marseilles, France and were collected through several techniques

by MASTRANDREA, FOURNET et BARRAT 2015 for 5 days in December 2013. Students belong to different classes, each one with a different specialization : “MP” for mathematics and physics, “PC” for physics and chemistry, “PSI” classes for engineering studies and “BIO” classes for biology. The data involve students of nine classes corresponding to the second year of such studies : 3 classes of type “MP” (MP, MP*1, MP*2), two of type “PC” (PC and PC*), one of type “PSI” (PSI*) and 3 of type “BIO” (2BIO1, 2BIO2, 2BIO3). Due to location of the classrooms of the various classes, the groups can be considered as almost closed populations whose contacts occur mostly within the same class.

In particular, we used two datasets of different nature :

- Dynamical contact list of the contacts between the students, as measured by the SocioPatterns infrastructure. The sensors used in this data collection are the same as those described above, with the difference that they were not embedded in custom designed boxes but in simple wearable conference-like badges. Students were asked to wear the sensors on their chests using lanyards, ensuring that the devices of two individuals can only exchange radio packets when the persons are facing each other. The information on face-to-face proximity events detected by the wearable sensors was relayed to radio receivers installed throughout the high school. Contacts data involve 327 students during the week of Dec. 2-6, 2013. The file contains a tab-separated list representing the active contacts during 20-second intervals of the data collection. Each line has the form “t i j Ci Cj“, where i and j are the anonymous IDs of the persons in contact, Ci and Cj are their classes, and the interval during which this contact was active is [ t – 20s, t ]. Time t was measured in seconds and expressed in UNIX ctime.

- Friendship surveys data. This dataset was collected at the end of the period of analysis, it involves 135 students and corresponds to the directed network of reported friendships. Students were asked to give the names of their friends in the high school. Each line has the form “i j”, meaning that student i reported a friendship with student j.

## 2.7. Conclusion

In this chapter we first presented several datasets involving both non-human primates, namely Guinea baboons, and humans (high school students) and collected through different methods :

1. Behavioral observations of non-human primates (one dataset collected in 2014 and another in 2019)

2. Contacts registered by wearable sensors between non-human primates

3. Automatically collected cognitive tests of non-human primates

4. Contacts registered by wearable sensors between students

5. Friendship surveys

We note that the ALDM cognitive tests dataset does not contain explicitly associations between individuals. Nonetheless, the timings and the position of individuals performing the tests can be used to construct a co-presence network (see 3.2.1), which has been shown by CLAIDIÈRE, GULLSTRAND, LATOUCHE et al. 2017 to be a good proxy of the underlying social relationships between individuals. In fact, the network obtained by CLAIDIÈRE, GULLSTRAND, LATOUCHE et al. 2017 from the co-presence of the baboons in ALDM testing booths turned out to be highly correlated to the one obtained through standard behavioral observation techniques.

In 3.3.1, we provide a further validation to this argument, comparing the social network obtained through the adjacent position and time concurrence of individuals in tests, with the one obtained by observational data.

We then compared, in terms of advantages and disadvantages, behavioral observations, which represent the traditional method of collecting pair-wise interactions in animals social studies, and the recent technique of automatic collection through wearable proximity sensors. It turned out that sensors and behavioral observations have different advantages and limitations that influence their ability to detect contacts and interactions between individuals. On the one hand, observational methods provide high-quality data, through which we can distinguish different behaviors and describe in depth social relationships between individuals. However, the data suffers from several sampling issues : only a limited amount of time can be spent observing each individual, and data may be completely absent on certain days for logistical reasons (the week-ends in our case). Biases related to the observation technique can also occur and are difficult to estimate. The cutoff on the duration of each individual observation leads moreover to an underestimation of the duration of long interactions, which can be particularly important to determine the social structure of a group. Finally, the total duration of the observation period is usually limited to a few weeks and the group can not be monitored continuously on very long time scales, for clear practical reasons. On the other hand, wearable sensors do not yield information on the type of behavioral interactions and they do not register contacts with individuals not wearing any sensor, such as very young individuals in our case. The quality of the collected data might also depend on infrastructure constraints and potential technical failures, so that sampling issues must also be considered carefully (GÉNOIS, VESTERGAARD, CATTUTO et al. 2015; VESTERGAARD, VALDANO, GÉNOIS et al. 2016). We will tackle the problem of the data loss in Section B.

We have performed a comparison of the two data sets at the level of single events. We have checked for each observed interaction whether a contact was registered by the sensors at the same time. This matching turns out to be very limited : about one third of the observed interactions was also recorded by the sensors, but this amount fluctuates and depends strongly on the type of interaction. In particular, for interactions that tend to last, such as grooming, the percentage of tracked events

rises to ~ 50% and is above ~ 80% in some days of observations. This is particularly important as grooming behavior is for primates one of the core social interactions allowing to define the social structure of the group (SEYFARTH 1977). For short and elusive interactions instead, like greeting, this percentage is only of about ~ 20%, which can be explained by the fact that greetings among baboons are most often not face-to-face interactions. Notably, our results are in line with ELMER, CHAITANYA, PURWAR et al. 2019; DAI, BOUCHET, NARDY et al. 2020. In ELMER, CHAITANYA, PURWAR et al. 2019 in particular, the correspondence was examined between data collected by wearable sensors and a video of the same interactions, yielding a sensitivity of 50% (about half of the interactions annotated on the video were present in the wearable sensor data).

In the next chapter we will look into the structure of the social group through social network analysis. We will show how we obtained different social networks from the datasets presented above, exploring different timescales through the aggregation over several time windows. Moreover, we will compare the network structures relative to data of different nature, to investigate whether the mismatch observed at the level of single events affect also the picture of social interactions.

# 3. From data to networks

## 3.1. Introduction

Network analysis represents a valuable and flexible framework to understand the structure of individual interactions at the population level in human and non-human societies. The versatility of network representations is suited to different types of datasets describing these interactions. Moreover, underlying associations between entities can be unveiled through network analysis even in cases of systems that do not possess an obvious “web-like” structure. However, depending on the data collection method, different pictures of the social bonds between individuals could a priori emerge from the corresponding network representations.

The availability of datasets of diverse nature and size provides a unique opportunity, in particular in animals social study, to assess the reliability of social studies based on different types of data. This precious asset allows to compare networks computed with different data, approaches and techniques and thus to understand the influence of these approaches on the picture of the network. On the one hand, different data may narrate different aspects of the evolution of a social system. On the other hand, the way a network is extracted from the data is not unique and could influence our perception of the dynamics : Castles, Heinsohn, Marshall et al. 2014 and Farine 2015 show how networks based on the same data but on different edge definitions may not be equivalent. Moreover, when dealing with temporally resolved data and networks, we can aggregate data on arbitrary time-windows that may not necessarily correspond to any intrinsic timescale of the system. The choice of the size of a time-window is a challenging problem (Caceres, Berger-Wolf et Grossman 2011 ; Psorakis, Roberts, Rezek et al. 2012 ; Psorakis 2013) because a too short time-window may create a noisy signal that may hide important structures of the network, whereas very large time-windows risk to "flatten" the underlying dynamics. There is no standard procedure to find a trade-off between these two scenarios and thus to distinguish between noise and meaningful association and even the choice of non-uniform time-windows might not be enough to solve the problem (Caceres, Berger-Wolf et Grossman 2011 ; Psorakis 2013 ; Psorakis, Roberts, Rezek et al. 2012).

Finally, underlying social processes inferred from networks based on individuals associations, such as proximity, might provide or not a reliable image of real social relationships depending on several factors : the edges definition, a correct use of statistical tests and null models, the amount and completeness of the data available (Farine et Whitehead 2015 ; Farine 2015 ; Génois, Vestergaard, Cattuto et al. 2015).

In this chapter we describe how different social networks were derived from the various data presented in Chapter 2 using different approaches and we compare these different networks. Section 3.2 is dedicated to the construction of temporal networks using a fixed aggregation time-window approach, while in section 3.3 we conduct two different comparative analyses : in the first, we compare the network obtained from cognitive tests data (see section 2.4) restricted to the month of July 2014 and the network obtained from 2014 behavioral observation (see section 2.2.1), taking only grooming behaviors ; in the second, the network computed from wearable sensors data (section 2.3) is compared with that obtained from 2019 observations (section 2.2.2). In both cases, we confront network weights using several well-established similarity and correlation metrics and results are then validated using a null model. In the case of the networks obtained by behavioral observations data and wearable sensors data, we examined multiple time windows, from few hours to the whole period of observations. While for the whole period of observations the networks appear extremely similar, we show how the selection of time windows of different sizes can have significant implications on the image of the social structures. In particular, the network obtained from wearable sensors proved to be more stable and less sensitive to a reduction of the timescale, with respect to the network obtained from observations data. In Appendix B, we moreover establish the sensors infracture to be robust to data loss.

Finally, in section 3.4 a new continuous-time model is presented and analysed as an alternative approach to represent temporal networks, that may overcome the issues cited above about time-windows aggregation, and which is generally applicable to any data stream containing dyadic interactions.

## 3.2. Computing aggregated networks

### 3.2.1. Co-presence network from ALDM data

Here we describe the construction of a temporal co-presence network based on the temporal and spatial proximity of the baboons (see Figure 3.1) using the ALDM dataset presented in section 2.4. Following the study of Claidière, Gullstrand, Latouche et al. 2017, this procedure aims to obtain a network of informative associations between individuals, starting from data that did not refer to social interactions, but including information about time and position of individuals in test workstations. We first aggregated the raw ALDM data in successive temporal windows of $\Delta t = 5$ seconds : this interval length was short enough to consider that the individuals performing tests in the same time window were in co-presence, and long enough to have a sufficient number of co-presence events. This interval length was also used by Claidière, Gullstrand, Latouche et al. 2017, and we show below that our results are robust with respect to changes in $\Delta t$. Note that a single co-presence event lasting for instance 1 minute gave rise to 12 successive time-windows in which the individuals were detected in co-presence.

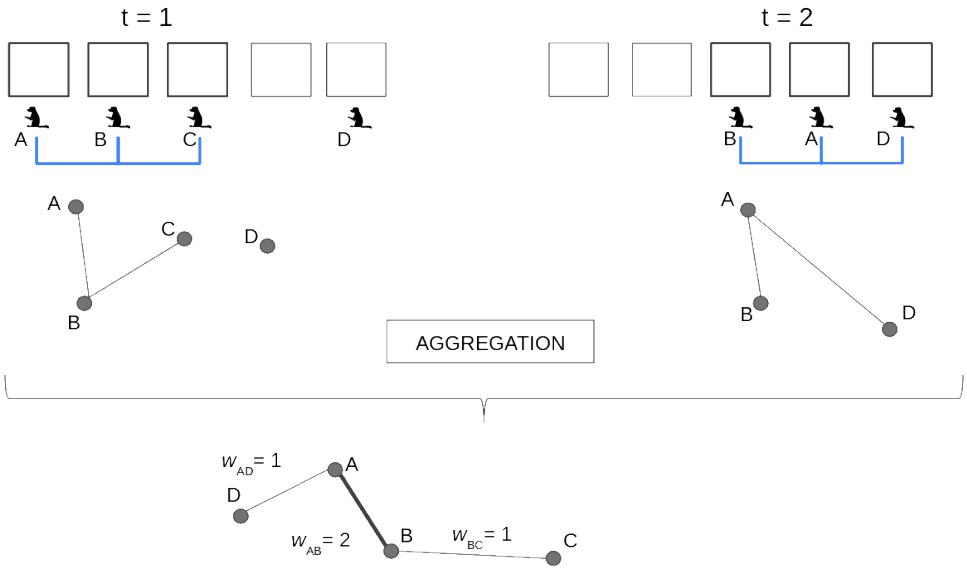


FIGURE 3.1. : **Sketch of the construction of the co-presence network** Top : Schematic of the network construction from the ALDM dataset. In each time-window of $\Delta t = 5$ seconds, links were created between individuals (nodes) if they were recorded in adjacent workstations, as depicted in the middle drawings : links $AB$ and $BC$ in the first time-window, and $AB$ and $AD$ in the second. The instantaneous networks were then aggregated to produce a weighted co-presence network (bottom sketch).

For each time window, we built a proximity network in which nodes represented baboons, and a link was drawn between two individuals if their presence had been recorded in two adjacent booths (see figure 3.1). We then aggregated these proximity networks on a monthly timescale, shown by CLAIDIÈRE, GULLSTRAND, LATOUCHE et al. 2017 to correspond to an adequate aggregation timescale : in each monthly network, nodes represented baboons and a weighted link between two baboons represented that they had been in co-presence at least once ; the weight of the link corresponded to the number of time windows in which co-presence of these individuals had been recorded (i.e., the weight represented the total co-presence time, in units of 5 seconds).

### 3.2.2. From weighted co-presence networks to affiliation and avoidance networks

A first analysis of the ALDM data revealed that the baboon's frequency of participation in cognitive tests was very heterogeneous (see Figure 3.2a), as in the study of CLAIDIÈRE, GULLSTRAND, LATOUCHE et al. 2017. This difference in participation could result in biased estimates of link strength in the co-presence network (defined in the previous subsection) for simple statistical reasons : individuals who are present more often in the ALDM booths have a larger probability of being found in co-presence

simply by chance, compared to individuals who participate less frequently. To take this behavioural heterogeneity into account and to determine which links could be interpreted as socially meaningful, we compared the observed co-presence to a null model based on the random permutation of the baboons' names for each month. This corresponds to the assumption that co-presence in the ALDM booths was independent from social relationships. To construct the null model, we considered the ALDM data of each month, which consists of the list of tests performed in that month, with for each test the date, identity of the individual performing the test and identification of the workstation (see Section 2.4). In this list, we reshuffled the identities of the individuals among the tests, swapping all observations at once and keeping the number of occurrences of each individual. This procedure ensured that the frequency of participation of each individual and the spatial and temporal organisation of the trials were preserved for each month in the null model (MANLY 1997; BEJDER, FLETCHER et BRÄGER 1998; FARINE 2017). We then used the randomized data to create a weighted co-presence network as previously. We performed the randomization procedure 100 times.

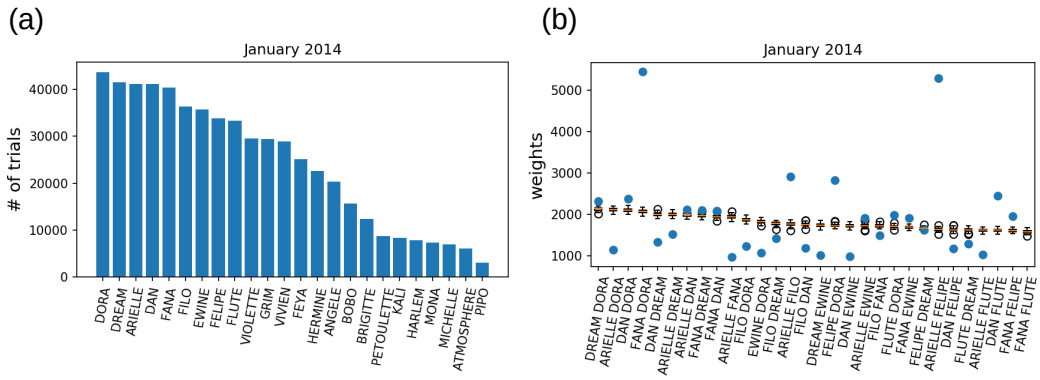


FIGURE 3.2. : **From the weighted co-presence network to the signed social network.** a) Bar plot representing the number of cognitive tests performed by each individual in January 2014. b) For a sample of 30 pairs of individuals, weights of the January 2014 co-presence network (blue dots) and boxplot showing the distributions of weights for the same pairs in networks resulting from the null model. In each box, the orange line marks the median and the extremities of the box correspond to the 25 and 75 percentiles; the whiskers give the 5 and 95 percentiles of each distribution.

The results showed that some links had weights compatible with the null distribution, while others had observed weights that were above the 95% confidence interval of the null distribution (see Figure 3.2b for illustrative examples), showing that the corresponding baboons were found in co-presence much more frequently than expected by chance and thus suggesting that they affiliated with each other. Interestingly,

some observed weights were significantly *lower* than expected by chance (below the $5^{th}$ percentile of the null model distribution), showing that these baboons were in co-presence much less often than predicted by chance : it was then natural to assume that they were actively avoiding each other (see BEJDER, FLETCHER et BRÄGER 1998). Note that pairs with no co-presence events, i.e. which were not linked in the original co-presence network, could be considered as avoiding each other if they were often found in co-presence in the null model.

This comparison with a null model allowed us to construct for each month a new signed network with both positive (affiliative) and negative (avoidance) links. In this new network, positive links were given by the co-presence links whose weights were above the $95^{th}$ percentile of the null model distribution. The negative links, on the other hand, joined the pairs of baboons with weights below the $5^{th}$ percentile of the null distribution. Moreover, the weight of each link in the weighted network was re-defined as the z-score value of the original weight with respect to the null model distribution, i.e.

$$Z_{ij} = \frac{w_{ij} - \mu_{ij}}{\sigma_{ij}} \,. \tag{3.1}$$

where $\mu_{ij}$ and $\sigma_{ij}$ are the mean and the standard deviation of the null model distribution for the link (ij), respectively. We hence obtained indeed positive values of $Z_{ij}$ for the affiliative links and negative values for the avoidance links. Finally, for each month we defined the set of positive links as the monthly *affiliative* network and the set of negative links as the monthly *avoidance* network.

### 3.2.3. Grooming network

From the observational data collected in 2014 and described in section 2.2.1, we used the number of grooming events observed between a pair of individuals during the observation month (July 2014) to build a weighted and undirected network. This network was then compared to the proximity network based on ALDM data of the same period. This network resulted in 216 links. A fully connected network with the same number of nodes would have had 231 links. The weights (i.e. number of grooming events per dyad) ranged from 1 to 778 and the average and the median were respectively 60.7 and 23.0.

### 3.2.4. Contact network and interaction network

Here we consider the observational and wearable sensors data collected between June and July 2019, introduced in sections 2.2.2 and 2.3, respectively. For each data set, we could in principle construct, on any temporal window, an aggregated network in which nodes represent individuals and weighted links give a summary of the recorded contacts or observed interactions during that time window. We first considered as time window the whole period in which observations were carried out, and we restricted the observational data to the 13 individuals with collars and sensors. We thus obtained

a "contact network" from the wearable sensor data and an "interaction network" from the observed interactions, both covering the period from June $27^{th}$ to July $10^{th}$, 2019. Both networks are undirected and weighted.

In the aggregated interaction network, a weighted link between nodes $i$ and $j$ is drawn if at least one interaction was observed between $i$ and $j$ during the aggregation time window. The weight $w_{ij}^{(I)}$ of the link between individuals $i$ and $j$ is given by the total number of interaction events recorded between $i$ and $j$ during this time. Note that we use here the number of interactions and not their total duration in order to account also for point events. Similarly, in the contact network, a link was drawn between $i$ and $j$ if at least one contact was recorded between them by the sensors infrastructure, and the corresponding weight $w_{ij}^{(C)}$ is given by the number of contacts recorded by the sensors between $i$ and $j$.

In addition to the whole observation time windows, we considered shorter time windows of 1 day, 3 days and one week and increasing time windows of $n$ days length.

## 3.3. Comparing networks

In this section we perform two separate comparative analysis, each time comparing a network obtained from data collected through an automated method with one obtained through observational data. This comparison analysis has a dual purpose : on the one hand it is meant to validate networks computed using automated collected data as reliable images of the underlying social relationships between individuals ; on the other hand it aims to quantify at what extent the image of the network structure is impacted by the nature of the data.

### 3.3.1. Co-presence vs Grooming

To validate the network obtained through the ALDM system, we compared the network obtained from the ALDM data of July 2014 to the one based on 2014 grooming behaviour (see 2.2.1 ). Since grooming is an affiliative behaviour, we used as a measure of similarity the Pearson correlation coefficient between the weights of the affiliative network (i.e., using only the positive links) and the weights of the grooming network. In addition, as it is known that the choice of the aggregation timescale can impact the characteristics of the network (see RIBEIRO, PERRA et BARONCHELLI 2013), we tested the robustness of the analysis by measuring the correlation between the affiliative and the grooming networks on various timescales, ranging from 3 to 25 days within the same period (July 1-29, 2014).

Note that, for timescales $T$ smaller than 14 days, we could define more than one observation period of such length within the period of interest (July 1-29, 2014) : we thus divided the total dataset in successive time windows of duration $T$ before building the affiliative and grooming networks, computing the correlation between their weights, and averaging over the time windows.

| Timescale (days) | Empirical value | Mean of the random distribution (90% CI) |
|---|---|---|
| 3 | 0.257 | 0.065 (0.045-0.085) |
| 5 | 0.309 | 0.066 (0.048-0.086) |
| 7 | 0.309 | 0.069 (0.047-0.091) |
| 10 | 0.396 | 0.094 (0.076-0.113) |
| 14 | 0.330 | 0.079 (0.053-0.111) |
| 18 | 0.413 | 0.105 (0.087-0.122) |
| 21 | 0.431 | 0.104 (0.085-0.123) |
| 25 | 0.389 | 0.094 (0.065-0.124) |
| 29 | 0.473 | 0.121 (0.103-0.138) |

Table 3.1. : **Pearson correlation value between grooming and co-presence networks** Pearson correlation coefficients between the grooming and co-presence networks calculated for various aggregation timescales. The last column gives the mean and 90% confidence interval of Pearson correlation coefficients computed between the co-presence affiliative network and 1000 randomized versions of the grooming network in which the baboon names were randomly reshuffled.

In addition, we compared the observed Pearson correlation to a null model based on the random reshuffling of the baboon names in the grooming network. We simulated for each time window 1000 such randomized networks and for each one we calculated the Pearson correlation coefficient with the real ALDM affiliative network. Finally, we computed the distributions of these Pearson correlation coefficients. The results (Table 3.1) show that the observed Pearson correlation was well above the $90^{th}$ percentile of the random distribution for all the timescales considered. We also observe that the correlation tends to increase for larger time windows, as also found by CLAIDIÈRE, GULLSTRAND, LATOUCHE et al. 2017, since more observational data is included and thus a more complete view of the social network is obtained.

The correlation between the grooming and ALDM networks is an overall measure of network similarity. Another well-known aspect of a social network's organisation, at an intermediate scale, is its community structure (FORTUNATO 2010). We determined the community structure of the affiliative and grooming networks using the Louvain algorithm (BLONDEL, GUILLAUME, LAMBIOTTE et al. 2008) implemented in the Gephi visualization software (www.gephi.org, see also BASTIAN, HEYMANN et JACOMY 2009). To compare the resulting partitions (see Figure 3.3), we calculated the adjusted Rand Index (ARI; RAND 1971; HUBERT et ARABIE 1985) implemented in the sklearn Python module (PEDREGOSA, VAROQUAUX, GRAMFORT et al. 2011). The Rand Index takes values between 0 and 1, with 1 indicating that the two partitions are the same and 0 corresponding to a case in which the two partitions disagree on all pairs of elements. The ARI is a version of the Rand index corrected for chance, i.e., yielding a value close to 0 when comparing two random partitions. Finally, we compared the observed

ARI value with a distribution of ARI values obtained by randomizing the community structure of the grooming network, keeping the number and size of communities fixed but reshuffling individuals among communities. We observed an ARI value of 0.23, well above the null distribution with mean −0.0001 (SD = .067), i.e., very close to 0 as expected between random partitions.

Both the results from the Pearson correlation analysis on different timescales and from the comparison between the communities structures through the Rand Index show a good accordance between the affiliative network and the grooming network, in all cases well beyond the results obtained with the null models.

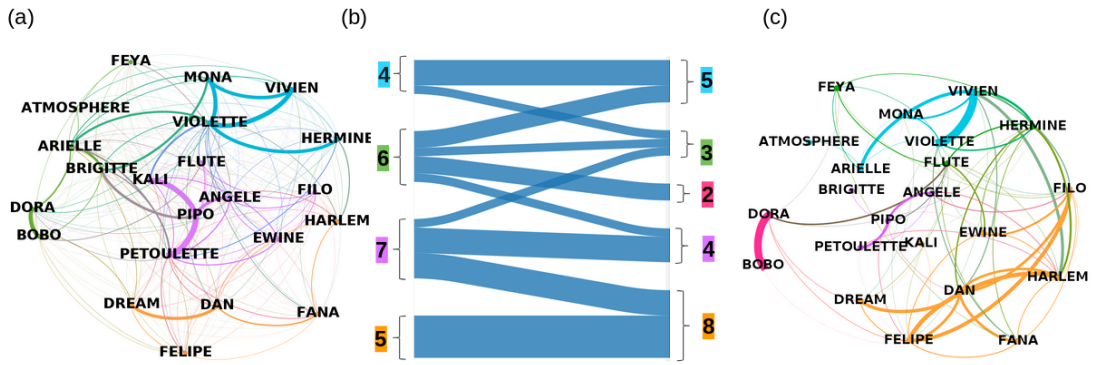


FIGURE 3.3. : **Affiliative network and grooming network.** (a) and (c) : Visualization, made using the Gephi software, of grooming (a) and affiliative (c) network of July 2014. The widths of the links are proportional to the weights of the networks (respectively number of grooming events and z-scores of the number of co-presence events), reflecting the strength of the relationships between nodes. Each colour correspond to a modularity class (i.e., a community) as assigned by the implementation (within Gephi) of the Louvain algorithm. The positions of the nodes were obtained by a Gephi layout implemented for the grooming network, and kept fixed for the affiliative network to facilitate visual comparison. (b) : Visualization of the differences in the community structures between the two networks by the flow of individuals across communities. Numbers give the community sizes and the widths of the lines are proportional to the number of individuals common to grooming and affiliative networks communities.

### 3.3.2. Wearable sensors vs Observations

In the previous chapter (section 2.5) we performed a comparison between wearable sensors data and observations, computing the number of observed events that had a correspondence in contacts data registered by wearable sensors, and vice-versa. This matching turned out to be overall very low (only $\simeq 30\%$ of the observed behaviors found a correspondent contact event registered by wearable sensors), despite many fluctuations depending on the type of behavior and the day of observation. Here we compare the networks resulting from these two datasets, both aggregating data on the whole period of investigation (static networks) and on shorter timescales.

**Static networks** Both interaction and contact networks, obtained from the aggregation over the whole period of observation (defined in subsection 3.2.4) were very dense, with respectively 70 and 78 links (in particular, the contact network is fully connected, i.e., with at least one contact registered between all pairs of individuals).

The two networks had by nature widely different weights, due to the differences in the methods of measurement. In particular, the number of observed interactions is strongly limited by the amount of time dedicated to the observation of each individual. As a result, the number of observed interactions between a given pair of individuals is at most of a few tens. On the other hand, sensors are active at all times and the weights of the contact network span several orders of magnitude, as common in such data sets (CATTUTO, BROECK, BARRAT et al. 2010). Despite these differences in the range of weights of the two networks, Figure 3.4 shows that the statistical distributions have very similar shapes.

In addition, Figure 3.5 gives a visualization of the two weighted networks in which the weights have been rescaled to have comparable widths. This figure highlights some important similarities in the structure of the strong links of both networks : relevant examples include the links Kali-Pipo (female-male) and Angele-Felipe (female-male), as well as the triad Atmosphere-Harlem-Violette (female-male-female) with two similarly strong links Atmosphere-Harlem and Harlem-Violette, and a very weak link Atmosphere-Violette.

To go further, we present in Table 3.2 a systematic comparison of the strongest links in both networks. The table reports the lists of the ten strongest links in each network. The two strongest links are the same in both networks, and more than half (6/10) of these links appear in both interaction and contacts networks. The links that are among the top ten of one network but not of the other are moreover within the top 20 strongest links of the other network, except for one. The exception is the only link between two adult males appearing in Table 3.2, namely the link BOBO-PIPO, ranked $8^{th}$ for the interaction network but only $55^{th}$ in the contact network. The interactions between adult males are usually short greetings ('presenting'), which are not face-to-face but face to rear (see the description of behaviors in table 2.1 in chapter 2), making this interaction harder for the sensors to detect. We checked that this was indeed the case for the BOBO-PIPO link, with almost only greetings and other point events (92%).

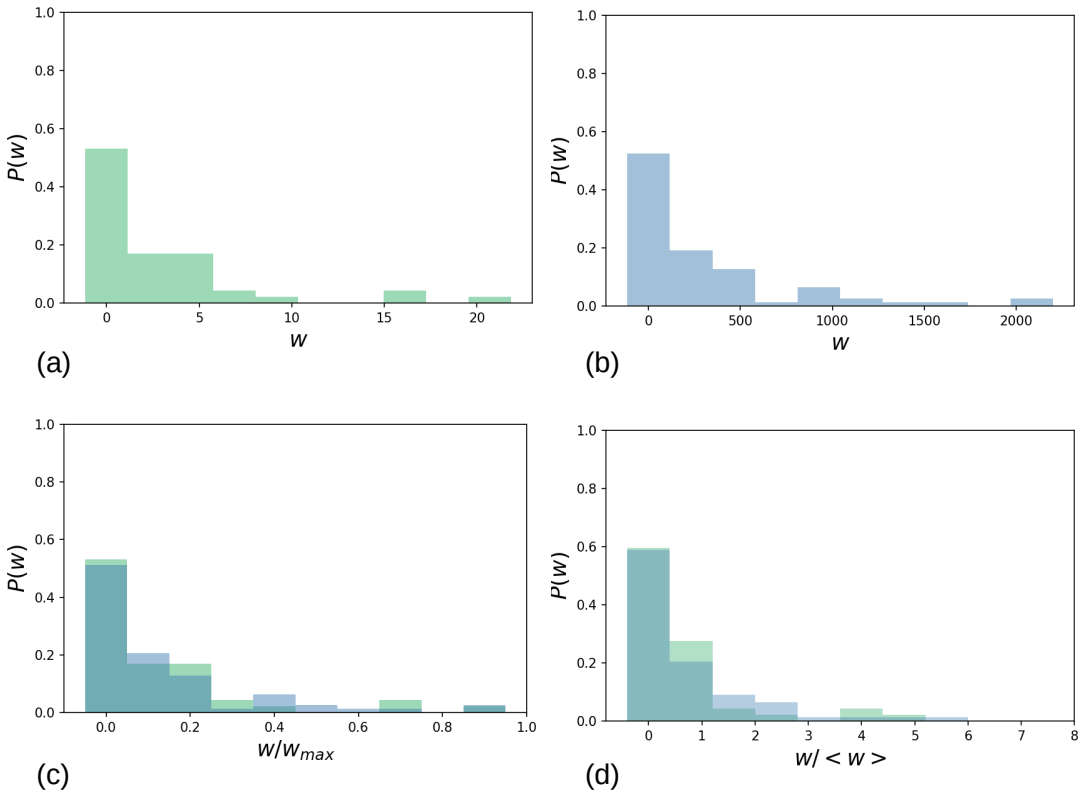


FIGURE 3.4. : **Distributions of weights.** Probability distributions of interaction (a) and contact (b) networks weights. Despite the very different values of the weights, their distributions have similar shapes. In panels (c) and (d) the same distributions are shown after rescaling the weights of each network by either the maximum weight (c) or the average weight (d).

Finally, we used four different indicators to give a quantitative estimation of the similarity between the networks. We computed the Pearson and Kendall's $\tau$ correlation coefficients between the two lists of weights to measure respectively the linear correlation and the similarity of the orderings of the weights in the two networks. We also considered two different versions of cosine similarity measures between the networks weights. A cosine similarity measure is in general defined between two vectors, and is bounded between $-1$ and $+1$. It takes the value 1 if the vectors are proportional with a positive proportionality constant, a value of $-1$ if the proportionality constant is negative, and 0 if they are perpendicular. For positive weights as in our case, it is bounded between 0 and 1. We considered first a Global Cosine Similarity (GCS) measure between the two networks as the cosine similarity between the two vectors formed by the list of all links weights in each network (using a weight 0 if a link is not

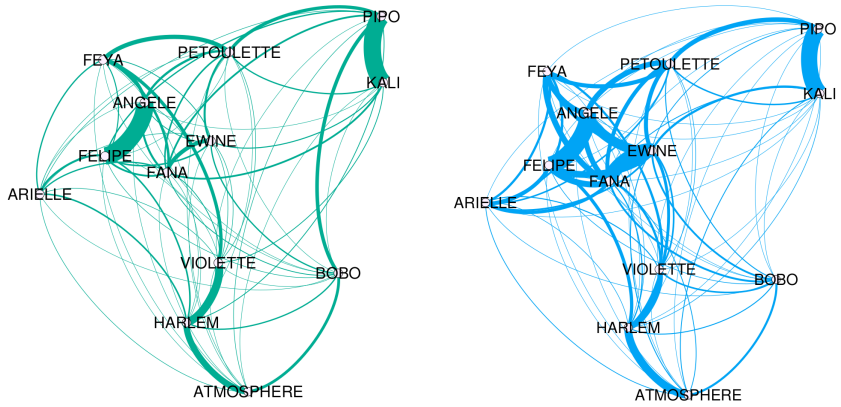


FIGURE 3.5. : **Graphs visualization.** Visualization realized with Gephi software (www.gephi.org, see also BASTIAN, HEYMANN et JACOMY 2009) of the interaction network (left) and the contact network (right), aggregated over the entire observation period. The thickness of the lines is proportional to the links weights (scaled in order to have comparable links widths in both networks). The figure shows in a qualitative way the high resemblance between the patterns of strong and weak links of the two networks.

| Rank | Interaction Network (observations) | Contacts Network (sensors data) |
|---|---|---|
| 1 | **FELIPE - ANGELE** | **FELIPE - ANGELE** |
| 2 | **KALI - PIPO** | **KALI - PIPO** |
| 3 | **VIOLETTE - HARLEM** | **FANA - EWINE** |
| 4 | **ATMOSPHERE - HARLEM** | EWINE - ANGELE |
| 5 | FEYA - PETOULETTE | **ATMOSPHERE - HARLEM** |
| 6 | **FANA - EWINE** | EWINE - FELIPE |
| 7 | PETOULETTE - PIPO | **VIOLETTE - HARLEM** |
| 8 | BOBO - PIPO | **FANA - FELIPE** |
| 9 | **FANA - FELIPE** | FANA - ANGELE |
| 10 | EWINE - PETOULETTE | FEYA - ANGELE |

Table 3.2. : **Top 10 strongest links.** For each network, links are ordered based on their weights, from the strongest to the weakest. The links in bold are the ones present in both top ten rankings.

present) :

$$GCS_{I,C} = \frac{\sum_{i>j} w_{ij}^{(I)} w_{ij}^{(C)}}{\sqrt{\sum_{i>j} \left(w_{ij}^{(I)}\right)^2} \sqrt{\sum_{i>j} \left(w_{ij}^{(C)}\right)^2}} . \tag{3.2}$$

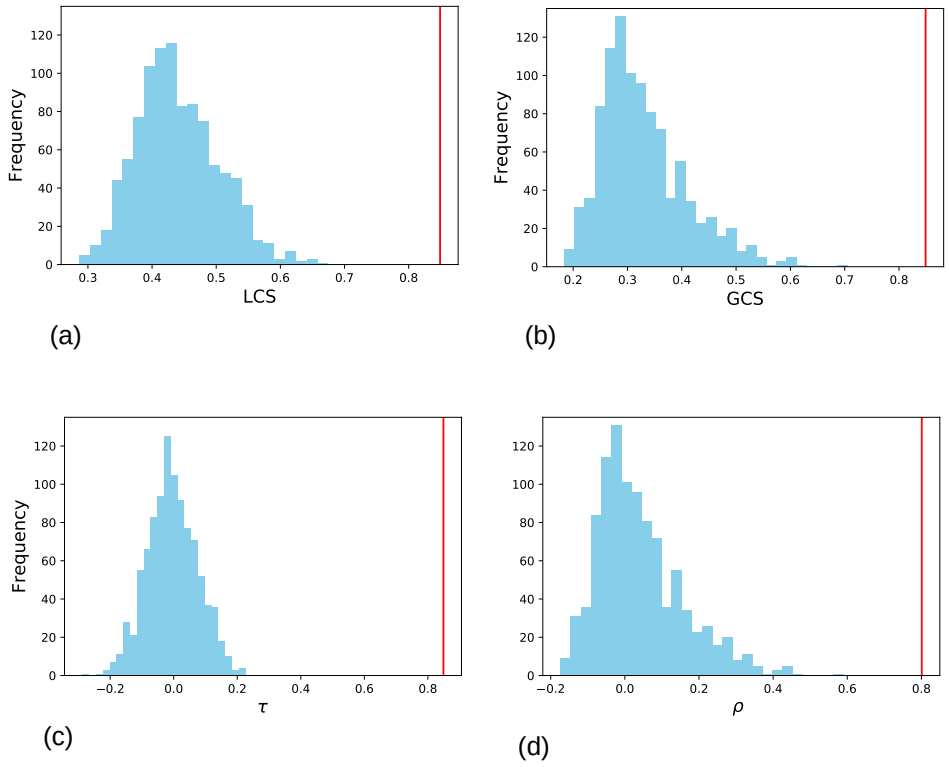


FIGURE 3.6. : **Similarity metrics.** Quantitative comparison between the contact network and the interaction network through several correlation and similarity measures. In each panel the empirical value is presented as a vertical red line, together with the distribution of 1000 values (light blue) obtained using a null model in which the weights of the contacts network were reshuffled and reassigned at random to the links. (a) average of the local cosine similarity, i.e. average of the cosine similarity between the ego-networks of single nodes (empirical value : 0.91, distribution : average = 0.44, std = 0.06) ; (b) global cosine similarity between the lists of weights of the two networks (empirical value : 0.84, distribution : average = 0.33, std = 0.08) ; (c) Kendall rank correlation coefficient between the weights of the two networks (empirical value : 0.58, distribution : average = −0.004, std = 0.080) ; (d) Pearson correlation coefficient between the weights (empirical value : 0.80, distribution : average = 0.04, std = 0.11).

We moreover considered local versions of the cosine similarity, in order to compare the two types of networks focusing on the ego-networks of single individuals, and thus investigate whether the global result is due to an homogeneity of individual patterns or to an average effect over very different outcomes. The Local Cosine Similarity (LCS) of a node $i$ is given by the cosine similarity between the vectors of weights involving $i$

in each network :

$$LCS_{I,C}(i) = \frac{\sum_j w_{ij}^{(I)} w_{ij}^{(C)}}{\sqrt{\sum_j \left(w_{ij}^{(I)}\right)^2} \sqrt{\sum_j \left(w_{ij}^{(C)}\right)^2}} . \tag{3.3}$$

$LCS_{I,C}(i)$ is thus equal to 1 if $i$ has been detected as linked with the same individuals in the two data sets with proportional weights. It is equal to 0 if $i$ has disjoints sets of neighbours in the two networks. Here we used the average LCS value over all individuals as a measure of similarity between the two networks.

To get a better grasp of the values obtained, we considered a null model in which the weights were reshuffled among the links for one of the networks.

Each indicator was computed for the two empirical networks and for 1000 realizations of the null model, obtaining a null distribution for each measure. In Figure 3.6, we show the comparison between the empirical value and the distribution of values obtained with the null model. The global and average local cosine similarity are extremely high (close to 0.9), as well as the Pearson correlation coefficient (0.83), while the Kendall rank correlation coefficient is still large (0.58) but more impacted by the large number of links with low weights, whose order is expected to be less stable than the one of the strong links. In all cases, the empirical values lie far above any value obtained in the null model realizations, as clearly seen also in Figure 3.7 where values of the local cosine similarities between ego-networks of each individual are computed.

**Temporal networks : fluctuations and convergence.** As mentioned in 3.2.4, we also considered other timescales on which to aggregate the data coming from the observations and from the sensors infrastructure. For each data set, in fact, the aggregation procedure yielding an aggregated network can be performed on any time window. Indeed, the time constraint of observational measures implies that the amount of information concerning each individual per day is relatively small. Building a reliable picture of the social bonds between individuals requires thus many days of observation and an aggregation window of one month is usually advocated (WHITEHEAD 2008; CLAIDIÈRE, GULLSTRAND, LATOUCHE et al. 2017; DAVIS, CROFOOT et FARINE 2018). In the case of data collected through wearable sensors on the other hand, a large amount of contacts is already recorded after a few hours. However, it is a priori unclear whether the structures present on short timescales such as e.g. one day of data fluctuate from day to day or are stable and already representative of the group social structure and of its strong links. Indeed, the structures present in the monthly aggregated network might result either from a superposition of different daily networks, or, on the contrary, from the repetition of the same contact network every day.

To investigate this issue, we computed aggregated interaction and contact networks over different timescales (1 day, 3 days, 1 week), obtaining in each case series of successive snapshots corresponding to the interactions observed or to the contacts measured in successive time windows. For each type of network, we computed the

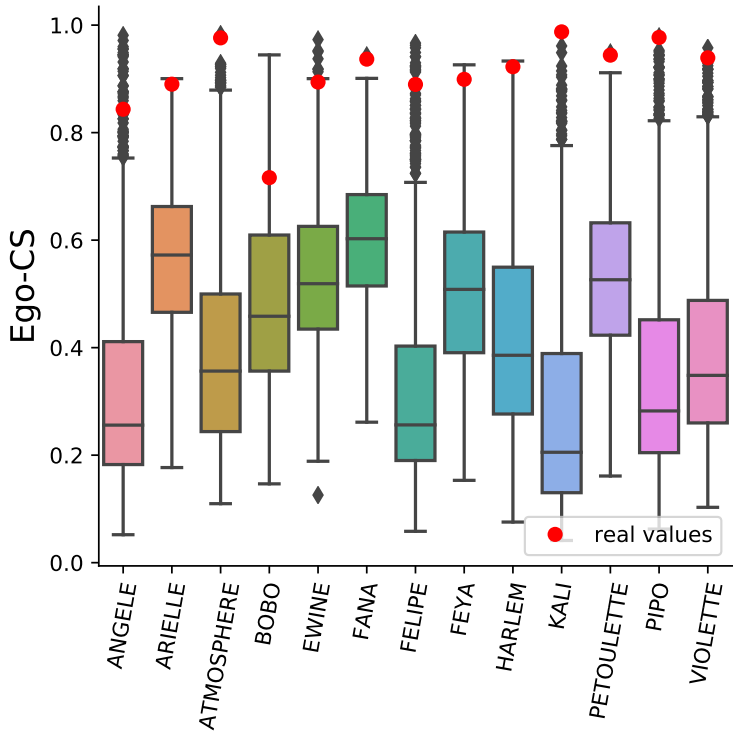


FIGURE 3.7. : **Cosine similarities between ego-networks obtained from the sensor data and from the observations.** Values of the cosine similarity between the ego-networks of each individual in the contact network and the interaction network (red dots) and distributions of the cosine similarity values obtained with the null model (boxplots, with the box going from the $25^{th}$ to the $75^{th}$ percentiles of the distributions, whiskers at the $5^{th}$ and $95^{th}$ percentiles, and outliers shown as dots).

cosine similarities (local and global) between each couple of snapshots to determine how stable networks are, once aggregated on such timescales. For instance, if we consider two different time periods $t_1$ and $t_2$, we denote by $w_{ij}^{(I,t_1)}$ and $w_{ij}^{(I,t_2)}$ the weights of the links between individual $i$ and $j$ in the interaction networks aggregated over $t_1$ and $t_2$ respectively, and the local cosine similarity of $i$ in the interaction network between $t_1$ and $t_2$ is

$$LCS_{I,t_1,t_2}(i) = \frac{\sum_j w_{ij}^{(I,t_1)} w_{ij}^{(I,t_2)}}{\sqrt{\sum_j \left(w_{ij}^{(I,t_1)}\right)^2} \sqrt{\sum_j \left(w_{ij}^{(I,t_2)}\right)^2}} . \tag{3.4}$$

We show in Figure 3.8 the resulting color-coded matrices for the average local cosine similarity : the values obtained for the interaction network are much lower than for the contact network, showing that the former fluctuates much more than the

latter. Interaction networks aggregated at daily scale are even more fluctuating (see Figure 3.9), and important differences are measured even between weekly aggregated successive networks (weekly interaction networks : min = 0.66, mean = 0.71 ; weekly contact networks : min = 0.85, mean = 0.91). On the other hand, daily networks obtained from sensor data are already quite stable.

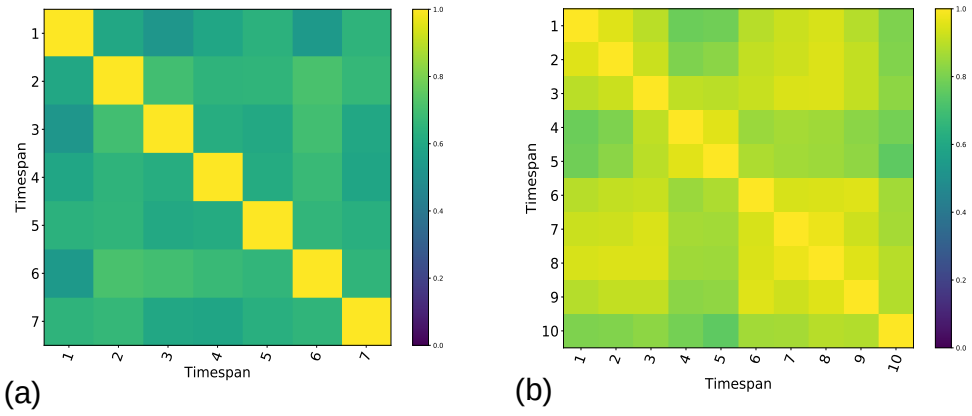


FIGURE 3.8. : **Cosine similarities between 3-days networks.** Color-coded matrices of average local cosine similarity values between every couple of 3-days (a) interaction networks (min = 0.52 ; mean = 0.63) and (b) 3-days contact networks (min = 0.75 ; mean = 0.89). A smaller number of snapshots is obtained for the interaction network because no observations were carried out during the week-ends.

We then built interaction and contact networks on time windows of increasing lengths, starting from the beginning of the observations (using only the first day of data, then the first two days and so on), and compared them with the aggregated network based on the whole observation time window. Figure 3.10 shows the resulting GCS and average LCS as a function of the length of the time window considered. The obtained similarities are already close to 1 when only one day of the sensors data is used (GCS = 0.93, Avg. LCS = 0.90), and remain at high values for longer time windows. In fact, the inset shows that similarity values rise above 0.8 as soon as about $10-12$ hours of data are collected.

Comparatively, the similarities with the final aggregated network increase much more slowly for the interaction data than for the contact data. For instance, the one-day interaction network has much smaller similarity with the monthly one (GCS = 0.68, Avg. LCS = 0.58). However, they reach very high values already after $9-10$ days of observation.

## 3.4. Beyond the aggregated approach :

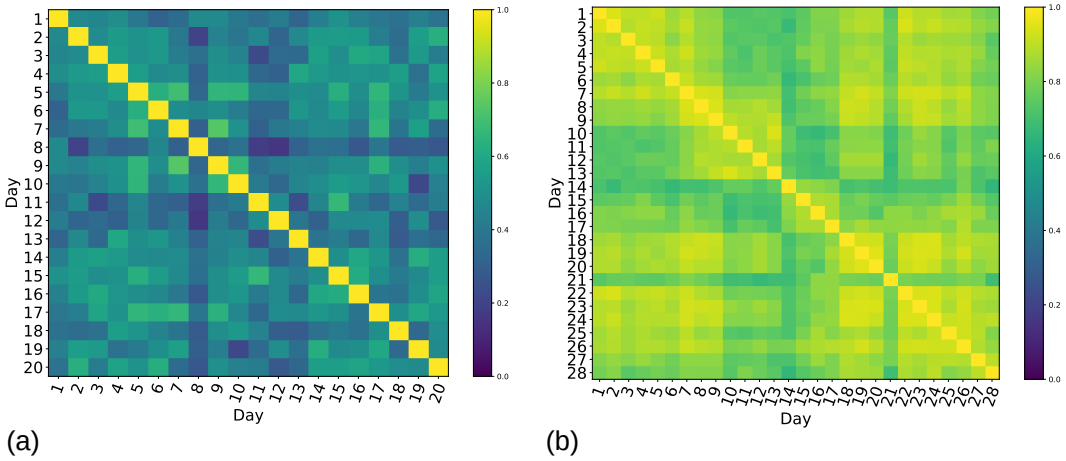


FIGURE 3.9. : **Cosine similarities between daily contact and interaction networks.** The figure represent colour-coded matrices of the average local cosine similarity values between every pair of (a) daily interaction networks (min = 0.16; mean = 0.45) and (b) daily contact networks (min = 0.66; mean = 0.83).

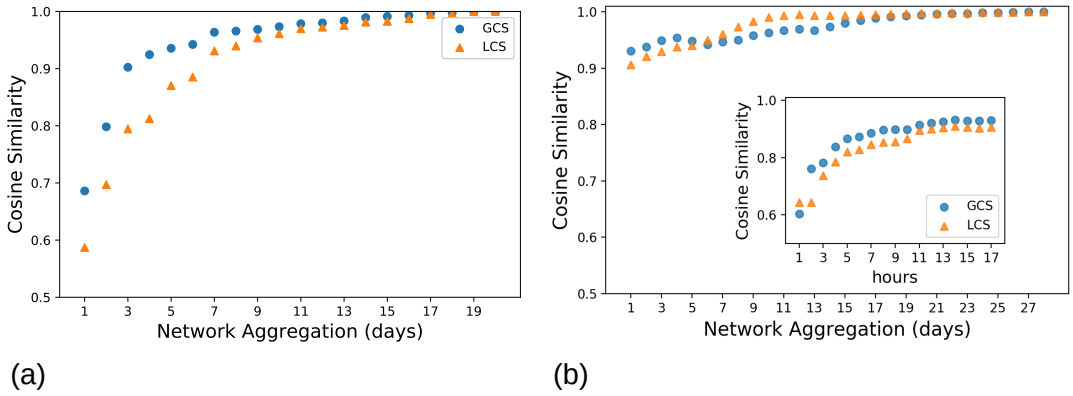


FIGURE 3.10. : **Global and average local similarities between the networks aggregated on the whole period of observation and networks aggregated on shorter time windows.** (a) : interaction networks; (b) : contact networks.

## a continuous-time framework

Social relationships are constantly evolving systems, developing over a variety of timescales (SARAMÄKI et MORO 2015). Some acquaintances are short-lived and soon replaced with new ones whereas some other friendships can flourish and last for

decades. Empirical data on social interactions (such as mobile phone communications, e-mails, letters, and face-to-face interactions...) allow to track and study the dynamics of social relationships in a variety of different contexts (MASUDA et HOLME 2019; NAVARRO, MIRITELLO, CANALES et al. 2017; HOLME et SARAMÄKI 2012; ONNELA, SARAMÄKI, HYVÖNEN et al. 2007; HIDALGO et RODRÍGUEZ-SICKERT 2008). Nevertheless, this dynamics can be bursty and irregular (BARABASI 2005; SARAMÄKI et MORO 2015). Determining the state of a relationship, establishing whether is still ongoing or not, or quantifying its strength in a given moment, is anything but trivial. Networks represent a fundamental tool to model and analyze these systems and the temporal representation of a social network (as well as other types of networks) is a challenging problem that has been receiving more and more attention in the literature (see MASUDA et HOLME 2019; HOLME 2003; HOLME et SARAMÄKI 2012; HOLME 2013; HOLME 2015).

A largely used representation of dynamic networks is a succession of graphs, each representing an aggregation over a discrete time interval of the continuous stream of interactions. In some cases the systems suggest a natural time interval (days, months), but mostly the choice of the interval is somehow arbitrary, not necessarily corresponding to any intrinsic timescale of the system. However, it could have great implications on the network structures observed and on the inferred underlying processes.

Aggregating on fixed time-windows or increasing-length time windows may not be efficient to grasp the heterogeneous underlying dynamics of social processes. In PSORAKIS, ROBERTS, REZEK et al. 2012; PSORAKIS 2013, authors examine the temporal dynamics of pairing behaviour on large-scale datasets of wild bird foraging records, showing that varying the size of a fixed time-window results in different network topologies and that there is no direct way of showing which one is the most appropriate. KRINGS, KARSAI, BERNHARDSSON et al. 2012 study the structure of networks emerging from aggregating mobile telephone call records data over time intervals of different lengths, highlighting that networks display different properties depending on the length of the time scale. Moreover, KRINGS, KARSAI, BERNHARDSSON et al. 2012 and KIVELÄ et PORTER 2015 show that the placement of the time window is also seen to affect the outcome of the network, due to inhomogeneities and burstiness of the system.

Just as importantly, aggregated approaches may result in ever-growing ties (KRINGS, KARSAI, BERNHARDSSON et al. 2012), neglecting phenomena of decaying and thus giving an unrealistic image of the social network. For these reasons, transforming a temporal network into a sensible continuously evolving representation of the social network appears to be a more appropriate solution (AHMAD, PORTER et BEGUERISSE-DÍAZ 2018; ZUO et PORTER 2019). Some frameworks represent social relationships as decaying continuously as a function of time, separating the concepts of interactions between individuals, that could have finite duration or could be instantaneous, and ties, that change continuously in time and are influenced by interactions. Already in early 2000s, JIN, GIRVAN et NEWMAN 2001 proposed a continuous-time growing network model, representing friendship strengths between people in a social net-

work. The model assumes that friendships disappear, following an exponential decay of tie strengths, if the people in question do not meet on a regular basis. More recently, AHMAD, PORTER et BEGUERISSE-DÍAZ 2018 proposed an approach for studying networks that evolve in continuous time in which ties, which represent strengths of relationships as functions of time, strengthen with repeated discrete interactions, and they decays exponentially in the absence of such interactions.

Starting from these models, in the next section we present a framework that transforms temporal network data of discretized dyadic interactions into a continuous-evolving weighted network. However, the formation and decay of social ties are not determined exclusively by individuals involved in the interactions, but also by the social patterns of their peers. We clarify that, even if it is not an actual model but rather a way to describe a dynamical system extracting social information from raw dyadic contacts data, from now on in the text we might refer to this framework using the term "model".

### 3.4.1. Construction of the temporal network : rationale and rule of update

**Rationale** Formation of strong and stable relationships play an essential role in humans and primates society both at the collective and individuals level, enhancing health and well-being (SILK 2007 ; HOLT-LUNSTAD, SMITH et LAYTON 2010).

However, previous studies demonstrate that the maintenance of these strong bonds is demanding, since it requires reciprocity, assiduity and persistence (HIDALGO et RODRÍGUEZ-SICKERT 2008 ; NAVARRO, MIRITELLO, CANALES et al. 2017). Therefore, the number of such ties is constrained by the limits that humans and other primates have, in terms of available time and cognitive capabilities (MIRITELLO, MORO, LARA et al. 2013 ; MIRITELLO, LARA, CEBRIAN et al. 2013 ; DUNBAR 1998 ; DUNBAR 2009).

The main idea underlying this new framework is thus to reproduce a continuous dynamics of relationships, identifying these limits as the mechanisms by which ties strengthen or decay.

We assume that each individual has a finite capital in terms of "attention" or available time that has to be divided among peers. Individuals interactions follow thus a strategic decision : when an individual interacts with another one, it chooses not to interact with all the others. We start constructing a temporal network so that nodes represent individuals and weights of the links between nodes, representing the strength of social ties, are updated at every event (interaction) occurred in the temporal network. As in other time-continuous networks models (AHMAD, PORTER et BEGUERISSE-DÍAZ 2018 ; JIN, GIRVAN et NEWMAN 2001), the tie between a pair of nodes depends on the history of interactions and it strengthens at every new interaction between nodes. However, the weakening of the tie between two individuals is not a consequence of time per se, as assumed in JIN, GIRVAN et NEWMAN 2001 and AHMAD, PORTER et BEGUERISSE-DÍAZ 2018, but the result of each individual interacting with others. In other words, when two individuals have a social interaction, the weight of the link

between the two increases at the expense of the relationships with other individuals. For example, an interaction of an node i with one peer j corresponds to increasing the weight of the relationship between i-j, and at the same time to a decrease in the weight of the relationships between i and any other peer k.

**Rule of update** Our framework takes as input any timestamped data stream of discrete dyadic interactions or contacts between entities or individuals, and yields a continuously-evolving weighted directed graph $G_t(\alpha, w_{max})$. The graph is characterized as follows : nodes of the network represent all individuals involved at least in one contact; weights $w_{ij}(t)$ of the links represent the strength of their social tie at time $t$ and are updated at every contact; $\alpha$ is the unique parameter of the model; $w_{max} > 0$ is the maximum value weights can assume (in our case $w_{max} = 1$ but it could priori assume any value). We start from a fully connected network with uniform weights inizialised to zero :

$$w_{ij}(0) = 0 \quad \forall i, j \tag{3.5}$$

We assume that there is an underlying continuous time, which we can measure in small increments $\delta t = 1$, and a pair of nodes can have an interaction during a time step. Nevertheless, the dynamics of the network is triggered exclusively by interactions among nodes, thus weights undergo an update only as a new interaction occur. Consequently, if at time t node i and j interact, the weight of their mutual link $w_{ij}$ ($w_{ji}$) increases, following the rule in Eq 3.6,

$$w_{ij}(t) = w_{ij}(t-1) + \alpha(w_{max} - w_{ij}(t-1)) \tag{3.6}$$

whereas the weight of the link between node $i(j)$ and any other $k$ different from $j(i)$, $w_{ik}(w_{jk})$ decreases :

$$w_{ik}(t) = w_{ik}(t-1)(1-\alpha) \tag{3.7}$$

Note that the rules defined above avoid negative weights or divergences. Nevertheless, a drawback might be the flattening of the strong weights (weights relative to couples of nodes that undergo frequent repeated interactions) towards $w_{max}$, while weak weights (those with low number of interactions) will tend to zero. As mentioned in the previous paragraph, the weight between the links of two nodes decays only if one of them has an interaction with another node, and not just as a function of time. In other words, weights change only if "something happens".

Finally, it is important to stress that while the input data are undirected, i.e. there is no *source* or *target* individuals, the network resulting from the model implementation is directed. The weight $w_{ij}$ evolves differently from $w_{ji}$ as a consequence of dynamics, opening the way for investigations on possible socially meaningful directions of the links. We will investigate on the nature of this asymmetry in subsection 3.4.3.

### 3.4.2. Dependence of the dynamics on $\alpha$ and on the timescale

In order to test the framework introduced in the previous subsection, we initially used the dataset of contacts registered by wearable sensors between baboons (see Section 2.3). In particular, this section is aimed to investigate to what extent the resulting temporal network was influenced by the parameter $\alpha$. Since weights are updated at every new interaction, we may have, in principle, a different configuration of weights (and therefore of the network) every 20s. This is in fact the time resolution of RFID sensors data. Such a short time spacing would make the visualization over long timescales almost unfeasible and would not allow the understanding of the social patterns underlying the contact data. Furthermore, contacts data embed information on social patterns at different timescales (SARAMÄKI et MORO 2015), from daily rituals (as feeding moments) to more complex expressions of social organization, as formation and consolidation of stable bonds between male and females in a unit (PATZELT, KOPP, NDAO et al. 2014; GOFFE, ZINNER et FISCHER 2016).

Visualizing pictures of the network in different moments and using different inter-observation time intervals may thus allow to "zoom" in and out over different time scales of the underlying dynamics.

Here, we show how the evolution of weights is influenced by the unique parameter $\alpha$ and how the choice of the inter-observation time interval can influence the visualization of this dynamics. In Chapter 4 we will analyse in detail the impact of these two elements in the detection of network instability. In Figure 3.11 we show the *link trajectories*, i.e. the evolution in time of the tie between two individuals, for different links, from the first day of data collection (June $11^{th}$) to November $30^{th}$ 2019, and for a wide range of values of $\alpha$, from 0.0001 to 0.5. Each subplot represents the dynamics of the weight of a given link on a weekly basis (i.e. the value of the weight at the end of each week). The 12 subplots represent the 12 links with the highest mean weight over all the considered period. These links are supposed to be the most relevant links in the dynamics of the network.

For both the timescales and time windows, we observe that different values of the parameter $\alpha$ lead to different regimes of the dynamics of weights. For very low values of $\alpha$ weights evolve very smoothly and the trajectories are almost stationary (e.g. blue line) ; for intermediate values the trajectories are still smooth but we observe non-trivial patterns of peaks and minima (e.g. green and red lines) ; finally, for high values of $\alpha$, the evolution of weights becomes noisy and bursty (e.g. grey line).

On the other hand, once the parameter $\alpha$ is fixed, in Figure 3.12 we can notice that sampling the link trajectories using different frequencies one day vs. 5-hours , influence the visualization and thus the perception of the weights dynamics. As more we shorten the time-spacing, as more jagged the weights appear, revealing the sub-dynamics which lies at different timescales. We note that the previous plots do not represent temporal networks aggregated over different time-windows, but rather pictures of the ongoing state of the network, taken with different frequencies.

We finally point out an effect of the asymmetry of the weights : in Figure 3.11 the

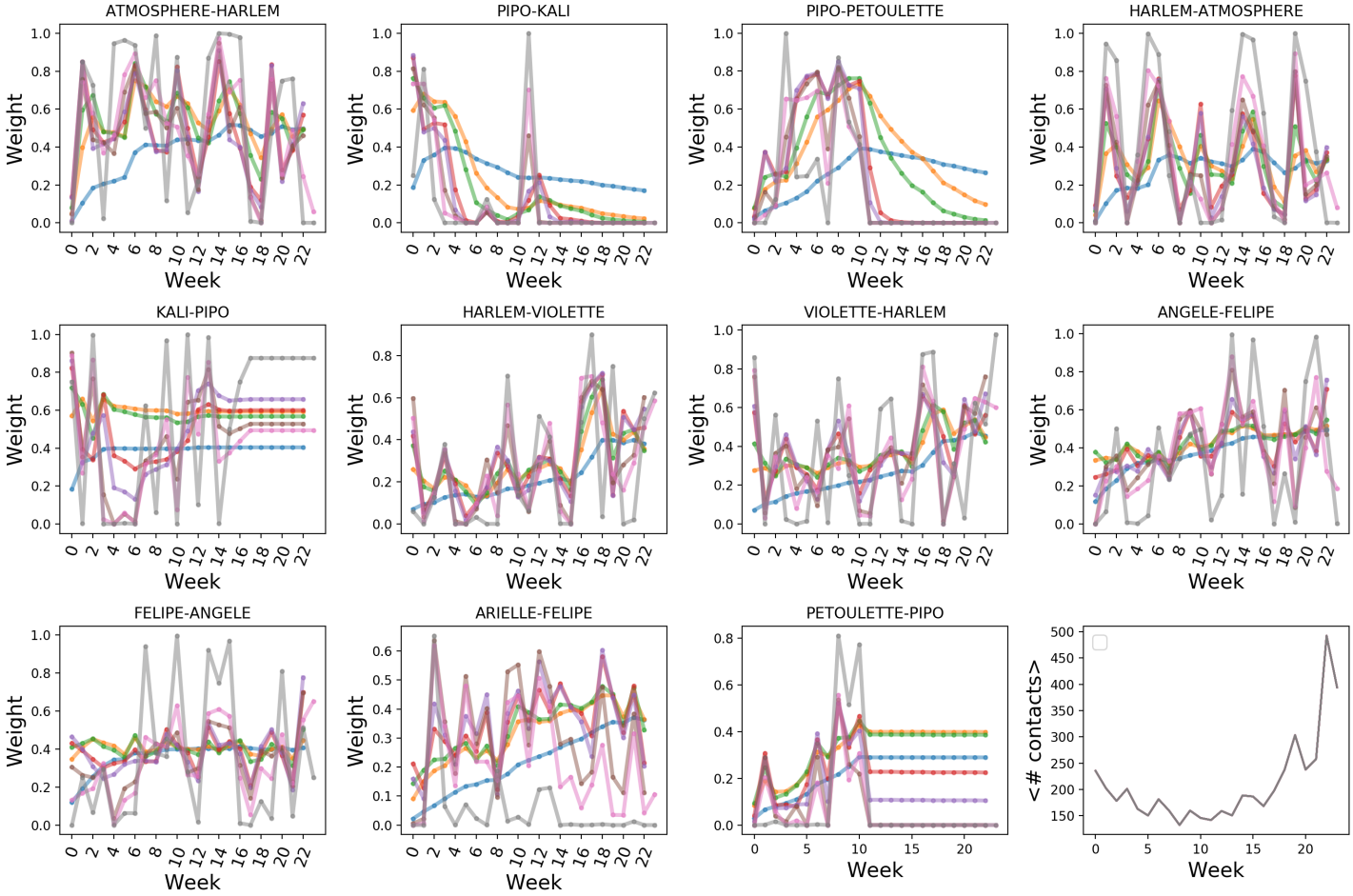


FIGURE 3.11. : **Link trajectories for different $\alpha$ on weekly basis** Each subplot of the figure represents the value of the weight of a given link at the end of each week, from June $11^{th}$ to November $30^{th}$ 2019, computed for different values of the parameter $\alpha$. Only the strongest links (which here are defined as the links with highest mean weights over the period of interest) are represented. The last subplot shows the average number of contact events per week, per couple.

link "PETOULETTE-PIPO" undergoes a sudden stop in correspondence of the $11^{th}$ week, whereas the link "PIPO-PETOULETTE" exhibit only a smooth decay. During this week, Petoulette removed its collar, and the sensor was consequently deactivated. If all the links were shown in the figure, we could notice that all the links from Petoulette towards other individuals stop evolving at the same time. Given the asymmetry of the links and noticing this synchronous stop in weights dynamics, allow thus to identify a failure of Petoulette sensor.

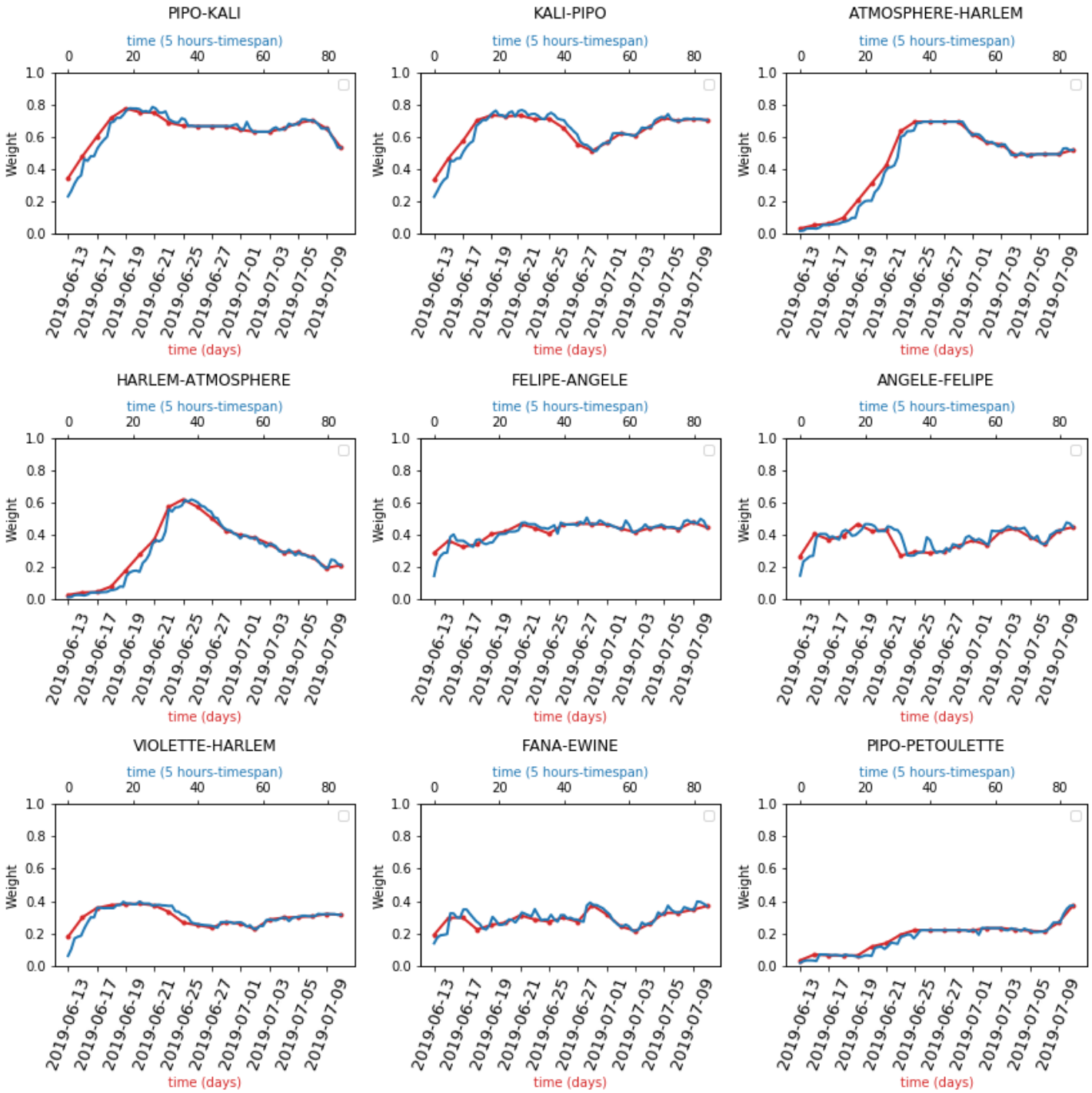


FIGURE 3.12. : **Links trajectories for the strongest links, 5-hours vs daily basis, $\alpha$ = 0.001** In each subplot, the blue line represents the value of the weight of a given link at every interval of 5 hours, whereas the red line represents the evolution of the weight on a daily basis. Trajectories are computed over the period of behavioral observations, i.e. from June $13^{th}$ to July $10^{th}$ 2019, for $\alpha = 0.001$.

### 3.4.3. Reciprocity

The model transforms streams of dyadic non-directional contacts, in a temporal directed network. This implies that, for a generic pair of nodes $i$ and $j$, $w_{ij} \neq w_{ji}$. As in the case of Pipo and Petoulette (see previous subsection), mutual links can have different evolutions and the cause of this difference may be due to the failure of a tag, to chance or to different activities of the two individuals involved. It is worth asking whether the directionality of links could give information about the nature of the relationships between the nodes. In other words, why does a link evolve differently to its mutual? Can this different evolution have a social meaning, such as the role of individuals in the social network or an imbalance in the social activity of the two individuals.

We attempted to address these questions through the study of network *reciprocity*.

Reciprocity is a theoretical concept that aims to quantify the tendency of pairs of vertices to be connected by two mutual links pointing in opposite directions (RAO et BANDYOPADHYAY 1987; WASSERMAN et FAUST 1994). Link reciprocity in binary networks (weight of a node is either 0 or 1) has been studied since the beginning of social network analysis, as it is traditionally considered as an indicator of balance or stability in social structure (RAO et BANDYOPADHYAY 1987). We deal with analysis of social stability also in Chapter 5. Moreover, many other real networks (WWW, World Trade Web, neural networks, networks of linked words..) have proven to show very different patterns of reciprocity, intended as the tendency of vertex pairs to form mutual connections between each other (GARLASCHELLI et LOFFREDO 2004). However, while in binary graphs establishing whether a link is reciprocated is trivial, that is not the case for weighted networks. The study of reciprocity of weighted networks has only recently received attention (KOVANEN, SARAMAKI et KASKI 2010; SQUARTINI, PICCIOLO, RUZZENENTI et al. 2013). Given a link $i, j$ of weight $w_{ij} > 0$ and its mutual $j, i$ with $w_{ij} > 0$, there is not a unique way to assess whether the interaction is reciprocated and measures of reciprocity can be defined at multiple levels, from the single link to the single node to the global network (SQUARTINI, PICCIOLO, RUZZENENTI et al. 2013).

We use here four different reciprocity metrics with the aim of measuring the tendency of link weights to be imbalance with respect to a symmetric situation and the the tendency of nodes to be associated with more in-strengths or out-strengths.

**Link reciprocity** Equations 3.8 and 3.9 define dyad-specific metrics, measuring deviations from a symmetric weights situation ($w_{ij} = w_{ji}$). Both metrics are defined in the interval [0,1] with the cases $r_{ij} = 1$ and $\Delta_{ij} = 0$ corresponding to symmetric weights and $r_{ij} = 0$ and $\Delta_{ij} = 1$ corresponding to a complete asymmetry, i.e. the case of a zero weight in one of the two directions. In case of $\Delta_{ij}$, the weight difference, i.e. the deviation from a symmetric situation, is normalized to take account for the fact that some relationships are overall stronger than others.

$$r_{ij} = \frac{min(w_{ij}, w_{ji})}{max(w_{ij}, w_{ji})} \tag{3.8}$$

$$\Delta_{ij} = \frac{|w_{ij} - w_{ji}|}{w_{ij} + w_{ji}} \tag{3.9}$$

**Node reciprocity** Equations 3.10 and 3.11 measure the imbalance between the in-strength and the out-strength of a node $i$. As for the links metrics, $r_i$ ranges from 0 to 1, with $r_i = 0$ corresponding to a maximum imbalanced situation (either all inward or all outward links have zero weights) and $r_i = 1$ corresponding to a node with in and out flows perfectly balanced. Contrarily from the other metrics, $\Delta_i$ ranges from $-1$ (only outward link weights) to 1 (only inward link weights). As in Equation 3.9, $\Delta_i$ takes account of the nodes heterogeneity : nodes with the same net imbalance between inwards and outwards link weights but absolute different strengths, present different $\Delta_i$.

$$r_i = \frac{min(S_{in}, S_{out})}{max(S_{in}, S_{out})} \tag{3.10}$$

$$\Delta_i = \frac{S_{in} - S_{out}}{S_{in} + S_{out}} \tag{3.11}$$

**Comparison with friendships data** We aimed to find out whether social meaningful patterns could emerge from the analysis of links reciprocity, in the evolving directed network obtained through our framework. We thus considered the datasets introduced in Section 2.6, which combines data of contacts registered by wearable sensors between students and friendship surveys data, implementing our framework on the contacts data and using surveys data as ground truth.

The surveys dataset is suitable to our purpose because it represents a directed network of friendships : a dyad "i j" exists, if an individual i declared a friendship with another individual j. In addition, the dyad "i j" is considered in the data only if j has declared other friendships. We thus defined a *mutual* friendship the case where the dataset contain both the lines "i j" and "j i". Conversely, we defined as a *non-mutual* friendship the case where the line "i j" exists but "j i" does not. Given these definitions, if we assume that the directions of the links computed with our framework from the contacts data had social meaning, we would expect links corresponding to mutual friendships to have more symmetric weights (high values of $r_{ij}$ and low values of $\Delta_{ij}$) in the network computed with our model. In contrast, links corresponding to non-mutual friendships should have more asymmetric weights (low values of $r_{ij}$ and high values of $\Delta_{ij}$).

The surveys data included 135 students ($\simeq$ 40% of the total) and 668 declarations. Among them, we counted 262 mutual friendships (declarations that were reciprocated) and 144 non-mutual friendships (non-reciprocated declarations). Since the surveys dataset was collected at the end of the period of analysis, we compared it with the weights of the network at the end of the dataset. The network obtained from the contacts data was denser than the network represented by the surveys data (11,514

edges). In fact, 88% of the declared friendships had a corresponding link in the contacts network, whereas only 5% of the contacts network was represented by the surveys data. These results are in line with MASTRANDREA, FOURNET et BARRAT 2015.

In the contact network, we found that for 17 of the links corresponding to mutual friendships ($\simeq$ 7%) and 41 of the links corresponding to non-mutual friendships ($\simeq$ 28.5%), $w_{ij} = w_{ji} = 0$. These links were therefore excluded from the analysis.

Figure 3.13 shows the distributions of the link reciprocity ($r_{ij}$ and $\Delta_{ij}$) values for both mutual and non-mutual declared friendships. Distributions show similar trend, with a general tendency of mutual weights to be symmetric (overall $r_{ij}$ shifted to high values and $\Delta_{ij}$ shifted to low values) both for mutual and for non-mutual friendships. Despite the similarity of the distributions, the average values reflect a tendency to lower symmetry for non-mutual friendships and higher symmetry for mutual friendships and the Mann Whitney tests rejects the null hypothesis of equal distributions at 5% significance level. This confirms a statistical relationship between values of the link reciprocity and mutuality (or not) of declared friendships

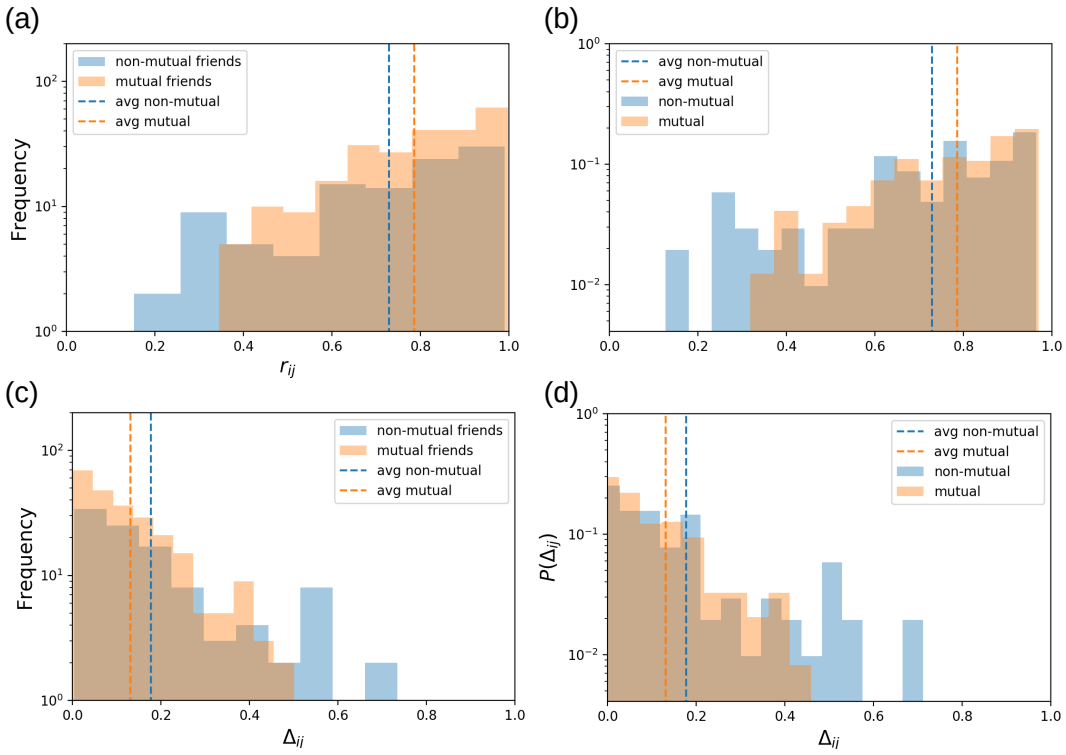


FIGURE 3.13. : **Distributions of link reciprocity measures, $\alpha$ = 0.001**. In each subplot links reciprocity values are presented, for mutual (orange) and non-mutual (blue) declared friendships. Dashed lines represent the averages. (a) Distribution of $r_{ij}$ values. (b) Probability distribution of $r_{ij}$ values. (c) Distribution of $\Delta_{ij}$ values. (d) Probability distribution of $\Delta_{ij}$ values..

## 3.5. Discussion

In this chapter we showed how we leveraged the data presented in Chapter 2 to construct and analyse different types of networks. First, we built different temporal networks using the method of aggregating into time-windows, i.e. obtaining the temporal network as a series of weighted static networks aggregated over a fixed timespan, from data concerning the group of baboons introduced in chapter 2 with the aim of studying their social dynamics. The datasets were of three different natures, namely automatically collected cognitive tests of non-human primates, behavioral observation of non-human primates and contacts registered by wearable sensors.

For the first type of data, we built a temporal network on monthly basis, based on the co-presence of individuals in the test stations. By comparing the observed co-presence to a null-model, generated under the assumption that the co-presence in neighbouring ALDM booths was due only to randomness and independent from the actual social relationships among the baboons (MANLY 1997; BEJDER, FLETCHER et BRÄGER 1998; FARINE 2017), we were able to establish a signed network representing both affiliative and avoidance relationships. This network building procedure has two main advantages. First, it takes into account the heterogeneity in the number of records of different individuals, thus reducing potential biases in the estimation of bond strength. Heterogeneity in the number of observations of individuals is a common feature of social network analysis in animals and several association coefficients have been developed to limit common biases (see e.g. WHITEHEAD 2008). Secondly, the null-model allowed us to determine both affiliative and avoidance relationships from positive interactions simply by assuming that individuals who meet more than chance are actively seeking each other's company while individuals who meet less than chance are actively avoiding each other (BEJDER, FLETCHER et BRÄGER 1998). Notably, negative interactions are more difficult to study in nature than positive interactions because they are often less evident (such as avoidance) and/or less frequent (such as open fights). Consequently, little attention has been paid to agonistic social networks. However, negative links are crucial to understand the social evolution of a group (according to social balance theory for instance, as we will discuss in Chapter 5) and using the lack of positive interactions, compared to a null-model, as an indicator of a negative relationship could therefore prove a useful general tool (ILANY, BAROCAS, KOREN et al. 2013).

Concerning the datasets of behavioral observations and of contacts registered by wearable sensors, we constructed two types of aggregated networks, both undirected and weighted, over the subgroup of individuals equipped with collars and sensors (see Section 2.3) and covering the period from June $27^{th}$ to July $10^{th}$ 2019. We moreover considered aggregations over different time-windows. We first consider as time window the whole period of observations. Interestingly, although the analysis at the single event level resulted in a limited matching between the two measurement systems (see Section 2.5), the global social structures resulting from the two networks were strikingly similar. The networks aggregated over the whole observation period turned

out to be similar as measured by several metrics : the weights of a link joining two individuals are highly correlated in the two networks, the top ranked links and the strong structures are preserved. We note that this result is at odds with the analysis of CASTLES, HEINSOHN, MARSHALL et al. 2014, in which an interaction network and a proximity network, built from the same set of direct observations of baboons, were shown to differ. However, our infrastructure detects very close proximity, which would be allowed only between animals sharing a certain level of trust, while the proximity criterion used by CASTLES, HEINSOHN, MARSHALL et al. 2014 was of 5 or 10 meters, thus not corresponding to a "contact" between individuals.

Moreover, we built aggregated networks at shorter timescales and investigated how quickly a reliable network (in this case with "reliable" network we mean a network as more similar to the network aggregated over the whole period of observations) could be obtained in each case. The observation network fluctuates strongly from day to day. It yields a very similar picture with respect to the whole observation period after about 10 days of observation. This is in agreement with recent results showing that limited amounts of observational data was enough to obtain a clear picture of the social structure of the group (DAVIS, CROFOOT et FARINE 2018). Comparatively, the structure of the aggregated network obtained with the sensors is very stable already at short timescales, and we obtain a network structure very similar to the one aggregated over one month even with only one day of data. This implies that the sensor data would potentially allow to pinpoint a change in the structure of the social network of the group on much shorter timescales than with observational data (we analyse in more detail the detection of changes in the social structure in Chapter 4). Moreover, we have actually deployed the sensors infrastructure on much longer timescales with no interruption (currently up to 6 months), while continuous observations cannot be carried out realistically on such timescales.

Furthermore, automated infrastructures are known to be prone to technical failures, with a consequent loss of data that could introduce some biases and alter the network structure. In Appendix B we tested the robustness of the sensors systems with respect to data incompleteness, simulating the failure of a reader. Both the correlation analysis and the cosine similarity between the weights of the incomplete and the complete networks proved the system to be very robust to data loss, as demonstrated also by CATTUTO, BROECK, BARRAT et al. 2010.

Despite the popularity of the aggregated approach in describing dynamically many social systems, a continuous-time approach could reveal even more effective because they take into account the fact that the influence of interactions can last far beyond the interaction itself and that ties between actors may deteriorate if relationships are not maintained (AHMAD, PORTER et BEGUERISSE-DÍAZ 2018; ZUO et PORTER 2019). We thus defined a new framework that generates a weighted, directed, continuous-evolving network, starting from any undirected stream of dyadic interactions. The model is based on the idea that a tie (weight) between two nodes reinforces if interactions between the two nodes are iterated, and deteriorates if one of the nodes interacts with other peers. The unique parameter $\alpha$ dictates the sensitivity of the weights to

every new interaction. Values of $\alpha$ too small do not allow the weights to update fast enough to detect changes in the network while high $\alpha$ produce a dynamics of the weights too sensitive to each interaction, resulting in abrupt variations and a general bursty trend.

In addition, once a value of $\alpha$ is set, the time interval used to observe the weights gives highly different pictures of the dynamics. In other words, the frequency with which we "give a peek" at the evolving weights of the network, may show us different social patterns at different scales.

Another potential interesting aspect of the model is the fact that, starting from symmetric interactions, we obtain asymmetric weights, i.e. $w_{ij} \neq w_{ji}$ for any couple of nodes i,j. We therefore investigated whether this asymmetry reflected a non-random effect of social dynamics. We first defined different reciprocity metrics to measure the level of symmetry between mutual weights, with the highest reciprocity corresponding to $w_{ij} = w_{ji}$ and the lowest reciprocity corresponding to one of the two weights equal to zero (either $w_{ij} = 0$ and $w_{ji} > 0$, or $w_{ij} > 0$ and $w_{ji} = 0$). We applied our model on the datasets of contacts between students registered by wearable sensors (see Section 2.6), and we then computed the different reciprocity measures on the weights of the final state of the network. Using as ground truth the dataset of declared friendships, we found that mutual declared friendships (a student i reported another student j as a friend and j also mentioned i) corresponded to more symmetric weights than those corresponding to non-reciprocated friendships, even if this effect was very small.

In general, this first analysis of the model suggests that extreme conditions (very low or high values) in the choice of the parameter $\alpha$ and of the time-span (very short or long time-windows), influence dramatically the picture of the social dynamics and this raises some questions. We may ask, for example, if one or more suitable values of the parameter do exist that give a reliable and readable image of the actual relationships between individuals, and if so, how to establish quantitatively whether a parameter value is more adequate than another. To address this problem, we will consider that an appropriate temporal network model associated to a suitable parameter value, should be able to react properly to changes of social structure, and thus to correctly detect instabilities and perturbations. In the next chapter we tackle this issue, implementing some methods to measure the capability of different frameworks (aggregated and time-continuous temporal networks) to detect instabilities in the network structure and thus within the social group.

# 4. Network dynamics : detection of social (in)stability

## 4.1. Introduction

Many real networks, such as social networks, change continuously over time. Describing this continuous dynamics is a challenging problem, as we mention in section 3.4. The information arising from a seamless ongoing stream of interactions can be nevertheless condensed into discrete states to uncover higher level structures in the network dynamics.

Many systems show patterns of periodicity and recurrence that can be modelled as a sequence of discrete states between which the system switches in correspondence of some change points : day-time and night time, for instance, can be treated as different macro states in many ecological and social systems. In other cases, change points may represent a collective response of the network to important events, like the loss of an individual or the breaking of a stable relationship. Such events can have serious consequences on the group social life : in primates for example, social stability can influence individuals fitness, (SILK 2007 ; SILK, BEEHNER, BERGMAN et al. 2010 ; ALBERTS 2019) offspring survival (SILK, ALBERTS et ALTMANN 2003 ; SILK, BEEHNER JACINTA, BERGMAN THORE et al. 2009) and reproduction (SCHÜLKE, BHAGAVATULA, VIGILANT et al. 2010). Detecting changes and patterns and developing models of periodicity of social networks is thus of paramount importance to understand the social life of both human and non-human animals.

Several models (MALMGREN, STOUFFER, MOTTER et al. 2008 ; VAJNA, TÓTH et KERTÉSZ 2013 ; RAGHAVAN, VER STEEG, GALSTYAN et al. 2014 ; JIANG, XIE, LI et al. 2016) defined discrete states of a network on the basis of different levels of the individuals' activity to account for long-tailed distributions of inter-event times generated by bursty patterns of human activities : MALMGREN, STOUFFER, MOTTER et al. 2008 demonstrate that the emergence of approximate power-law scaling of the inter-event time distribution in e-mail correspondence patterns is a consequence of circadian and weekly cycles of human activity ; RAGHAVAN, VER STEEG, GALSTYAN et al. 2014 develop a probabilistic model of user activity that explicitly takes into account the interaction between users and in which users transition between states are influenced by the activity of the neighbors.

More recent approaches hypothesise that the state of a networked system is encoded in the edges (i.e., pairwise interactions) of the network, rather than in the behaviour of individual nodes, and show that the network dynamics can be summarized as

a series of state changes. MASUDA et HOLME 2019 propose a method based on the combination of different analyses (namely, division of temporal network data into snapshots using aggregation approach; definition of a graph distance measure; application of a clustering algorithm to the distance matrix), to categorise aggregated temporal network snapshots at different times into groups, defining each group as a state. This method allows to represent the dynamics of the system as a succession of discrete states of the temporal network, differing from each other in internal structure, regardless of whether they have similar event rates. The network's evolution appears thus as a series of contiguous periods of relative structural stability, divided by change points or moments of instability. SUGISHITA et MASUDA 2020 apply this method to analyse evolution of air transport networks patterns from the viewpoint of recurrence. They found that the network structure of the single carriers abruptly changes from time to time, and that network change reflects actual changes occurred in the systems. However, when dealing with empirical data, underlying structure and change point are often unknown. Establishing whether and to what extent a certain network states dynamics is actually responding to a change in the system is an important issue, as well as uncovering triggering local factors that influence the network (e.g. single nodes which contribute the general instability of the network).

In the spirit of MASUDA et HOLME 2019 approach, in this chapter we use different methods to detect change points and instabilities emerging from temporal network dynamics, testing them directly on empirical data of different nature. We then study these patterns for two main purposes : (i) to link network changes at global scale to instability patterns at level of single nodes, (ii) to study to what extent the procedure used to compute the temporal network from the data influences the detectability of the network change points.

In section 4.2 we deal with the first point, analysing the (in)stability of the monthly aggregated co-presence network computed using the ALDM cognitive tests data (see section 3.2.1). We use quantitative similarity measures to compare static networks built in different periods. This procedure allow us to investigate the rearrangements of the network at various scales. It is indeed possible to measure the similarity at the scale of the whole network but also at more detailed levels such as subgroups or for each single individual, identifying individuals whose pattern was more affected by rearrangements than others. We highlight in particular how the local ego-network of some individuals could be completely altered while others were left unchanged, with only partial rearrangements of the overall social network. Notably, some of the periods of interest and rearrangements of the ego-network of some individuals revealed by the analysis were confirmed by external observations.

In section 4.3, we instead tackle the issue (ii), focusing on the continuous-time framework defined in section 3.4 for different values of the parameter $\alpha$ and comparing it with different aggregated representations, in order to estimate its ability to detect perturbations in a social system. The analysis is carried out on datasets concerning different systems, i.e. the group of baboons under study during this PhD and humans, to investigate whether some parameters or approaches are generally suitable

regardless of the system or instead if they are system-specific. To better distinguish significant changes from mere noise, and to have a ground truth for assessing the performances of the networks, we simulate a change in the group social structure. As in the first section, we first use similarity measures to compare the networks over all pairs of times $t, t'$ (once a timescale is chosen) and then, similarly to MASUDA et HOLME 2019 and SUGISHITA et MASUDA 2020, we apply different clustering algorithms to group different periods in "meso-states".

Our analysis aims to be a method not only to detect instabilities and change points in network's dynamics, but also to provide a benchmark for evaluating qualitatively the performance of different temporal networks representations.

## 4.2. Aggregated approach : (In)stability of affiliative co-presence network

As we mention in section 2.4, the group of baboons under study changed in composition and size over the time. In this section, we refer to the period between January 2014 and May 2017 during which ALDM cognitive tests data on a total of 29 individuals were collected. During this years the size of the group varied from 19 to 24 individuals with a monthly average size of $\simeq 22$, because of several births and natural deaths, as well as the composition in terms of males and females (7.3 [7;9] males and 14.4 [12;17] females (mean [min ; max]),) and age of individuals (ranging from 0 to 21 years old). This evolution of the group characteristics naturally led to rearrangements of the social structure over time. Here we analyse the dynamics of the monthly aggregated co-presence network presented in section 3.2.1, and in particular the resulting affiliative network, to detect periods of (in)stability of the network itself. We aimed in fact to pinpoint periods during which the social ties undergo some important rearrangements, which are supposed to be encoded in the weights dynamics.

Our method consisted in measuring the similarity between monthly network snapshots using the local cosine similarity measure, which we calculated for every individual and for every pair of months. The cosine similarity values at the group level (averaged over all individuals) are shown in Figure 4.1(a). The figure clearly shows that the average cosine similarity between different months remained very high in certain periods (yellow blocks along the diagonal). For instance, the average of the values obtained between two different months between January and July 2014 was 0.794 (SD = 0.07). The average of the values over different months taken between September 2014 and May 2015 was 0.784 (SD = 0.054). These examples are shown as blocks 1 and 2 in Figure 4.1(b). Such large values of the average cosine similarity between different months imply that the ego-networks of the individuals did not change much, and therefore highlight periods of high network stability.

On the other hand, at some moments the average cosine similarity between successive months was lower, such as between July and September 2014 ($CS = 0.577$) and between July and September 2015 ($CS = 0.65$). These lower values indicate that

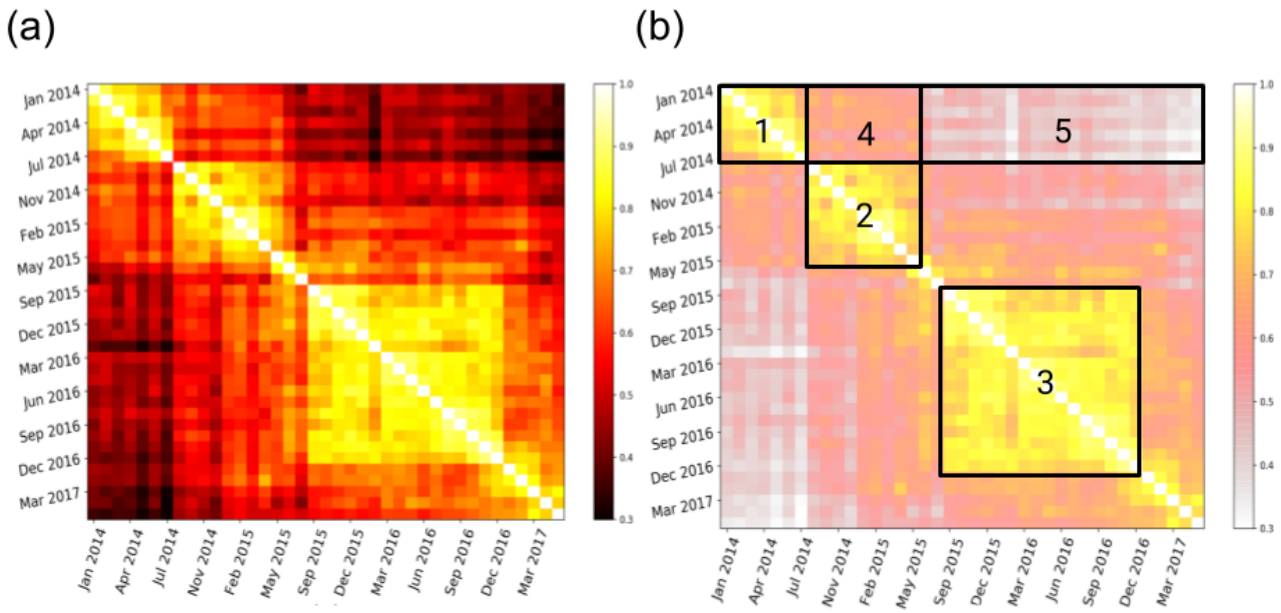


FIGURE 4.1. : **Dynamics of the social network at the group level.** (a) : Colour-coded matrix of the average cosine similarity values for all pairs of months. Several periods of strong structural stability clearly appear as blocks of lighter (yellow-white) colour. In contrast, the average CS between July and September 2014 was 0.577, and the one between July and and September 2015 was 0.65. (b) : the same matrix is represented with highlighted periods of particular interest. The principal periods of stability are shown as block 1 (January-July 2014 : the average of the average CS values, excluding the diagonal, was 0.794, SD = 0.07), block 2 (September 2014-May 2015 : average of values 0.784, SD = 0.054), and block 3 (September 2015-December 2016 : average of values 0.814, SD = 0.044). Note that values tended to be progressively smaller away from the diagonal, i.e. for months separated by longer and longer times. For example, the block 4, which represents the average CS values between the periods January-July 2014 and September 2014-May 2015, had a mean of 0.61 and a SD = 0.045, while in block 5, between January-July 2014 and September 2015-December 2016, the mean value was 0.454 and a SD = 0.047.

the networks in those cases differed between the successive months, i.e., that some social network rearrangements took place, suggesting potential periods of network instability.

We also note that the average cosine similarity values tended to be progressively

lower away from the diagonal, i.e. for months separated by longer and longer times. For instance, the block 4 in Figure 4.1(b) corresponds to all pairs of months $(t_1, t_2)$ with $t_1$ between January and July 2014 and $t_2$ between September 2014 and May 2015 : the average of the values within this block was 0.61 (SD = 0.045). When considering instead block 5 in Figure 4.1(b), which corresponds to comparing a month in the period January-July 2014 to a month between September 2015 and December 2016, the average of the cosine similarity values was 0.454 (SD = 0.047). This is consistent with the fact that the social network became more and more different, and did not come back to a previous structure during the period of study.

Figure 4.2 sheds more light into these two types of periods by presenting the distributions of individual cosine similarity values for two periods corresponding to high and low group level similarity. When the similarity is high (Figure 4.2(a)), the distribution is highly skewed with most individual's cosine similarity values close to 1. This shows that the network global stability was the result of the stability at the individual's level. In contrast, when the average similarity is lower (Figure 4.2(b)), the distribution of the individual cosine similarity values is broader with some individuals maintaining their ego-network (large value of the cosine similarity) while others changed dramatically (cosine similarity values close to 0). This implies that the instability of the network was not a global one but that some parts of the network remained stable while others underwent important changes.

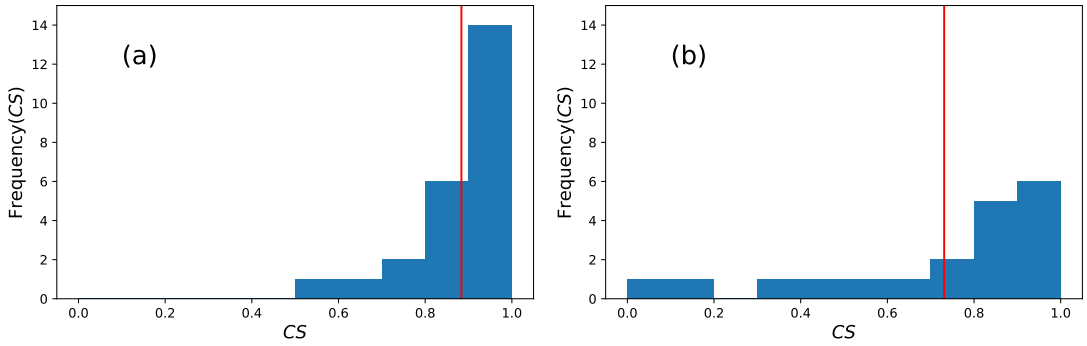


FIGURE 4.2. : **Ego-network dynamics.** Histograms of individual's cosine similarity values between weighted ego-networks for two different pairs of successive months : (a) April 2014, May 2014; (b) April 2015, May 2015. For each panel, the histogram corresponds to the cosine similarity values of all the ego-networks of the individuals present in both months. The vertical line gives the average value of the cosine similarity (i.e., the value shown in Fig. 4.1a), that correspond to 0.884 and 0.731 for April 2014, May 2014 and for April 2015, May 2015 respectively.

In order to better understand the network's dynamic, we studied the evolution of ego-networks independently. Figure 4.3 shows the cosine similarity between the ego-networks of specific individuals in successive months. The resulting patterns differed

greatly between individuals. For instance, as can be seen in Figure 4.3(a), Vivien (adult male) and Angele (adult female) had on average high cosine similarity values over the entire study (0.96 and 0.95 respectively), showing prevalently a strong stability of their ego-networks. However, such average values hide an interesting pattern : in a synchronized way, these two baboons went through a strong rearrangement of their ego-networks, between July and September 2014, with cosine similarity values of respectively 0.23 and 0.01. Both individuals had thus very stable ego-networks before and after this period, but their ego-networks between the first and second stability periods differed strongly. In particular, between these two periods Angele lost her strong link with Pipo (adult male), the links between Vivien and most of his females became much weaker, and a strong link between Angele and Vivien appeared. On the other hand, both individuals kept a stable ego-network during other structural changes observed in the matrix of Figure 4.1(a), such as between March and June 2015 : this highlights once again, as deduced also from Figure 4.2(b), that a low average cosine similarity between two different months can be the result of a large variation of some ego-networks while others remain completely unchanged. Figure 4.3(b) shows that other individuals went through very different patterns of ego-network stability and instability : some kept a relatively stable ego-network throughout the whole period, with only small changes (for instance, Petoulette, adult female, in Figure 4.3(b)), and some had much more important and frequent changes in their local ego-network (such as Brigitte, adult female).

Finally, we sought to analyse in more details the important change in the network between July and September 2014 (see Figure 4.1(a)). Indeed, the average cosine similarity between these months was equal to 0.577, while the average between May and July was 0.779, and 0.845 between September and November 2014. As already discussed above, these average values hide a heterogeneous amount of local rearrangements, as shown by the distributions of Figure 4.2. Figure 4.4 shows a visualization of the affiliative networks in these months, as well as the flux of individuals between communities obtained by the Louvain algorithm. The ARI (Adjusted Rand Index; RAND 1971; HUBERT et ARABIE 1985, see also section 3.3.1) between the resulting partitions in July and September was equal to 0.16, while it was equal to 0.67 between the partitions in communities of the September and November networks and to 0.41 between partitions in communities of May and July networks.

The visualization reveals several important changes in the network :

- Angele moved from a community to another. The strong link with Pipo disappeared and a new strong link with Vivien emerged ;
- Links between Vivien and other females of his community weakened as the link with Angele abruptly became very strong ;
- The number of individuals went from 23 to 22 because Grim was removed from the group for a medical reason unrelated to the experiment.

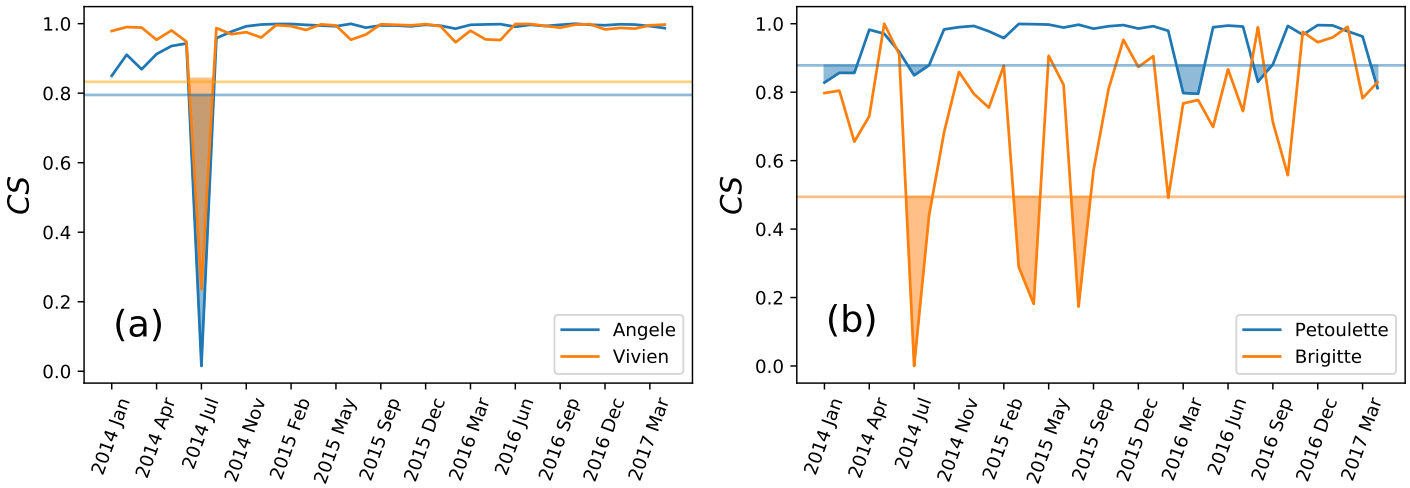


FIGURE 4.3. : **Dynamics of ego-networks.** Evolution of ego-network cosine similarity values computed between one month and the next for several individuals ($CS_i(t, t+1)$ for each month $t$). The lines give for each individual the average of its cosine similarity value over time, minus one standard deviation. The filled areas correspond therefore to very unstable periods, i.e. to periods where the ego-network cosine similarity between successive months are more than a standard deviation below the average. The two individuals in panel (a) showed a stable ego-network overall (Vivien : mean = 0.96, SD = 0.12 ; Angele : mean = 0.95, SD = 0.15) but displayed a sudden and synchronized change between July and September 2014. The two individuals in panel (b) had very different patterns of ego-network stability and instability both in terms of variability of values (Petoulette : mean = 0.94, SD = 0.12 ; Brigitte : mean = 0.71, SD = 0.06) and in terms of (absence of) synchronization : for instance in August 2016 we note that while Brigitte's trajectory has a local maximum (0.93), Petoulette's trajectory undergo a local minimum (0.83).

The two first points are clearly related to the synchronization in the timelines of Figure 4.3(a). The visualization also makes clear how certain parts of the network were on the contrary quite stable between these months, as discussed above in relation to Figure 4.2(b).

Note that all these points were deduced only from the study of the affiliative network built from the proximity in ALDM booths, without any external knowledge. Interestingly, it turned out that direct annotations of observations of the group in the period of the summer 2014 confirmed that two important changes occurred in July 2014, namely : (i) Grim died and (ii) Angele changed primary male during that month.

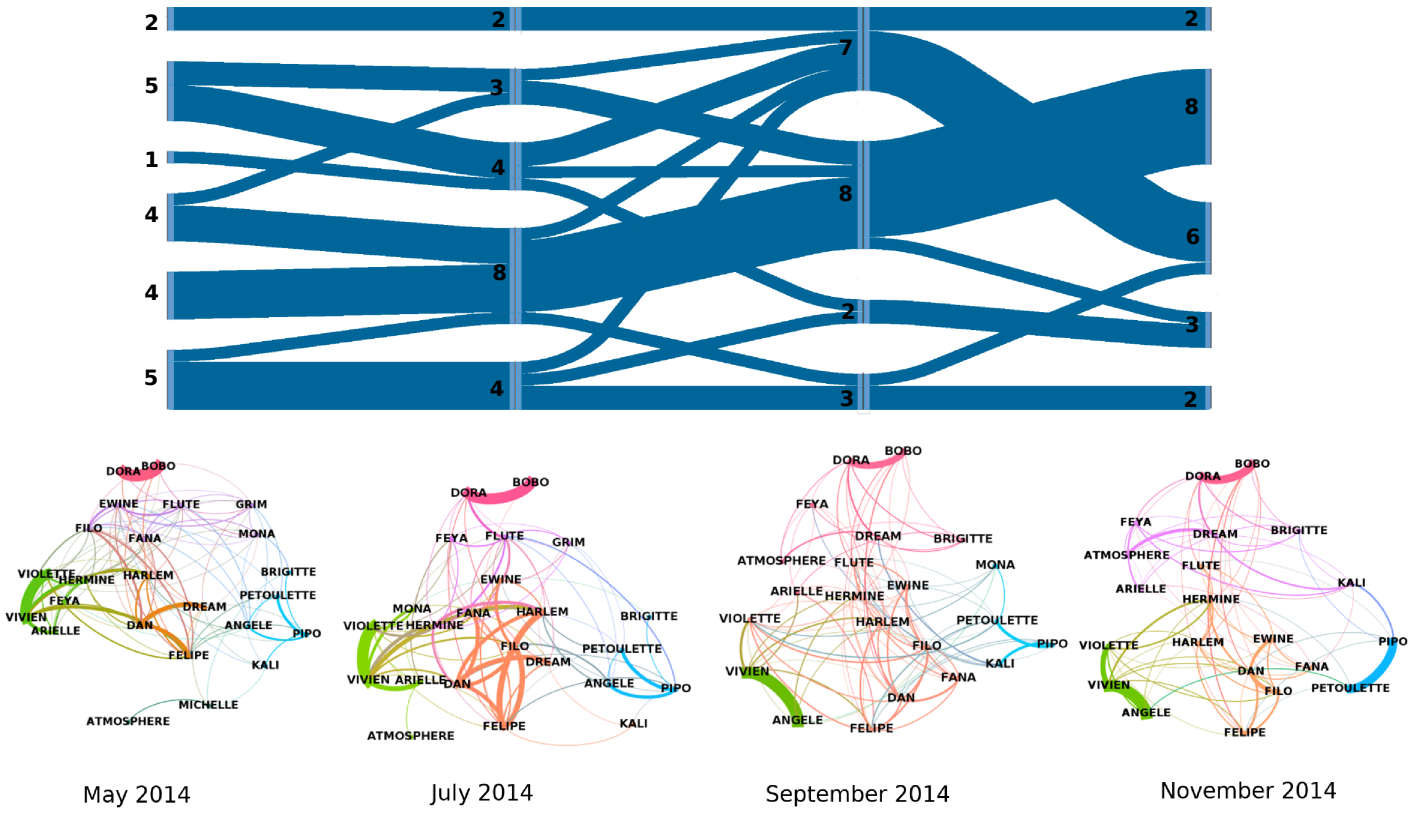


FIGURE 4.4. : **Visualization of the co-presence networks and of the flow between communities across the months of May, July, September and November 2014.** Different colours in the graphs correspond to different communities. In he flow diagram, the numbers specify the community size and the widths of the lines are proportional to the number of individuals common to the communities joined by the lines.

## 4.3. Time-continuous model : perturbations

In the previous chapter (see section 3.4.2), we presented a new framework that allows to represent a sequence of pairwise interactions in a temporal network with time-dependent weights that evolve at each interaction. The sensitivity of the framework, i.e. the rate at which weights increase or decrease at every new interaction, is modulated by a unique parameter $\alpha$, which determines the way the network reacts to the underlying dynamics of the system, and thus to its changes. The choice of the value of this parameter is therefore crucial to construct a network that allows to interpret the evolution of social relationships. We now may ask : is there a unique "best choice" for the value of $\alpha$ or rather are various values suitable for representing a given system? Does a range of values of $\alpha$ exist, that is universally adequate for social systems of different natures? Given the higher computational cost of the framework with respect to aggregating in time-windows, is our framework actually better than aggregated

approaches in representing the social dynamics? In this section we define a method to evaluate the effectiveness of different temporal network, representing the same temporally resolved data, to uncover the underlying social dynamics. This effectiveness is measured based on the capability of the network to detect perturbations or significant changes. In our case, we are interested to compare several representations of the network resulting from our framework, each corresponding to a different choice of the value of parameter $\alpha$. Once set the time window (which in case of our framework determines the frequency at which we visualize network snapshots), we use two types of aggregated temporal networks as possible baselines : (i) a network computed aggregating contacts over each time window and (ii) a network computed aggregating contacts over an increasing number of time windows (at t=1 we aggregate only contacts $\in [0,1]$ ; at t=2 only contacts $\in [0,2]$ and so on). This method will allow us not only to assess the choice of a parameter $\alpha$, but also to compare the performance of our framework with that of aggregated approaches. Our assumption is that a proper temporal network should be able to detect changes in the social structure, in particular to detect them promptly (without delays) and clearly, i.e. significant and informative social changes have to be distinguished from the noise represented by "ordinary" social activity. However, to verify whether or not a significant structural change actually occurred, one needs ground truth data or external information (e.g. surveys, direct observations, reports), which are not always accessible. As a work-around, we simulated temporary perturbations in the social group of interest, switching the identity of two or more individuals for a period $\Delta t$ and we then verified for which $\alpha$ and for which aggregated approach the perturbation is better detected. In the section below we present the method, based on the clustering analysis associated with the use of validation indices, and the results obtained with two different datasets are shown, namely : contacts registered by wearable sensors on baboons (presented in section 2.3) and contacts between students (presented in section 2.6).

### 4.3.1. Method

MASUDA et HOLME 2019 implemented a procedure to detect the state dynamics of an aggregated temporal network from pairwise interactions data, that we may summarize in three steps : i. transforming the data stream into a temporal network as a sequence of static networks, i.e., snapshots ; ii. Measuring the distance between all pairs of snapshot networks. iii. Run a hierarchical clustering algorithm on the distance matrix to categorise the snapshots into discrete states. Our method follows a similar approach but at the same time it moves beyond, aiming to compare different network representations on the basis of their capability to better detect the system states. The flow of the analysis is schematically shown in Figure 4.5.

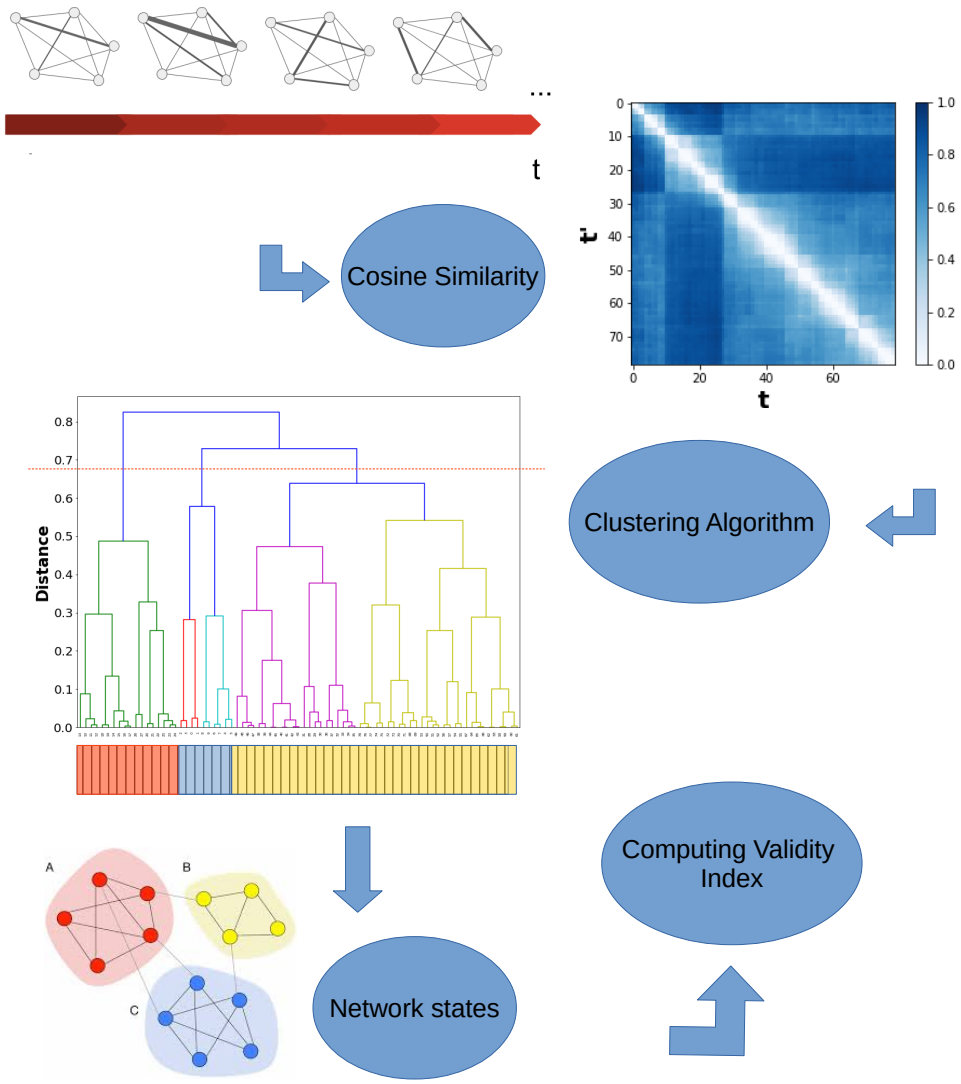


FIGURE 4.5. : **Workflow for defining discrete states and detecting perturbations of temporal networks.** Once both the time resolution and the framework to compute temporal network are set (if we use our continuous-time framework, we have to choose a value of the parameter $\alpha$, otherwise if we use an aggregated approach we can choose either a fixed or an increasing time-window), we obtain a sequence of network snapshots. Then, the cosine similarity is computed between each pair of snapshots $(t, t')$. The distance matrix is obtained from the cosine simlarity matrix as $d(t,t') = 1 - CS(t,t')$. A hierarchical clustering (or k-means) algorithm is run on the distance matrix, where each cluster represent a state and the time sequence of the states is thus obtained. A perturbation is said to be well detected if one of the states includes all snapshots concerned in the perturbation itself and only those. A validity index (silhouette or others) is finally computed to assess the quality of the clustering configuration. This procedure is repeated for different representations of the temporal network (different values of $\alpha$ or aggregated approaches).

Considering empirical data describing pairwise interactions in discrete time, we first fake a significant change in the group's social structure by switching the identity of 2 or more individuals in the data at a certain time $t_0$. Moreover, we impose this "perturbed" state of the network to last for a certain interval of time $\Delta t$. This way, we provide a simulated state that will be used as ground truth to assess whether the discrete states resulting from our method actually reflect the system dynamics. Then, we compute a temporal network based on the modified data, using aggregated or continuous-time approaches, and once defined a timescale, network snapshots are obtained. As in section 4.2, we compute a $t_{max} \times t_{max}$ matrix in which each entry is the global cosine similarity between each pair of snapshots $(t, t')$. The visualisation of the matrix can give a first insight on whether the network correctly detected the simulated perturbation and thus the underlying social dynamics. The more the temporal network matches with the actual dynamics of the system, the more recognizable the discrete states are in the matrix. In particular, if the perturbation is significant enough, we should be able to distinguish a block of side $\Delta t$ around the diagonal in correspondence of $t_0$, similarly to the block-wise structure identified in Figure 4.1(b), where block 2 was formed in correspondence of a significant rearrangement of the social structure. To obtain discrete system states we have to assign each snapshot a label. We then first transformed the cosine similarity matrix in a distance or dissimilarity matrix defining $d(t, t') = 1 - CS(t, t')$ as the distance between each pair of snapshots. We finally used different clustering algorithms, namely hierarchical clustering and k-means, to group snapshots in clusters that represent the discrete states of the network.

**Clustering methods** For the hierarchical clustering, we used the function "fcluster" of the *scipy.cluster.hierarchy* library from the SciPy module in Python. The function can be applied directly on the $t_{max}$x$t_{max}$ distance matrix. To define the distance between clusters, we used the "average" method in the "linkage" function of the library. The hierarchical clustering provides a set of partitions of the network snapshots into states, represented by a dendrogram, where the number of states $C$ ranges between 1 and $t_{max}$. When the correct partition is unknown, there are several methods to chose the number or states. For the sake of completeness, we note that generally one validates a partition focusing on internal characteristics of the clustered data and measuring the compactness and separation of the clusters (ARBELAITZ, GURRUTXAGA, MUGUERZA et al. 2013). A conventional procedure is in fact to adopt the value of $C$ that maximizes some validity index. We may assume that the dendrogram allows to pinpoint a hierarchy of dynamics over different scales, in which the greater the number of the clusters, the more complex and enriched is the description of the dynamics, with the possibility to detect also minor changes. The utility of the validation index is therefore usually to set a tradeoff between a too synthetic description of the dynamics and an excess of information. We may compare the validity index to a technique for preventing underfitting, i.e. the inability of a model capture the underlying structure of the data, or overfitting, i.e. extracting superfluous information (i.e. noise) from the data as if that variation represented underlying significative structure. However, here

we use validity indices not, as conventionally, with the aim of determining the number of states $C$, but rather to measure the capability of different ways of representing the data as networks to detect changes. We present them in more detail below. Going back to the choice of $C$, our interest is to assess whether the main significant change was detected in the network, i.e. the one we simulated, filtering out the "secondary dynamics" and the potential noise. We thus set $C = 3$, assuming to have a correct detection if the algorithm clusters the network snapshots so that the three states correspond to the phases of pre-perturbation, perturbed and "back-to-normality". The same argument is applied when using the k-means cluster algorithm. In this case we used the "KMeans" function from sklearn in Python, which however requires as input the datapoints instead of the matrix of distances. We thus used The Multi Dimensional Scaling (MDS) method to get inferred data points from a distance matrix. MDS is a technique to seek low-dimensional representation of the data in which the distances respect well the distances in the original high-dimensional space and it is implemented in Python as a function of the "sklearn.manifold" class.

**Validity indices : assessing partition quality** Once obtained the discrete states, assuming the clustering method to have well detected the perturbation (grouping the network snapshots so to have a unique cluster corresponding to the perturbation), we need to evaluate "quality" of the partition, in order to compare which network representation is more appropriate to describe the system dynamics. We thus assign the partition a validity index and we regard it as an assessment of the temporal network. We considered different indices reported in literature, namely Silhouette index, Calinski-Harabasz (CH) index and Dunn index. The silhouette measures how close each point in one cluster is to points in the neighboring clusters and is defined by

$$s(i) = \frac{b(i) - a(i)}{\max\{a(i), b(i)\}}$$

where $a(i)$ is the mean distance between $i$ and all other data points in the same cluster and $b(i)$ is the smallest mean distance of $i$ to all points in any other cluster, of which $i$ is not a member. It takes values in [-1, 1], where a silhouette value near to 1 indicates that the point is far away from the neighboring clusters and thus it is well matched to its own cluster and poorly matched to neighboring clusters. Low or negative values indicate that the point might have been assigned to the wrong cluster. The silhouette score is implemented in Python as "sklearn.metrics.silhouette_score" accepting as input a distance matrix, associated with a clustering method that provides a partition.

The Calinski-Harabasz Index (CALIŃSKI et JA 1974) is defined as the ratio of the between-clusters dispersion mean and the within-cluster dispersion and is implemented in the Python module "sklearn.metrics".

The Dunn index includes a family of indices (DUNN 1973) defined by

$$DI_m = \frac{\min\limits_{1 \leqslant i < j \leqslant m} \delta(C_i, C_j)}{\max\limits_{1 \leqslant k \leqslant m} \Delta_k}.$$

Based on how the inter-cluster distance $\delta(C_i, C_j)$ and the diameter of a cluster $\Delta(C_k)$ are defined, we obtain in fact a different formulation of the index. To compute the Dunn index we used the function implemented in the GitHub repository (*dunn-sklearn.py*), where combinations of different methods are implemented both to compute the inter-cluster distance ('nearest' or 'farthest' for the distances between the two nearest or farthest points in each cluster) and the diameter of a cluster ('mean_cluster' for the mean distance between all elements in each cluster, or 'farthest' for the distance between the two points furthest from each other).

We repeated this workflow for each of the network representations, i.e. our framework for different values of the parameter $\alpha$, and the aggregated temporal networks with the two different approaches cited above. The representation assigned with the higher index is assumed to be the one that better detected the perturbation and thus that better represents the system dynamics.

### 4.3.2. Baboons data

Here we apply the method described above to contacts data between baboons concerning the period between June $13^{th}$ and July $10^{th}$ 2019 (see section 2.3). These contacts data involve a subset of the whole baboons group, i.e. the 13 individuals collared with RFID sensors, and were collected concurrently with behavioral observation data. In the previous chapter (see section 3.3.2) we already presented different temporal network representation of these data, aggregating contacts over different timescales. Then, in section 3.4 we presented a time-continuous temporal network representation as a possible suitable alternative to the aggregated approach, noting that the image of the dynamics provided by this framework is heavily influenced by the choice of the value of its unique parameter $\alpha$. Here we assess, through the method described in the previous section, the more suitable approach and the most suitable value(s) of $\alpha$ to describe the social dynamics underlying the baboons contacts data.

Figure 4.6 shows matrices of global cosine similarity between network snapshots computed for all couple of times, using a daily time resolution, taking some values of the parameter $\alpha$ of different order of magnitude ((a), (b), (c) correspond to $\alpha$ equal to 0.0001, 0.001 and 0.01 respectively) and for the two types of aggregation ((d), (e)), i.e. with a fix daily time-window and an increasing time-window, that is, aggregating on the [0,t] period. The perturbation consisted in the switch of two adult males id for $\Delta t$=3 days, from July $1^{st}$ to July $4^{th}$ 2019. The 2 individuals were involved overall in the 34% of the total interactions. The matrices show qualitatively that the detection of the perturbed period depends on the value of the parameter $\alpha$ and on the type of aggregation. In particular, the cases of very low values of $\alpha$ (0.0001) and of the increasing time-window result in a very flat and stable dynamics (all the pairs of time

frames are extremely similar). For higher values of $\alpha$ and for the case of fixed time-window aggregation we observe that the dynamics of the network starts to emerge. Not only the simulated perturbation is distinguishable, but also several different sub-structures of the network dynamics. In the case of the fixed time-window this pattern appears even noisy. Panel (f) shows the values of the average silhouette index resulting from the hierarchical clustering analysis, setting the number of clusters equal to 3, both for the networks computed with our framework for different values of $\alpha$ and for the aggregated representation with fixed time window. The plot compares the ability of different representations to detect the perturbation. Our framework appears to detect the perturbation for several values of $\alpha$, with silhouette values that range from 0.2 ($\alpha = 0.2$) to 0.5 ($\alpha = 0.003$) and it yields a quantitatively better detection (higher silhouette value) with respect to the aggregated approach (0.38) for 2 values of $\alpha$, i.e. 0.003 and 0.005. The silhouette value concerning the aggregated network with increasing time window does not appear in the panel since it did not detect the perturbation.

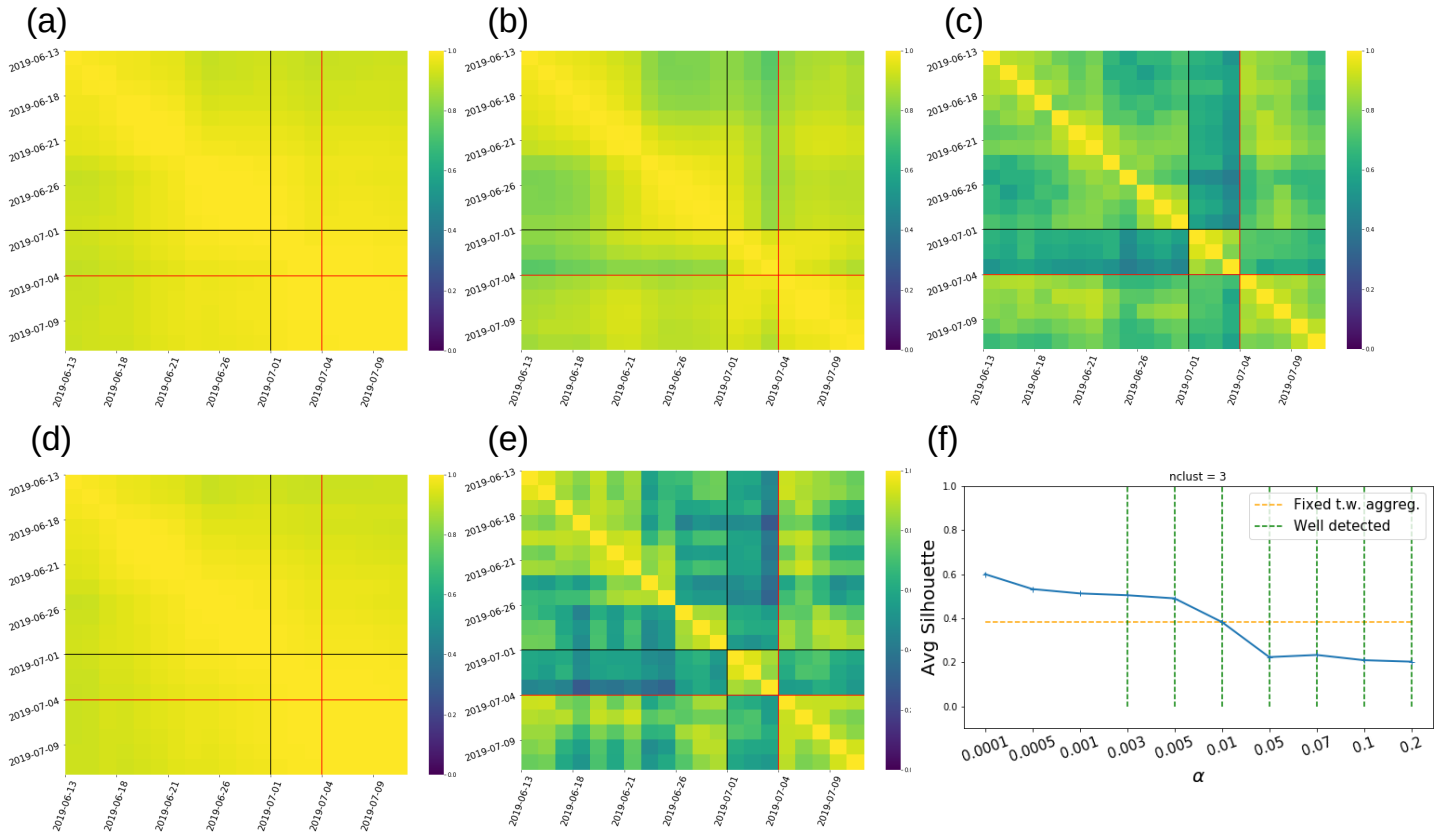


FIGURE 4.6. : **Comparison between various network representations in response to a simulated perturbation on baboons contact data (i.e. exchange of two nodes' id in the network for $\Delta t$ = 3 days and $t_0$ = 2019-07-01)** The entries of the matrices in (a), (b), (c), (d), (e) represent the values of global cosine similarity between all possible couple of network snapshots relative to different days (d,d') for several temporal network representations. In particular, (a), (b), (c) are the representations obtained with our framework, using different values of the parameter $\alpha$ (0.0001, 0.001 and 0.01, respectively) ; panels (d), (e) concern the two aggregated representations, using an increasing time windows [0,d], and a fixed daily time window, respectively. Black and red lines correspond to the time of the beginning and of the end perturbation, respectively. (f) : Average silhouette values over all data points, resulting from the hierarchical clustering analysis applied to the matrices, with the number of clusters $C = 3$. The value measures the ability of our framework to detect perturbations, for different values of $\alpha$, and for the one of the two aggregated representations that succeeded in detecting the perturbation. Green vertical dashed lines correspond to the values of $\alpha$ for which the perturbation is well detected, i.e. the clustering algorithm classified the snapshots corresponding to $\Delta t$ as a single (perturbed) state on its own ($0.2 \lessapprox avg.silh \lessapprox 0.5$ ). For the other values of $\alpha$, the clustering algorithm failed in identify the perturbation as a separate state, therefore even in the values of the silhouette may be high, they refer to "incorrect" partitions. Orange horizontal dashed line correspond to the result of the clustering obtained with the fixed time window aggregated network (avg.silh. = 0.38). For $\alpha = 0.003$ and 0.005, our framework yield thus a quantitatively better detection of the perturbation than the aggregated network.

Figure 4.7 shows the robustness of the results obtained with the silhouette index and the hierarchical clustering analysis with respect to a different clustering method, i.e. k-means, and different validity indices, i.e. CH index and Dunn index. All the panels show that our framework show a better capability to compute the discrete states of the network, in particular in a range of values of $\alpha$ between 0.003 and 0.01.

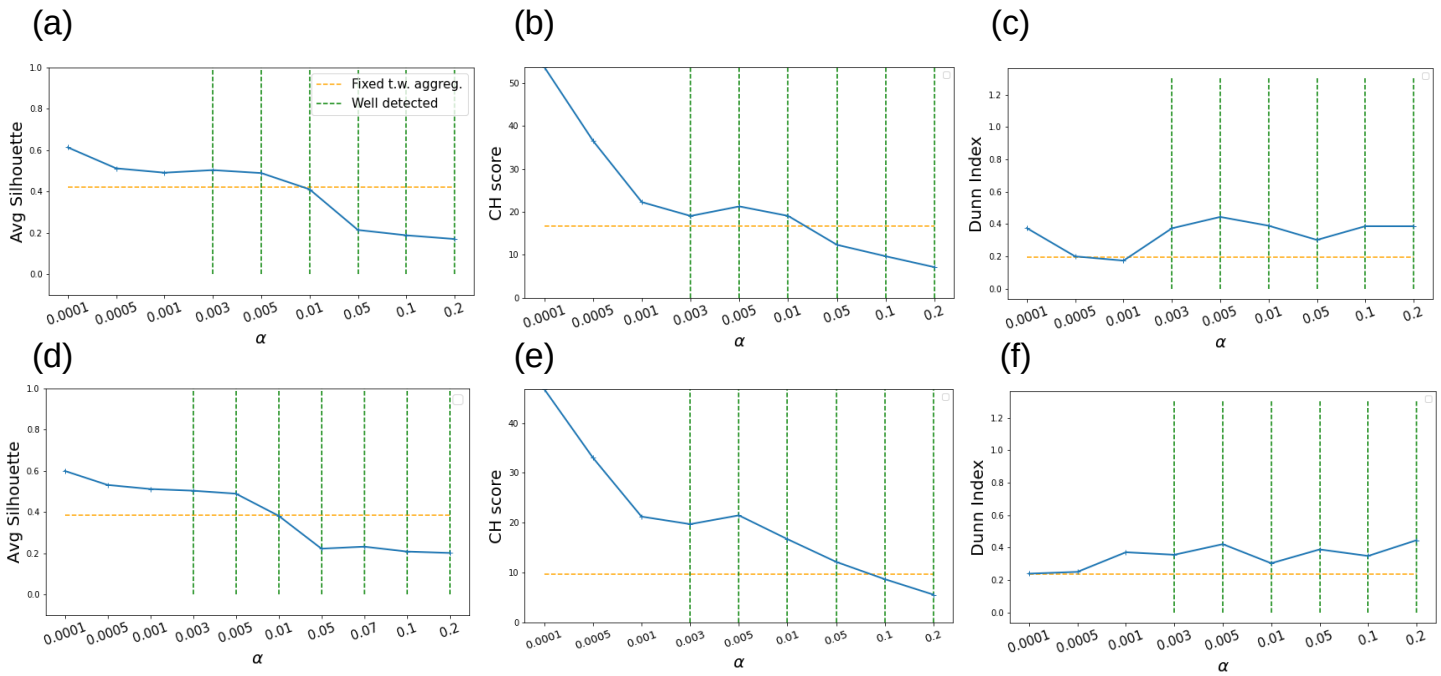


FIGURE 4.7. : **Combinations of clustering analyses and validity indices for evaluating the response of the network to the simulated perturbation (see Figure 4.6).** Each panel represent values of a validity index, associated to a clustering method : the v.i. evaluate the "quality" of the partition computed by the corresponding clustering method, and thus gives a qualitative estimation of detection of the perturbation for different values of the parameter $\alpha$ (in case the network was computed with our framework), and for the aggregated network (dashed horizontal orange line). As for Figure 4.6(f), green vertical dashed lines correspond to the values of $\alpha$ for which the perturbation is well detected, i.e. the clustering algorithm classified the snapshots corresponding the perturbation as a single state. For the other values of $\alpha$, the clustering algorithm failed in identify the perturbation as a separate state, therefore even in the values of the silhouette may be high, they refer to a wrong partitions. We note that in (c) and (e) the values of the Dunn Index represent the mean values between different methods adopted for computing both the inter-cluster distance and the diameter of a cluster. Only the aggregation with fixed time window is showed because is the only case in which the perturbation was detected. In particular, for panels (a), (b), (c) we used the k-means method to infer the clustering configuration, whereas for panels (d), (e), (f) we used hierarchical clustering. For both methods, the number of clusters was set to 3. For $\alpha = 0.003$ and $\alpha = 0.005$, the model always outperforms the aggregated approach.

### 4.3.3. Students data

In this section we refer to contacts data between students introduced in section 2.6. We are here interested in testing the generality of the previous results (that there is a range of values of $\alpha$ for which our models outperforms aggregation in detecting perturbations of the system). We therefore consider a completely different dataset, concerning human interactions. As the previous one, this dataset contains face-to-face proximity interactions between individuals. The data concern a group of students (in total 327), belonging to different classes (each class with a different specialization), in a high school in Marseilles, France and were collected by MASTRANDREA, FOURNET et BARRAT 2015 for 5 days in December 2013. Here we show analogue analyses, carried out using the same procedures, as those obtained in the the previous section, in this case referred to the dataset of contacts between students. Nonetheless, we note that the scale of this system is different with respect of that of baboons data. First, the data collection lasted for only few days and the social dynamics of a school fluctuates strongly throughout the day, punctuated by specific daily patterns such as class breaks and lunches. In this case we thus chose a shorter temporal resolution of the order of the hours. Moreover, the higher number of nodes required the perturbation to be re-sized to have a comparable impact on the network structure, therefore instead of simply switching 2 individuals, we reshuffled the identities of an entire group of individuals.

Figure 4.8 (analogue to the Figure 4.6), shows the matrices of global cosine similarities between perturbed network snapshots, using a time resolution of 0.5 hours, for different network representations. The simulated perturbation consisted in reshuffling the identities of the 10% most active individuals, i.e. individuals associated to the highest numbers of interactions, for the entire second day of data collection (2013-12-03). Overall, the individuals were involved in 39% of the interactions occurred during the entire period of interest, we can thus regard the scale of the perturbation as comparable to that performed in the case of the baboons dataset (in the previous section we showed that the 2 switched individuals were involved and 34% of all interactions). Panels (a), (b), (c) concern the networks computed with the continuous-time framework, using $\alpha$ equal to 0.0001, 0.01 and 0.1, respectively. Panels (d) and (e) concern the two types of aggregated networks, namely with increasing time-window [0,t] and with fixed time-window. Differently from baboons data, the matrices show block-wise patterns that reflect the multi-scaled dynamics of the underlying system. For relatively high values of $\alpha$ (0.01 and 0.1), the pattern of the 3 discrete macro-states corresponding to the simulated perturbation, overlaps with the underlying dynamics of the system at different scales (the dynamics we would have observed if we had not added the simulated perturbation). We can distinguish in fact the transition of the systems from the non-perturbed to perturbed state (switch of individuals identities) and the second transition in which individuals are re-assigned with their original identities. Figure 4.8(f) shows the average silhouette plot for each network representation, referring to clusters configurations obtained using the hierarchical clustering algorithm. The

panel reveals that our representation performs a better detection of the perturbation for multiple values of $\alpha$ (avg. silhouette = 0.48 for $\alpha = 0.01$ ; 0.31 for $\alpha = 0.05$ ; 0.38 for $\alpha = 0.1$) with respect to the fixed time-window aggregation (avg. silhouette = 0.23).

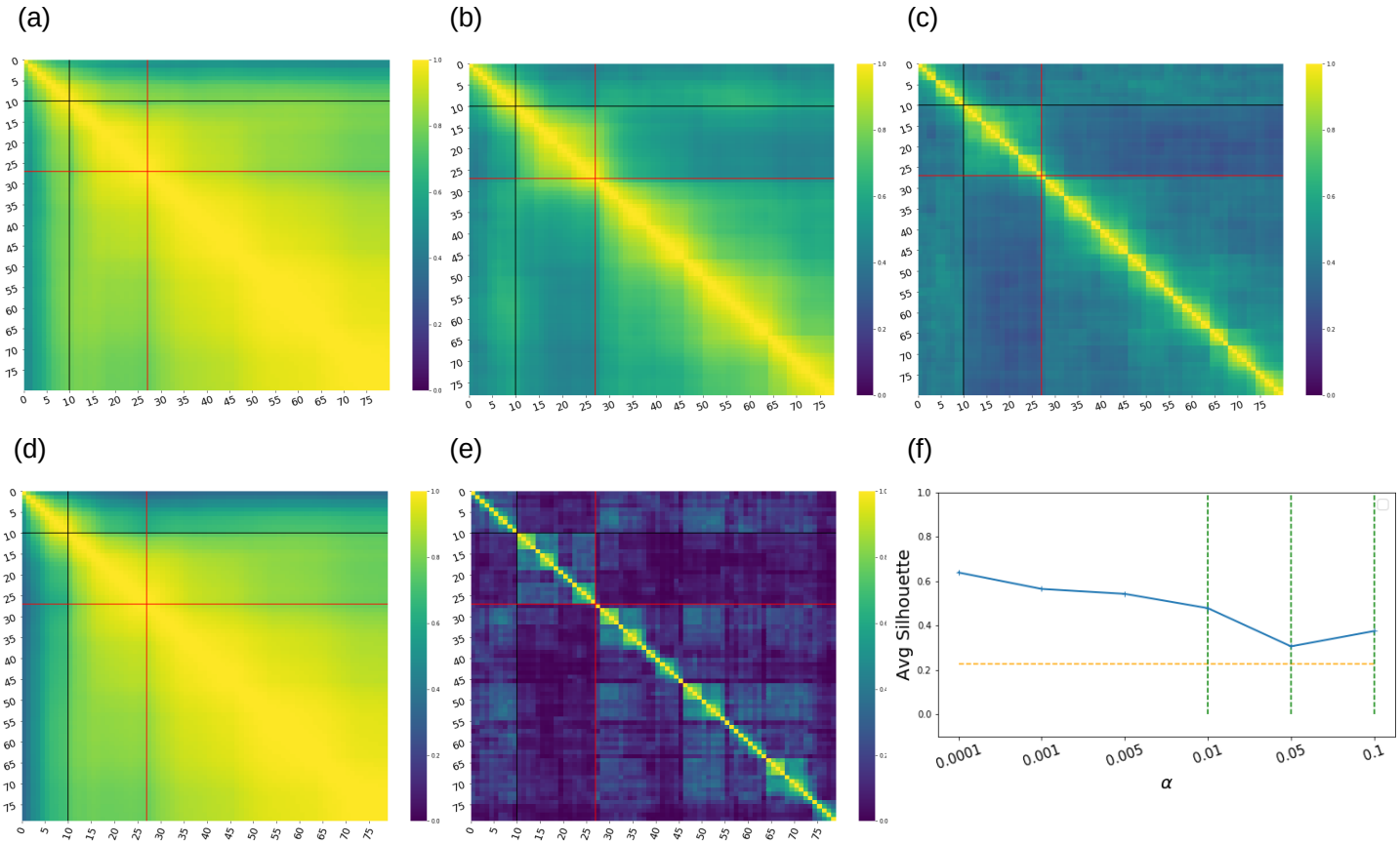


FIGURE 4.8. : **Comparison between various network representations in response to a simulated perturbation on students contact data.** The entries of the matrices in (a), (b), (c), (d), (e) represent the values of global cosine similarity between all couples of network snapshots (t,t') for several temporal network representations, using a time resolution of 0.5 hours. The simulated perturbation consisted in re-shuffling the identities of the 32 (10%) most active individuals (i.e. involved in highest numbers of interactions) for the entire $2^{nd}$ day of data collection 2013-12-03 (in this case, $\Delta t = 17$ snapshots of 0.5 hours, covering a time period from 8am to 17pm). Panels (a), (b), (c) concern the representations obtained with our framework, using different values of the parameter $\alpha$ (0.0001, 0.01 and 0.1, respectively) ; panels (d), (e) concern the two aggregated representations, using an increasing time windows [0,t], and a fixed time window of 0.5h. Black and red lines correspond to the time of the beginning and of the end perturbation, respectively. (f) : Average silhouette values over all data points, resulting from the hierarchical clustering analysis applied to the matrices, with the number of clusters $C = 3$. Green dashed lines correspond to the values of $\alpha$ for which the perturbation is well detected, while for all other values of $\alpha$ the silhouette, even if higher, the cluster algorithm that failed to detect the perturbation (network snapshots were incorrectly grouped). The orange horizontal dashed line corresponds to the silhouette relative to the aggregated network with the fixed time window. The silhouette relative to the aggregated representation with increasing time windows is not showed here, since it failed to detect the perturbation.

Similarly as for the analysis on baboons data, Figure 4.9 report the plots of all combinations of each of the three validity indices associated to each clustering method. All the panels show that our time-continuous framework performs a better detection with respect to the aggregated approach. Notably, the range of $\alpha$ for which the perturbation is detected $(0.01 - 0.1)$ appears to be shifted of about an order of magnitude with respect to the case of baboons data, suggesting that suitable parameters $\alpha$ are related to specific characteristics of the system under consideration.

In the Appendix (see Figure A.1) we provide some partial confirmation of this argument, showing that the range of suitable $\alpha$ remains almost stable, given a system, changing both the time and the individuals involved in the perturbation.

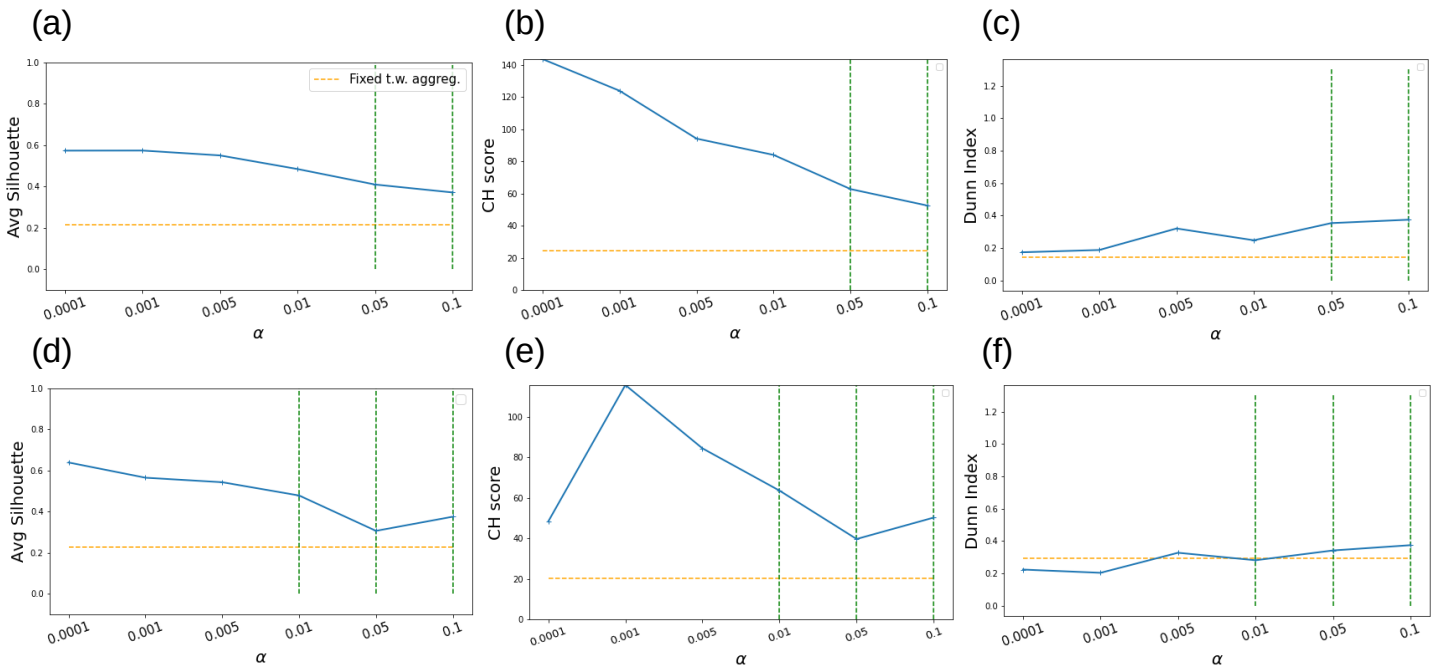


FIGURE 4.9. : **Combinations of clustering analyses and validity indices for evaluating the response of the network to the simulated perturbation (see Figure 4.8)** Each panel shows the plot of a validity index values associated to a clustering method, estimating the detection of the perturbation for different values of the parameter $\alpha$, and for the aggregated network (analogue of Figure 4.7 and Figure 4.8(f)). For all the combinations, the model outperforms the aggregated network in a range of $\alpha \in [0.01, 0.05, 0.1]$

.

## 4.4. Conclusion

In this chapter we have analysed the patterns of (in)stability of different networks, computed on different empirical datasets, both using an aggregated and a time-continuous approach.

We first considered the monthly aggregated affiliative co-presence network compu-

ted from cognitive tests data and we studied the social network's dynamics using the cosine similarity between the affiliative ego-networks in successive months, comparing networks across two different scales, i.e. single individuals and the entire network. This analysis represents a first illustration that CS is a useful measure to detect change points in a temporal network. Indeed, the group averaged cosine similarity value allowed us to visualize periods of global stability, and to identify moments of instability (Figure 4.1(a)). More detailed investigation of the cosine similarity values showed that the periods of stability corresponded to high stability (large similarity values) for almost all individuals, as could be expected. However, the instability revealed by the average did not necessarily come from an instability of the entire network, but rather from a mixture of locally stable and changing structures (Figure 4.2). Following individual cosine similarities therefore allowed us to identify, for each period of interest, individuals with more or less stable ego-networks, as well as interesting patterns of synchronization of ego-networks evolution (Figure 4.3). The patterns we identified on a monthly timescale often suggest sudden and important changes that correspond, at least in some cases, to adult females changing primary males, as observed in the wild (GOFFE, ZINNER et FISCHER 2016). We suspect that stronger perturbations of the network could be linked to high ranking females changing males (such as Angele), whereas smaller perturbations could be linked to more peripheral females (such as Brigitte) changing principal male.

The use of a similarity measure proved to be a sensitive and versatile method to understand changes in the individuals' social relationships and their consequences at the group level. In particular, our results show that behind what, at first glance, looks like a stable social network, there is a complex and subtle mixture of stable and unstable ego-networks.

We then aimed to test the ability of our continuous-time model with respect to traditional aggregated approaches (see section 3.4) in detecting discrete systems states. We thus provided a systematic approach that, starting from a data stream of contacts between individuals, allows to detect discrete meso-states and change-points of the system under study (see Figure 4.5). Using different empirical datasets, considering data streams of direct contacts both between non-humans (baboons individuals under study) and humans (students), we moreover aimed to uncover for which values of the parameter $\alpha$ of the model the detection was more effective.

We simulated a temporary perturbation for a period $\Delta t$, by switching identities of individuals in the data streams and, as for the study of aggregated monthly network described above, we computed the cosine similarity between network snapshots for each couple of times. Already from a qualitative visual analysis, the matrices showed a block-wise structure around the diagonal from which we infer the presence of different epochs or states, each state corresponding to a stable configuration of the network. We assumed the temporal network to have successfully detected the perturbation if we were able to identify unique block of size $\Delta t$ corresponding to the perturbed period. In case of the continuous representation, the perturbation resulted more or less distinguishable, depending on the value of $\alpha$ used. In fact, we already

observed in the previous chapter (see Figure 3.11) that the choice of the parameter value heavily influences the description of the system dynamics. This variability is reflected in the matrices of similarity between network snapshots (Figures 4.6 and 4.8. For low values of $\alpha$ the matrices show stable flat patterns, meaning that network weights do not vary enough to detect the underlying system dynamics and thus the perturbation is not detected; for high values of $\alpha$ the perturbation is distinguishable in the matrices visualization and in addition, the dynamics of the system at various levels also appears : as $\alpha$ increases, the perturbation gradually overlaps with minor fluctuations of the system. Also in case of aggregated representation, different patterns are shown for the two different types of aggregation. For the increasing time-window approach, already after few snapshots the network appears extremely stable : the time window is clearly too large to detect changes in the system dynamics, which then appears completely flattened. Contrarily, in case of the fixed time-window the similarity matrix shows the underlying dynamics of the system at multiple scales : the three macro-states produced by the presence of the simulated perturbation (before, during and after the perturbation) overlaps with a "noisy" residual dynamics. We thus noticed that the fixed time-window approach was overall more effective than the increasing time-window approach. However, the size of the time-window turned out to affect the ability of detection. In fact, for very short timescales (few hours) the noise prevails, preventing us to detect the simulated perturbation (see Figure A.1).

We then applied different clustering methods (Hierarchical Clustering Analysis and k-means) to matrices of distances obtained from the similarity matrices to detect the network states and thus the simulated perturbation. In order to validate and compare the partitions obtained through the clustering methods, we computed several validity indices, that confirmed a better performance of our model with respect of the aggregated approaches. Interestingly, given a certain system and a set a perturbation, all the combinations between the two clustering methods and the three validation indices indicate the same range of values of $\alpha$ as more suitable to detect the perturbations. In particular, we identified, both for baboons dataset and for students dataset, a range of parameters $\alpha$ for which the network computed with the model representation outperforms the aggregated approaches in detecting of changes ($\alpha = 0.003 - 0.005$ for baboons data and $\alpha \in [0.01, 0.05, 0.1]$ for students data). In the Appendix (see A) we show that these values are rather stable also in case of different types of perturbations and time resolutions. These results suggest that the range of suitable values of $\alpha$ could be independent from the time scale and the type of perturbation and thus a system-specific characteristics. Nonetheless, more datasets and further investigations would be needed to confirm this.

Generally, we showed that the method proposed effectively allows to detect the underlying states of the social system described by the temporal network. This confirms the results already shown in very recent works (MASUDA et HOLME 2019; SUGISHITA et MASUDA 2020; PEDRESCHI, BERNARD, CLAWSON et al. 2020). Moreover we show that, when associated with validity indices, this method allows to evaluate the capability of a network representation to reflect the underlying system dynamics and thus allows

for comparison between different network representations. Based on this comparison, we demonstrated that the continuous-time approach, that we proposed as alternative to the aggregated approaches, is actually better to reflect the dynamics of the social systems, at least for a proper choice of the value of the parameter $\alpha$.

# 5. Triads and Social Balance

So far we studied the nature and evolution of dyadic relationships and their consequences on the whole network structure. Starting from different network representations, using either aggregated weights over different timescales or continuously-evolving link weights (new framework defined in section 3.4), we investigated how dyadic relationships appear and disappear or change in time in different ways, either abruptly or smoothly, and how these changes can be interpreted as transitions between states of the entire network.

We moreover considered the fact that dyadic relationships are not isolated and are to be studied in relation to other dyads of the group (section 3.4). Indeed, in social systems, as in a wide range of complex systems, interactions can occur in groups of more than two nodes and to understand the evolution of single dyads, we might need to consider at least the evolution of dyads involving neighbor nodes. The presence of subgraphs, *motifs* and local structures formed by dyads at various scales, such as triangles, have proven to provide further insights to characterize and interpret the whole network structure (SHEN-ORR, MILO, MANGAN et al. 2002; ONNELA, SARAMÄKI, KERTÉSZ et al. 2005) and also the system dynamics, in case of time-dependent networks (BRAHA et BAR-YAM 2009; KOVANEN, KARSAI, KASKI et al. 2011).

Few tools are however yet available to study temporal network structures at various temporal scales and group-scales, especially regarding non-human animal social networks.

In this chapter we will take advantage of the signed network presented in section 3.2.2 to analyze the social dynamics of the group of baboons under interest in this PhD project in terms of particular sub-groups structures, i.e. triads and triangles. We remind that the just mentioned signed network was derived by the weighted co-presence temporal network obtained from baboons cognitive tests during a period of 39 months (from january 2014 to May 2017). In fact, in the previous chapters we have dealt only with weighted networks in which the links were intended as "positive" social relationships. However, disliking exists between individuals. Here we are able to exploit the binary signed network discussed previously (in which links assume either + or - value) to test whether the social network is "balanced", according to social balance theory, and to then investigate the triadic closure dynamics. In doing so, we thus aim to provide additional ways of investigating social groups and their evolution.

## 5.1. Triads, triadic closure, social balance

Triads are the simplest social structures beyond dyadic associations, since they involve three individuals, among which at most three links can exist. In social networks, a group of three individuals $A, B, C$ such that $A$ and $C$ are both friends of $B$ are called a triad centered at $B$. The triad is *open*, forming a "wedge", if the link from $A$ to $C$ is missing. The process of closing an open triad to create a triangle is called *triadic closure* and is a well-known mechanism of evolution of social networks (RAPOPORT 1953; GRANOVETTER 1973). In signed networks with positive and negative links, there are three possible wedge types : $++$, $+-$ and $--$ (THURNER 2018). Triadic closure refers to the fact that, if only two links are known to be present in a triad (e.g., between three individuals A B and C, only the links AB and BC are known to exist), the third link AC is predicted to exist as well or to appear in the future. This phenomenon helps to characterize and predict the development of ties within a network and the progression of its connectivity (THURNER 2018; RAPOPORT 1953; GRANOVETTER 1973). Evidence of triadic closure in primates has been reported by BORGEAUD, SOSA, BSHARY et al. 2016 in three groups of vervet monkeys, finding that two individuals are more likely to be associated if they are both linked with a mutual third party associate. The notion of triadic closure is however limited to binary associations (a link is either present or not) and does not consider that links can be weighted or of different types (see however BRANDENBERGER, CASIRAGHI, NANUMYAN et al. 2019 for a recent extension to multi-edge social networks).

Triadic structures become richer when it is possible to assign signs (positive or negative) to the links of a social network, to denote on the one hand positive associations such as friendship or trust, and on the other hand antagonistic relationships such as dislike, distrust or aggression. In this case, social balance theory (HEIDER 1946; HEIDER 1958; WASSERMAN et FAUST 1994; CARTWRIGHT et HARARY 1956) provides a theoretical framework to understand the dynamic (in)stability of signed social networks by studying the closed triangles, which have each either 0, 1, 2 or 3 negative links (see Figure 5.1). In its strong formulation, social balance theory states that a triangle is balanced if all three links are positive (the three nodes are all "friends"), or if two links are negative and one is positive (two "friends" are "non-friends" with the third). The remaining two configurations (either three negative links or two positive links and one negative, see Figure 5.1) are called unbalanced and are considered to be a symptom of tension and social stress. For instance, the configuration with two positive links and one negative is in contradiction with the common belief that "a friend of a friend is a friend". A network should thus tend towards more balanced configurations (KUŁAKOWSKI, GAWRONSKI et GRONEK 2005; MARVEL, KLEINBERG, KLEINBERG et al. 2011) as, in Heider's words, "If no balanced state exists, then forces towards this state will arise". Studying social balance is therefore an interesting direction for investigating the dynamics of social networks, as the numbers of balanced and unbalanced triads could be expected to be predictors of changes and instability.

Social balance theory has received a lot of theoretical attention (MARVEL, KLEINBERG,

| |  |  |  |  |
|---|---|---|---|---|
| Weak | B | U | B | B |
| Strong | B | U | B | U |

FIGURE 5.1. : **Principle of social balance theory.** We show the four possible signed triads. In the original "strong" formulation of the social balance theory, two triads are balanced (B) and two are unbalanced (U). In the "weak" formulation put forward by DAVIS 1967, triangles with three negative edges are also considered balanced because such configurations can arise when more than two subgroups exist within the social network under consideration.

KLEINBERG et al. 2011 ; KUŁAKOWSKI, GAWRONSKI et GRONEK 2005) but relatively little empirical validation in human social networks (DOREIAN et MRVAR 1996 ; DOREIAN et MRVAR 2009 ; SZELL, LAMBIOTTE et THURNER 2010 ; LESKOVEC, HUTTENLOCHER et KLEINBERG 2010 ; THURNER 2018). This is most probably due to the difficulty in defining signed social networks, i.e., in having information on both affiliative (positive) and antagonistic (negative) ties between individuals. The study of social balance theory in non-human animals is even more difficult, as their social networks are often built using only information of positive nature (such as proximity). Notably, negative interactions are often less evident : behaviors like avoidance or open fights are difficult to observe and ascertain and/or less frequent. Consequently, little attention has been paid to agonistic social networks but according to social balance theory for instance, negative links are crucial to understand the social evolution of a group. We know of only one study that explicitly tested social balance in a wild, non-human system. In social rock hyrax (*Procavia capensis*), ILANY, BAROCAS, KOREN et al. 2013 considered two individuals who did not share a positive interaction within a year to be 'non-friends' (negative link), and individuals who shared at least one positive interaction to be friends (positive link). By counting the number of balanced and unbalanced triangles, the authors confirmed the predictions of social balance theory in its strong version. They also showed that unbalanced triangles tended to change to become balanced, as predicted by the theory, but that some level of imbalance remained in the network, mostly due to new individuals entering the group and forming unbalanced structures. A useful general tool could be therefore to compare the number of positive interactions to a null model : having less positive interactions than expected by the null model could be then an indicator of a negative relationship.

This is in fact what we did in section 3.2.2 when computing a signed social net-

work from the co-presence network built on baboons cognitive tests data, using a null-model of social interaction to estimate link strength. In this way, we were able to determine both affiliative and avoidance relationships from positive interactions simply by assuming that individuals who met more than chance were actively seeking each other's company while individuals who meet less than chance are actively avoiding each other (BEJDER, FLETCHER et BRÄGER 1998).

In the following, we will consider this signed social network to both validate social balance theory on empirical data and to use tools linked to social balance theory to explore network dynamics. These tools, such as counts of the numbers of triangles and triangle creations, will serve to seek possible alternative methods to detect changes in the network structure, aside from the quantitative similarity measures between networks built in successive periods presented in the previous chapter (see section 4.2), considering intermediate-levels between the individual and the whole group's dynamics.

## 5.2. Social Balance validation

The procedure described in section 3.2.2 yielded a signed social network for each month, with both positive and negative links, from a data which in principle were not collected for assessing social relationships. To substantiate the social significance of the positive and negative links obtained through our method, we first tested the social balance theory on the networks, counting the triangles of each of the four possible types, i.e. with 0, 1, 2 or 3 negative links (see Figure 5.1) in each monthly network snapshot. Then, we compared the results in each case to a null model in which network structure was fixed but the signs were reshuffled among the links, to check whether the balanced triangles were over-represented and the unbalanced ones under-represented with respect to this null model.

Figure 5.2 shows that both the total number of triangles and the number of triangles for each case fluctuated between months, but in all months balanced triangles were more numerous than the unbalanced ones. This was true both within the strong and the weak versions of the social balance theory.

In particular, triangles with three positive links were strongly over-represented in each month (100% of the months) with respect to the null model and triangles with only one positive link (balanced in both weak and strong balance theory) were also over-represented in most months (74% of the months). In contrast, unbalanced triangles with two positive and one negative links were clearly under-represented (95% of the months) and triangles with three negative links tended to be moderately under-represented (82% of the months). We recall that these triangles are unbalanced in the strong version but balanced in the weak version of the social balance theory. Overall, balanced triangles were over-represented and unbalanced ones were under-represented with respect to the null model, showing that the signed monthly networks built from co-presence data did respect social balance theory.

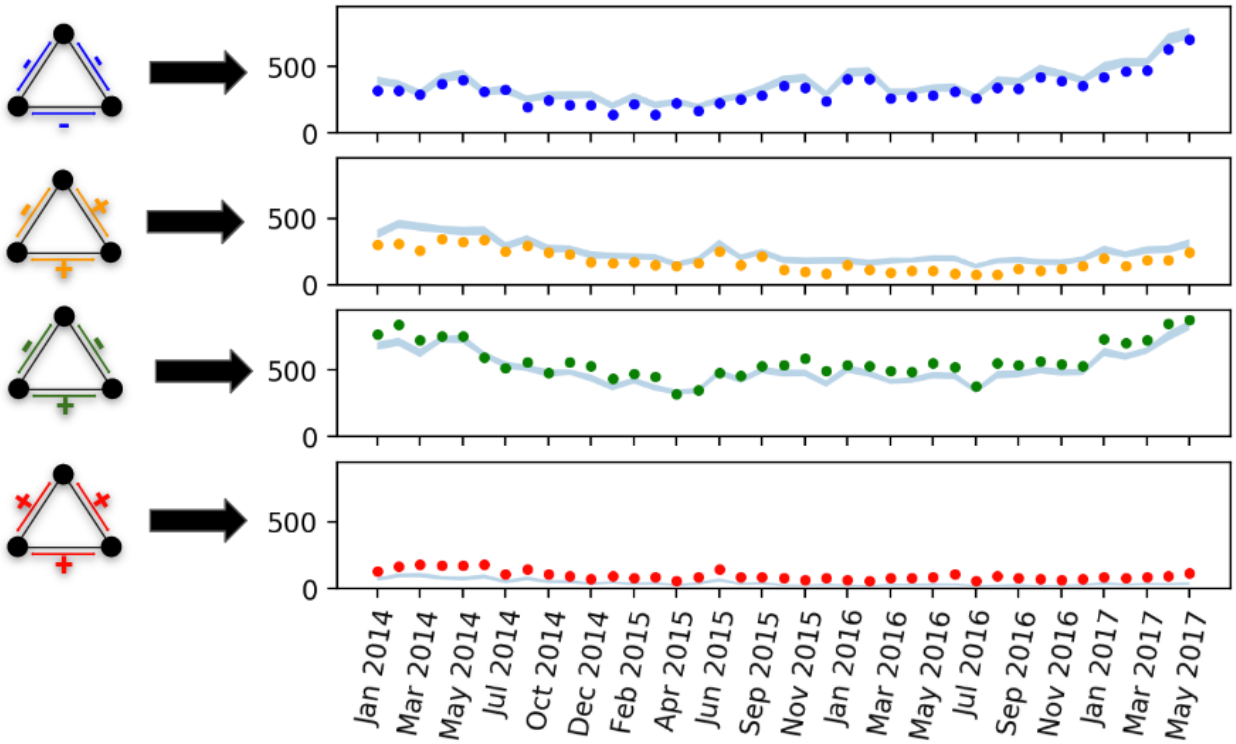


FIGURE 5.2. : **Evolution of the number of signed triangles through time.** Coloured filled circles : Number of triangles of each type (shown on the left part of the figure) in the empirical monthly signed co-presence networks (union of affiliative and avoidance networks). Shadowed area : confidence interval ($5^{th}$ to $95^{th}$ percentiles) of the distributions of numbers of triangles of each type in the randomized monthly networks. In the strong version of social balance theory, the triangle types in the two bottom panels are balanced, while the ones in the two top panels are unbalanced. In the weak version, triangles with three negative links (top panels) are also considered balanced.

## 5.3. Triadic closures

**Aggregated analysis** To investigate the dynamic aspects of social balance, we considered the triadic closure events between successive months, in which an open "wedge" in a month $t$ became a closed triangle in the following month $t+1$. We thus counted, for each wedge type in month $t$, how many became triangles of each of the four

possible types (Figure 5.1) and thus whether closing wedges became preferentially balanced or unbalanced triangles (SZELL, LAMBIOTTE et THURNER 2010).

Social balance theory implies that wedges should preferentially close by forming balanced triangles.

Figure 5.3 gives the global number of triadic closure events from one month to the next. The results, aggregated over all values of $t$, showed that the total number of triadic closure events producing balanced triangles was larger than the total number of events producing unbalanced triangles, both using the strong or the weak version of the social balance (see Figure 5.3). Note that we obtained a substantial number of events in which a $--$ wedge became a $---$ triangle, which is considered balanced only in the weak formulation of social balance theory.

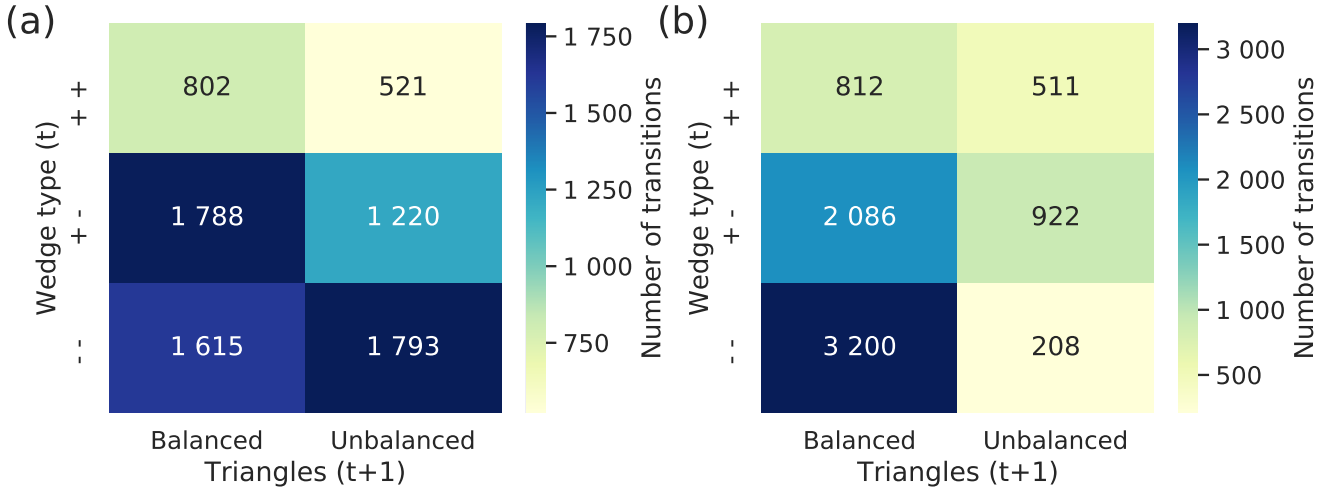


FIGURE 5.3. : **Total triadic closures in the signed monthly networks.** Total numbers of triadic closures of each type from a month $t$ to the next one $t+1$, i.e., numbers of transitions from the various types of wedges (from bottom to top, $--$, $+-$, $++$) to balanced triangles (left column of each table) or unbalanced triangles (right column of each table). We present the numbers of transitions summed over all the period of investigation (39 months) and for both the (a) strong and (b) weak formulations of social balance. For instance, over the whole period there were 3,200 transitions from a wedge $--$ to balanced triangles, and 208 to unbalanced ones, in the weak social balance formulation.

**Dynamical analysis** We moreover investigated triadic closure events taking into account the events of every single month. We remind that the study of the stability of the co-presence weighted network through similarities between couples of network snapshots (see section 4.2) showed that the network instabilities detected at global level were linked to individuals patterns. For instance, the instability detected

during the period between July and September 2014 was linked the fact that a high ranking female changed primary male. We thus investigated whether triadic closure dynamics reflected the same instability patterns found at individual and global level in the previous chapter. Indeed, given the interpretation of the social balance theory that unbalanced triangles are a sign of tension and social stress, one could expect (i) an increase in the number of balanced triangles and a decrease in the number of unbalanced ones during periods of stability, and (ii) that a large number of unbalanced triangles could lead to an instability of the network and thus to important rearrangements in the following month. Figure 5.4 shows the temporal evolution of the number of balanced and unbalanced triangles and the number of triadic closure events of each type. For each panel, blue lines represents the number of transitions from each type of wedge to balanced close triangles, whereas orange lines represent the number of transitions from each type of wedge to unbalanced close triangles. The first row refers to the strong theory (balanced triangles are $'+++'$ and $'+--'$) while the second row refers to weak theory (balanced triangles are $'+++'$, $'+--'$, $'---'$). Based on the assumptions mentioned above, we would have expected inverse trends for the two lines, e.g. relative peaks of the blue lines in correspondence of relative minima of the orange lines (periods of stability) and viceversa (instabilities). However, contrarily to the results obtained from cosine similarity analysis, the numbers fluctuate widely from one month to the next, and variations showed no clear temporal signal or trend.

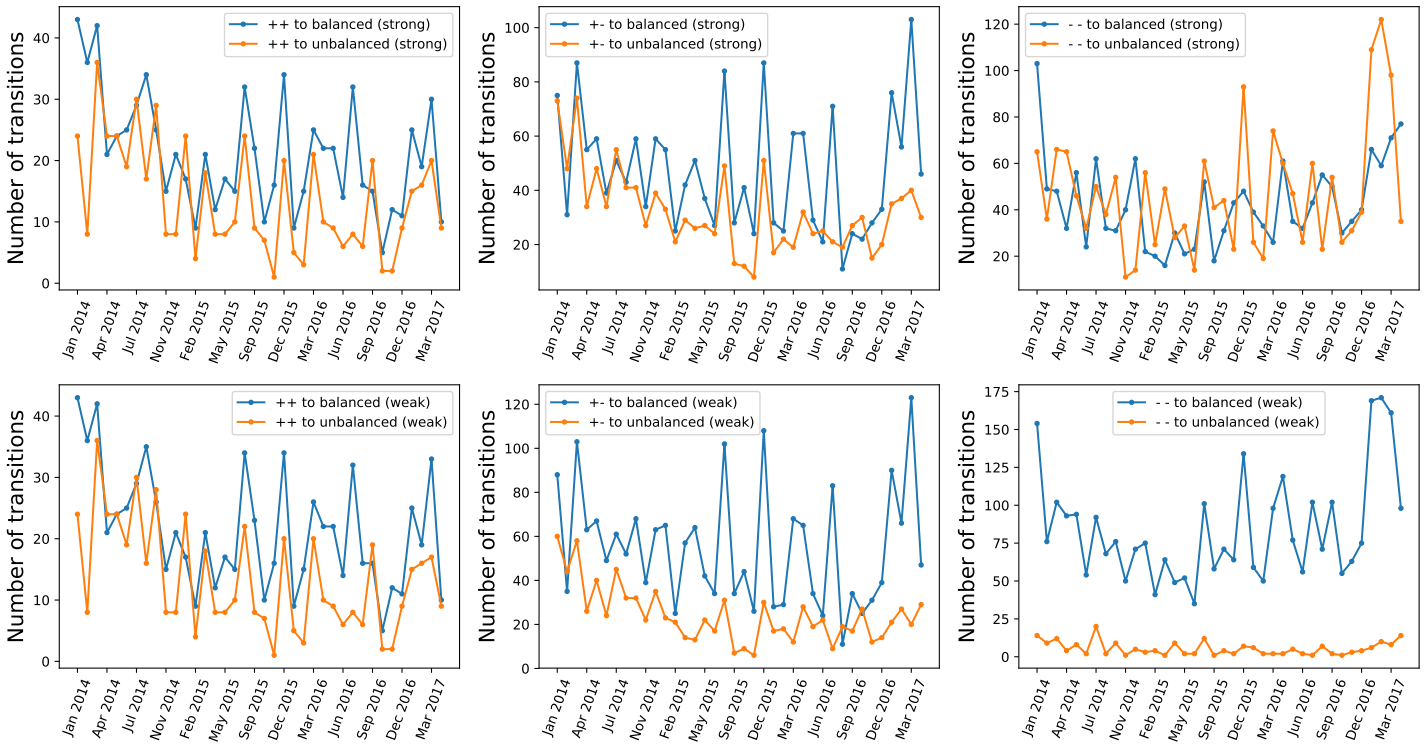


FIGURE 5.4. : Numbers of transitions from one month to the next, from wedges of each type to balanced and unbalanced triangles, where balanced and unbalanced triangles are defined either according to the strong (top row) or to the weak (bottom row) version of social balance.

## 5.4. Discussion

In this chapter we analyzed the co-presence network obtained from baboons cognitive tests in terms of particular sub-groups structures, i.e. triads. In particular we considered the signed network derived from the weighted co-presence network (the procedure is illustrated in section 3.2.2), which allowed us to test social balance theory by combining positive (affiliative) and negative (avoidance) social networks. We showed that the networks followed the predictions of social balance theory (HEIDER 1946). From a static point of view, the results showed that balanced triangles were over-represented and unbalanced triangles under-represented when compared to a null distribution based on random permutation of the networks' edge signs. Furthermore, from a dynamic point of view, we found that wedges (unclosed triangles) tended to close into balanced triangles more frequently than into unbalanced ones. Interestingly, we also observed many closure events towards triangles with three negative edges : this could be linked to the fact that the group of baboons was composed of more than two sub-units, so that triangles with three avoidance links were not rare.

Our results are in line with two previous studies that aimed at testing social balance theory directly. SZELL, LAMBIOTTE et THURNER 2010 in an online game with more than 300,000 participants and ILANY, BAROCAS, KOREN et al. 2013 in a study of rock hyraxes both found that their networks were generally balanced with an over-representation of balanced triangles (especially + + + triangles) and an under-representation of unbalanced triangles (especially + + − triangles). In these two studies, as in ours, there was substantially more support for the weak formulation of social balance theory DAVIS 1967, compared to its stronger alternative. Finally, SZELL, LAMBIOTTE et THURNER 2010 also studied the triangle closure dynamics and also found, like us, that more wedges (unclosed triangles) closed into balanced triangles than unbalanced ones. Based on these three studies with different species and in very different contexts, it is tempting to conclude that (weak) social balance theory may represent general principles of social organisation, as envisaged by HEIDER 1946. Surprisingly however, very few studies have tested social balance theory and in our opinion it deserves more scrutiny especially because it provides a clear static and dynamic theoretical framework to understand the structure of social networks and their evolution.

Unfortunately, the analysis of the temporal evolution of social balance measures (in proportion or number of balanced vs. unbalanced triangles with both the weak or strong interpretation) did not yield clear insights into the temporal evolution of the structure of the social network. There were no clear changes in the different measures between periods of social stability and instability that were instead revealed by the analysis of the cosine similarity. One explanation could be that our analysis did not consider the correct timescale on which changes in social balance occur. For instance, there is some evidence in chacma baboons (*Papio ursinus*) that individuals adapt their social strategies on very different timescales (SICK, CARTER ALECIA, MARSHALL HARRY et al. 2014; HENZI, LUSSEAU, WEINGRILL et al. 2009; SILK, BEEHNER, BERGMAN et al. 2010). If the social network we studied can be reorganised rapidly, going from balanced to unbalanced to balanced again on a scale of a few days, then we should expect to find a large difference in a similarity measure (the network has changed) but little difference in terms of the number of balanced-unbalanced triangles on a monthly timescale. This problem may not be easy to solve because networks established on shorter timescales are subject to imprecise estimates of link strengths, which in turn could mask changes in the network. In the previous chapter, for instance (see section 4.2), the monthly timescale usually recommended (WHITEHEAD 2008) turned out to be a good compromise between a precise estimate of link strength and the possibility to detect temporal changes. However, the best aggregation timescale is likely to change depending on the situation, study species, group and data gathering technique (FARINE et WHITEHEAD 2015; DAVIS, CROFOOT et FARINE 2018). The investigation of the cosine similarity measure also shows a limit of the social balance theory. The important changes we observed in the structure of the network using the cosine similarity method in the previous chapter (see section 4.2) were in fact not reflected by changes in the social balance of the social network, probably because they were linked to changes occurring in the relationships of only some of the individuals and not

involving triads. This suggests that the measure of social balance through the counting of balanced and unbalanced triangles may be a too coarse and too global measure to be able to detect and follow changes in the relationships between individuals. In particular, social balance focuses only on the sign of these links, whereas approaches that take into account weights and hence the relative importance of the relationships in the social network are probably more suitable to study the network dynamics.

However, flexible approaches might be useful that characterize dynamic changes across different levels of description of the social network (pairs, triads, subgroups of individuals, entire network) and that have started to be developed in the context of temporal networks (HOLME 2015; FOURNET et BARRAT 2014; DARST, GRANELL, ARENAS et al. 2016; CROFT, DARDEN et WEY 2016; FARINE 2018). We note that the study of specific frameworks that naturally describe more complicated structures, called *high-order interactions*, is beyond the network representation. This study brings in fact difficult issues that require the development of new mathematical tools and it has been only recently receiving attention in literature (for a review see BATTISTON, CENCETTI, IACOPINI et al. 2020).

# Conclusion

Social interactions are an important fitness component of group living animals

and social network analysis provides powerful tools to describe these social interactions. In particular, the notion of temporal network is the natural means to represent this highly dynamic system, allowing for the analysis of its evolution and a for deeper mechanistic understanding. However, the availability of high resolution and longterm time-resolved datasets is still uncommon in the study of animal social dynamics : differently from the widespread availability of digital traces on human social patterns, infrastructures and protocols based on digital devices have only recently become more easily available for the study of animal groups. Such techniques are foreseen to be a less costly and reliable alternative to current traditional data collections methods, such as behavioral observations, and could a priori provide further insights on social dynamics especially on very short and very long timescales. Moreover, not only the data collection method but also the network representation may influence the image of the social bonds between individuals : temporal networks are often constructed by aggregating empirical data over time windows, such that a link represents a social tie between two individuals and the link weight, which represents the intensity of such interaction, is defined using the interaction frequency within the aggregation time window. The choice of the length of this time window, often dictated by the availability of data rather than specifics of the system, plays therefore a crucial role in the structure of the resulting network and in the description of its dynamics.

The work carried out during this PhD has attempted to contribute to the study of the dynamics of animals social patterns, through the case study of a group of captive Guinea baboons. Our main focus has been in particular on a twofold objective : on the one hand the investigation of temporal network dynamics through high-resolution and long-term datasets, accompanied by the development of an infrastructure to collect data on individuals interactions based on proximity sensors ; on the other hand the design of a novel framework to investigate the social system dynamics through a continuous time description of networks weights evolution.

In chapter 2 we presented several temporal empirical data of pair-wise associations between non-human primates individuals, namely behavioral observations, which represent the traditional method to collect social data on animals, automatically collected time-stamped data on cognitive tests and contacts registered by wearable sensors between individuals through a ad-hoc system designed, tested and realized during this PhD. In order to further compare human and non-human social patterns, we also introduced two datasets concerning human interactions, i.e. contacts registered by wearable sensors between students and friendship surveys. We then

focused on the comparison between the traditional collecting method of behavioral observations and the technique of automatic collection through wearable proximity sensors, highlighting different advantages and limitations of the two methods. For instance, observational methods provide high-quality data, through which we can distinguish different behaviors and describe in depth social relationships between individuals, but the data suffers from several sampling issues and biases. The aim of this comparison was originally to assess the reliability of our infrastructure in providing meaningful social information, and we thus performed a matching between the two datasets at the level of single events, to verify to what extent the observed behaviors were detected by the sensors systems. The result might have seemed to be discouraging, since the overlap between the events registered by the two systems was very limited : about one third of the observed interactions was also recorded by the sensors. Nevertheless, when we considered the global social structures resulting from the networks constructed from the two datasets, we found surprisingly completely different results. Indeed, in chapter 3 we focused to the construction, analysis and comparison of temporal networks built from the data previously presented. In the first instance, we represent temporal networks as a succession of weighted static networks aggregated over fixed time-windows. Notably, data on baboons cognitive tests were not originally collected to inform on social associations between individuals. However, we have been able to build a temporal network based on the co-presence of individuals in the test stations that had revealed to be informative on the actual social relationships between individuals, as shown by the high correlation between weights of co-presence network and of the network obtained by observational data collected in the same period. Moreover, comparing the observed co-presence to a null-model, we were able to build a signed network representing both affiliative and avoidance relationships, simply by assuming that individuals who met more than chance were actively seeking each other's company while individuals who met less than chance were actively avoiding each other. As anticipated above, we then compared the network images emerged from behavioral observations and of contacts data registered by wearable sensors, discovering that the two networks aggregated over the whole observation period turned out to be striking similar as measured by several metrics. When considering the aggregations over different time-windows, the observational method reveal its limitations in providing a reliable image of the social structure at short timescales : while the observations network fluctuated strongly from day to day, the sensors network appeared very stable, suggesting to be potentially suitable to reliably pinpoint changes in the social structure of the group. With this in mind, we analysed the detection of changes and period social instability in the next chapter.

The analysis of shortest timescales revealed however that when presenting temporal network data as a succession of static networks aggregated on successive time windows, the length is somehow arbitrary and it does not necessarily correspond to any intrinsic timescale of the system. In the last part of the chapter we thus presented a new framework that generates a weighted, directed, continuously-evolving network, starting from any undirected stream of dyadic interactions. This approach is based

on the idea that the tie between two nodes reinforces if interactions between the two nodes are iterated, and deteriorates if one of the nodes interacts with other peers. The unique parameter $\alpha$ dictates the sensitivity of the weights to every new interaction. From an initial test of the framework on the contacts data registered from wearable sensors, two main aspects emerged.

First, the model generates asymmetric weights with different level of reciprocity, meaning that given two nodes $i$ and $j$, we might have $w_{ij} \simeq w_{ji}$ (high reciprocity) or $w_{ij}(w_{ji}) >> w_{ji}(w_{ij})$ (low reciprocity). We would have expected these different levels of symmetry to reflect a non-random effect of social dynamics. We thus computed the temporal network from contacts data between students and we compared the different levels of weights symmetry to the friendship surveys data, where individuals declared who among other individuals they considered as their friends. We expected that individuals that have a mutual declaration resulted in a more symmetric link in the temporal network. However, this effect was slightly visible. The question about whether or not the asymmetry of links have a social meaning might therefore deserve further investigation.

Second, the dynamics of the network is heavily influenced by the value of the parameter : values of $\alpha$ too small do not allow the weights to update fast enough to detect changes in the network while high $\alpha$ produce a dynamics of the weights too sensitive to each interaction, resulting in abrupt variations and a general bursty trend. The possibility to have such different scenarios of evolution of weights raised the question of how to estimate a suitable value of the parameter that could better reflect the actual social dynamics of the underlying system. To address this problem, in chapter 4 we focused on the ability of different network representations to detect change points and instabilities in the social structure. In the first part of the chapter we considered the monthly aggregated affiliative co-presence network computed from cognitive tests data and we studied the social network's dynamics using a similarity measure between the affiliative ego-networks in successive months, comparing networks across two different scales, i.e. single individuals and the entire network. The use of a similarity measure proved to be a sensitive and versatile method to understand changes in the individuals' social relationships and their consequences at the group level. In particular, we showed that the global social stability of a group is the result of a continuous reorganizations of dynamical pattern at ego-network scales, and that only the synchronizations of these patterns might generate a visible change at the macro-scale. In the second part of the chapter we instead tested the ability of the framework early presented to detect discrete system states, with a dual aim : (i)uncovering for which values of the parameter $\alpha$ of the model the detection was more effective and (ii)comparing the performance of the model with respect to the traditional aggregated approaches. We provided a method based on clustering algorithms that, starting from a data stream of dyadic contacts, allows to detect meso-states and change points of the system and to give also an estimation for the quality of this detection. Based on this method we thus were able to compare different network representations, i.e. the model with different values of the parameter $\alpha$ and two different aggregated network

approaches, in two different contexts, namely human and non-human primates interactions. Interestingly, for both systems we found a range of parameter values for which the network constructed with the model outperformed the aggregated representations in the ability of detecting changes in the system and these values seem to be system-characteristics. Nonetheless, more datasets and further investigations would be needed to confirm this hypothesis. Either way, our findings support the assumption, already advanced in the recent literature (AHMAD, PORTER et BEGUERISSE-DÍAZ 2018), that temporal networks represented through continuous-time approaches appear more suitable than the aggregation in time-windows to describe the dynamics of social systems. Finally, in chapter 5 we analysed the signed network derived from the weighted affiliative and avoidance network obtained in chapter 3 in terms of its internal sub-group structure, i.e. triadic structures. First, we assessed that the network respected the predictions of social balance theory, that is, a social group tends to have more balanced than unbalanced triangles. We showed in fact that balanced triangles were over-represented and unbalanced triangles under-represented when compared to a null distribution based on random permutation of the networks' edge signs. A more ambitious purpose was to analyse the temporal evolution of social balance measures (in proportion or number of balanced vs. unbalanced triangles with both the weak or strong interpretation) to eventually uncover similar patterns of (in)stability than those found in chapter 4. Nevertheless, this analysis did not yield clear insights into the temporal evolution of the structure of the social network. There were no clear changes in the different measures between periods of social stability and instability that were instead revealed by the analysis of the cosine similarity. The reason why these changes are not reflected in the analysis of triads can be structural, i.e. the changes occurring in the relationships involve other scales of the system, e.g. single individuals, and not triads. Alternatively, considering only the sign of the links could be a too simplistic approach with respect to taking into account weights and hence the relative importance of the relationships in the social network are probably more suitable to study the network dynamics.

However, very few studies have tested social balance theory and in our opinion it deserves more scrutiny especially because it provides a clear theoretical framework to understand the structure of social networks. In addition, it might be useful to characterize dynamics changes at a sub-group level of description, which is an intermediate scale between the individual and the global, which are more frequently taken into consideration.

To conclude, we have shown that new infrastructures, that produce long-term high-frequency data on non-human animal social interactions, could unlock the investigation of the social dynamics at scales (both in time and at group level) that that seemed unreachable until few years ago. This data availability, together with the advance of temporal network frameworks, could help in the future to understand ecological and evolutionary processes underlying social network formation and organization, and to study how changes in the environment, composition of the group or single key-relationships influence the entire network structure. This thesis aimed

to represent a small step forward in this direction and a bridging between different disciplines, network science and animal social science.

# References


[APBD18] Walid AHMAD, Mason A PORTER et Mariano BEGUERISSE-DÍAZ. « Tie-decay temporal networks in continuous time and eigenvector-based centralities ». In : *arXiv preprint arXiv :1805.00193* (2018) (cf. p. 31, 68, 69, 78, 116).

[Alb19] Susan C. ALBERTS. « Social influences on survival and reproduction : Insights from a long-term study of wild baboons ». In : *Journal of Animal Ecology* 88.1 (2019), p. 47-66. DOI : 10.1111/1365-2656.12887. eprint : https://besjournals.onlinelibrary.wiley.com/doi/pdf/10.1111/1365-2656.12887. URL : https://besjournals.onlinelibrary.wiley.com/doi/abs/10.1111/1365-2656.12887 (cf. p. 27, 80).

[Alt74] Jeanne ALTMANN. « Observational study of behavior : sampling methods ». In : *Behaviour* 49.3 (1974), p. 227-266 (cf. p. 39, 40).

[And+13] James R. ANDERSON, Hika KUROSHIMA, Ayaka TAKIMOTO et al. « Third-party social evaluation of humans by monkeys ». In : *Nature Communications* 4 (2013), p. 1561. URL : http://dx.doi.org/10.1038/ncomms2495 (cf. p. 30).

[Arb+13] Olatz ARBELAITZ, Ibai GURRUTXAGA, Javier MUGUERZA et al. « An extensive comparative study of cluster validity indices ». In : *Pattern Recognition* 46.1 (2013), p. 243-256 (cf. p. 90).

[Bar05] Albert-Laszlo BARABASI. « The origin of bursts and heavy tails in human dynamics ». In : *Nature* 435.7039 (2005), p. 207-211 (cf. p. 68).

[BBV08] Alain BARRAT, Marc BARTHELEMY et Alessandro VESPIGNANI. *Dynamical processes on complex networks*. Cambridge university press, 2008 (cf. p. 29).

[BBV04] Alain BARRAT, Marc BARTHÉLEMY et Alessandro VESPIGNANI. « Modeling the evolution of weighted networks ». In : *Physical Review E* 70.6 (2004). ISSN : 1550-2376. DOI : 10.1103/physreve.70.066149. URL : http://dx.doi.org/10.1103/PhysRevE.70.066149 (cf. p. 28, 33).

[BC13] Alain BARRAT et Ciro CATTUTO. « Temporal Networks of Face-to-Face Human Interactions ». In : *Temporal Networks* (2013), 191–216. ISSN : 1860-0840. DOI : 10.1007/978-3-642-36461-7_10. URL : http://dx.doi.org/10.1007/978-3-642-36461-7_10 (cf. p. 34).

[Bar+13] Alain BARRAT, Ciro CATTUTO, Vittoria COLIZZA et al. « Empirical temporal networks of face-to-face human interactions ». In : *The European Physical Journal Special Topics* 222.6 (2013), p. 1295-1309 (cf. p. 34).

[Bas+13] Danielle S BASSETT, Nicholas F WYMBS, M Puck ROMBACH et al. « Task-based core-periphery organization of human brain dynamics ». In : *PLoS Comput Biol* 9.9 (2013), e1003171 (cf. p. 34).

[BHJ09] Mathieu BASTIAN, Sebastien HEYMANN et Mathieu JACOMY. « Gephi : An Open Source Software for Exploring and Manipulating Networks ». In : *Third international AAAI conference on weblogs and social media*. 2009. URL : https://www.aaai.org/ocs/index.php/ICWSM/09/paper/view/154/1009 (cf. p. 58, 62).

[Bat+20] Federico BATTISTON, Giulia CENCETTI, Iacopo IACOPINI et al. « Networks beyond pairwise interactions : structure and dynamics ». In : *Physics Reports* (2020) (cf. p. 112).

[Bea+14] Michaël BEAULIEU, Sylvère MBOUMBA, Eric WILLAUME et al. « The oxidative cost of unstable social dominance ». In : *Journal of Experimental Biology* 217.15 (2014), p. 2629-2632. DOI : 10.1242/jeb.104851 (cf. p. 27).

[Bei+11] Brianne A. BEISNER, Megan E. JACKSON, Ashley N. CAMERON et al. « Detecting Instability in Animal Social Networks : Genetic Fragmentation Is Associated with Social Instability in Rhesus Macaques ». In : *PLOS ONE* 6.1 (jan. 2011), p. 1-11. DOI : 10.1371/journal.pone.0016365. URL : https://doi.org/10.1371/journal.pone.0016365 (cf. p. 28).

[BFB98] Lars BEJDER, David FLETCHER et Stefan BRÄGER. « A method for testing association patterns of social animals ». In : *Animal Behaviour* 56.3 (1998), p. 719-725 (cf. p. 55, 56, 77, 106).

[Bet+15] EM BETTANEY, Richard JAMES, JJH ST CLAIR et al. « Processing and visualising association data from animal-borne proximity loggers ». In : *Animal Biotelemetry* 3.1 (2015), p. 27 (cf. p. 30, 35, 37).

[Blo+08] Vincent D BLONDEL, Jean-Loup GUILLAUME, Renaud LAMBIOTTE et al. « Fast unfolding of communities in large networks ». In : *Journal of Statistical Mechanics : Theory and Experiment* 2008.10 (2008), P10008. URL : http://stacks.iop.org/1742-5468/2008/i=10/a=P10008 (cf. p. 58).

[Bor+16] Christèle BORGEAUD, Sebastian SOSA, Redouan BSHARY et al. « Intergroup variation of social relationships in wild vervet monkeys : a dynamic network approach ». In : *Frontiers in psychology* 7 (2016), p. 915 (cf. p. 104).

[BBY09] Dan BRAHA et Yaneer BAR-YAM. « Time-dependent complex networks : Dynamic centrality, dynamic motifs, and cycles of social interactions ». In : *Adaptive Networks*. Springer, 2009, p. 39-50 (cf. p. 103).

[Bra+19] Laurence BRANDENBERGER, Giona CASIRAGHI, Vahan NANUMYAN et al. « Quantifying Triadic Closure in Multi-Edge Social Networks ». In : *arXiv preprint arXiv :1905.02990* (2019) (cf. p. 104).

[CBWG11] Rajmonda Sulo CACERES, Tanya BERGER-WOLF et Robert GROSSMAN. « Temporal scale of processes in dynamic networks ». In : *2011 IEEE 11th International Conference on Data Mining Workshops*. IEEE. 2011, p. 925-932 (cf. p. 52).

[CJ74] Tadeusz CALIŃSKI et Harabasz JA. « A Dendrite Method for Cluster Analysis ». In : *Communications in Statistics - Theory and Methods* 3 (jan. 1974), p. 1-27. DOI : 10.1080/03610927408827101 (cf. p. 91).

[CH56] Dorwin CARTWRIGHT et Frank HARARY. « Structural balance : a generalization of Heider's theory. » In : *Psychological review* 63.5 (1956), p. 277 (cf. p. 104).

[Cas+14] Madelaine CASTLES, Robert HEINSOHN, Harry H MARSHALL et al. « Social networks created with different techniques are not comparable ». In : *Animal Behaviour* 96 (2014), p. 59-67 (cf. p. 37, 38, 52, 78).

[Cat+10] Ciro CATTUTO, Wouter Van den BROECK, Alain BARRAT et al. « Dynamics of Person-to-Person Interactions from Distributed RFID Sensor Networks ». In : *PLOS ONE* 5.7 (juil. 2010), p. 1-9 (cf. p. 29, 36, 39, 41-43, 60, 78, 141).

[CP03] Tanzeem CHOUDHURY et Alex PENTLAND. « Sensing and Modeling Human Networks using the Sociometer ». In : *Proceedings of the 7th IEEE International Symposium on Wearable Computers*. ISWC '03. Washington, DC, USA : IEEE Computer Society, 2003, p. 216-. ISBN : 0-7695-2034-0. URL : http://dl.acm.org/citation.cfm?id=946249.946901 (cf. p. 37).

[Cla+15] N. CLAIDIÈRE, A. WHITEN, M.C. MARENO et al. « Selective and contagious prosocial resource donation in capuchin monkeys, chimpanzees and humans ». In : *Scientific Reports* 5 (2015), p. 7631. DOI : 10.1038/srep07631 (cf. p. 30).

[Cla+17] Nicolas CLAIDIÈRE, Julie GULLSTRAND, Aurélien LATOUCHE et al. « Using Automated Learning Devices for Monkeys (ALDM) to study social networks ». In : *Behavior Research Methods* 49.1 (2017), p. 24-34. ISSN : 1554-3528. DOI : 10.3758/s13428-015-0686-9. URL : https://doi.org/10.3758/s13428-015-0686-9 (cf. p. 31, 38-40, 45, 50, 53, 54, 58, 64).

[Con+12] Rosaria CONTE, Nigel GILBERT, Giulia BONELLI et al. « Manifesto of computational social science ». In : *The European Physical Journal Special Topics* 214.1 (2012), p. 325-346 (cf. p. 28).

[Cra+15] JD CRALL, N GRAVISH, AM MOUNTCASTLE et al. « BEEtag : A Low-Cost, Image-Based Tracking System for the Study of Animal Behavior and Locomotion ». In : *PLoS ONE* 10 (2015), e0136487 (cf. p. 30, 37).

[CDW16] D.P. CROFT, S.F. DARDEN et T.W. WEY. « Current directions in animal social networks ». In : *Current Opinion in Behavioral Sciences* 12 (2016), p. 52-58 (cf. p. 112).

[CJK08] D.P. CROFT, R. JAMES et J. KRAUSE. *Exploring animal social networks*. Princeton University Press, 2008. ISBN : 0691127522 (cf. p. 29).

[Dai+20] Sicheng DAI, Hélène BOUCHET, Aurélie NARDY et al. « Temporal social network reconstruction using wireless proximity sensors : model selection and consequences ». In : *EPJ Data Science* 9 (déc. 2020). DOI : 10.1140/epjds/s13688-020-00237-8 (cf. p. 47, 51).

[Dar+16] Richard K. DARST, Clara GRANELL, Alex ARENAS et al. « Detection of timescales in evolving complex systems ». In : *Scientific Reports* 6 (déc. 2016), p. 39713. URL : https://doi.org/10.1038/srep39713 (cf. p. 29, 112).

[DCF18] Grace H. DAVIS, Margaret C. CROFOOT et Damien R. FARINE. « Estimating the robustness and uncertainty of animal social networks using different observational methods ». In : *Animal Behaviour* 141 (2018), p. 29-44. ISSN : 0003-3472. DOI : https://doi.org/10.1016/j.anbehav.2018.04.012. URL : http://www.sciencedirect.com/science/article/pii/S0003347218301210 (cf. p. 36, 64, 78, 111).

[Dav63] James A DAVIS. « Structural balance, mechanical solidarity, and interpersonal relations ». In : *American journal of sociology* 68.4 (1963), p. 444-462 (cf. p. 27).

[Dav67] James A DAVIS. « Clustering and structural balance in graphs ». In : *Human relations* 20.2 (1967), p. 181-187 (cf. p. 105, 111).

[DM96] Patrick DOREIAN et Andrej MRVAR. « A partitioning approach to structural balance ». In : *Social Networks* 18.2 (1996), p. 149-168. ISSN : 0378-8733. DOI : https://doi.org/10.1016/0378-8733(95)00259-6. URL : http://www.sciencedirect.com/science/article/pii/0378873395002596 (cf. p. 105).

[DM09] Patrick DOREIAN et Andrej MRVAR. « Partitioning signed social networks ». In : *Social Networks* 31.1 (2009), p. 1-11. ISSN : 0378-8733. DOI : https://doi.org/10.1016/j.socnet.2008.08.001. URL : http://www.sciencedirect.com/science/article/pii/S0378873308000397 (cf. p. 105).

[Dor10] Sergey DOROGOVTSEV. *Lectures on Complex Networks*. Jan. 2010. DOI : 10.1093/acprof:oso/9780199548927.001.0001 (cf. p. 33).

[Dun98] Robin IM DUNBAR. « The social brain hypothesis ». In : *Evolutionary Anthropology : Issues, News, and Reviews : Issues, News, and Reviews* 6.5 (1998), p. 178-190 (cf. p. 69).

[Dun09] Robin IM DUNBAR. « The social brain hypothesis and its implications for social evolution ». In : *Annals of human biology* 36.5 (2009), p. 562-572 (cf. p. 69).

[Dun73] Joseph C DUNN. « A fuzzy relative of the ISODATA process and its use in detecting compact well-separated clusters ». In : (1973) (cf. p. 91).

[Dun] *dunn-sklearn.py*. URL : https://gist.github.com/douglasrizzo/cd7e792ff3a2dcaf27f6 (cf. p. 92).

[EP06] Nathan EAGLE et Alex PENTLAND. « Reality mining : sensing complex social systems ». In : *Personal Ubiquitous Comput.* 10.4 (2006), p. 255-268. ISSN : 1617-4909. DOI : http://dx.doi.org/10.1007/s00779-005-0046-3 (cf. p. 37).

[EMS04] J. P. ECKMANN, E. MOSES et D. SERGI. « Entropy of dialogues creates coherent structures in e-mail traffic ». In : *PNAS* 101 (2004), 14333-14337 (cf. p. 29, 36).

[Elm+19] Timon ELMER, Krishna CHAITANYA, Prateek PURWAR et al. « The validity of RFID badges measuring face-to-face interactions ». In : *Behavior research methods* 51 (2019), p. 2120-2138 (cf. p. 47, 51).

[FB10] Joël FAGOT et Elodie BONTÉ. « Automated testing of cognitive performance in monkeys : Use of a battery of computerized test systems by a troop of semi-free-ranging baboons (Papio papio) ». In : *Behavior Research Methods* 42.2 (2010), p. 507-516. ISSN : 1554-3528. DOI : 10.3758/BRM.42.2.507. URL : https://doi.org/10.3758/BRM.42.2.507 (cf. p. 44).

[FP09] Joël FAGOT et Dany PALERESSOMPOULLE. « Automatic testing of cognitive performance in baboons maintained in social groups ». In : *Behavior Research Methods* 41.2 (2009), p. 396-404. ISSN : 1554-3528. DOI : 10.3758/BRM.41.2.396. URL : https://doi.org/10.3758/BRM.41.2.396 (cf. p. 45).

[Far18] D. FARINE. « When to choose dynamic vs. static social network analysis ». In : *Journal of Animal Ecology* 87 (2018), p. 128-138 (cf. p. 29, 112).

[Far15] Damien R FARINE. « Proximity as a proxy for interactions : issues of scale in social network analysis ». In : *Animal Behaviour* 104 (2015), e1-e5 (cf. p. 38, 52).

[Far17] Damien R FARINE. « A guide to null models for animal social network analysis ». In : *Methods in Ecology and Evolution* 8 (2017), p. 1309-1320 (cf. p. 55, 77).

[FW15] Damien R. FARINE et Hal WHITEHEAD. « Constructing, conducting and interpreting animal social network analysis ». In : *Journal of Animal Ecology* 84.5 (2015), p. 1144-1163. ISSN : 1365-2656. DOI : 10.1111/1365-2656.12418. URL : http://dx.doi.org/10.1111/1365-2656.12418 (cf. p. 30, 36, 52, 111).

[For10] Santo FORTUNATO. « Community detection in graphs ». In : *Physics Reports* 486.3 (2010), p. 75 -174. ISSN : 0370-1573. DOI : https://doi.org/10.1016/j.physrep.2009.11.002. URL : http://www.sciencedirect.com/science/article/pii/S0370157309002841 (cf. p. 58).

[FB14] Julie FOURNET et Alain BARRAT. « Contact Patterns among High School Students ». In : *PLoS ONE* 9.9 (sept. 2014), e107878. DOI : 10.1371/journal.pone.0107878 (cf. p. 29, 30, 36, 41, 43, 112, 141).

[GL04] Diego GARLASCHELLI et Maria I LOFFREDO. « Patterns of link reciprocity in directed networks ». In : *Physical review letters* 93.26 (2004), p. 268701 (cf. p. 74).

[Gel+19] Valeria GELARDI, Joël FAGOT, Alain BARRAT et al. « Detecting social (in)stability in primates from their temporal co-presence network ». In : *Animal Behaviour* 157 (2019), p. 239 (cf. p. 32).

[Gel+20] Valeria GELARDI, Jeanne GODARD, D. PALERESSOMPOULLE et al. « Measuring social networks in primates : wearable sensors versus direct observations ». In : *Proceedings of the Royal Society A* 476 (2020) (cf. p. 32).

[G+15] Mathieu GÉNOIS, Christian VESTERGAARD, Ciro CATTUTO et al. « Compensating for population sampling in simulations of epidemic spread on temporal contact networks ». In : *Nature Communications* 8 (2015), p. 8860. DOI : 10.1038/ncomms9860 (cf. p. 41, 50, 52, 141).

[GZF16] Adeelia S. GOFFE, Dietmar ZINNER et Julia FISCHER. « Sex and friendship in a multilevel society : behavioural patterns and associations between female and male Guinea baboons ». In : *Behavioral Ecology and Sociobiology* 70.3 (2016), p. 323-336. ISSN : 1432-0762. DOI : 10.1007/s00265-015-2050-6. URL : http://dx.doi.org/10.1007/s00265-015-2050-6 (cf. p. 30, 71, 100).

[GWH07] Scott A GOLDER, Dennis M WILKINSON et Bernardo A HUBERMAN. « Rhythms of social interaction : Messaging within a massive online network ». In : *Communities and technologies 2007*. Springer, 2007, p. 41-66 (cf. p. 29, 36).

[Gra73] Mark S. GRANOVETTER. « The Strength of Weak Ties ». In : *American Journal of Sociology* 78.6 (1973), p. 1360-1380. ISSN : 00029602, 15375390. URL : http://www.jstor.org/stable/2776392 (cf. p. 27, 28, 104).

[Gra+19] Jacob M GRAVING, Daniel CHAE, Hemal NAIK et al. « DeepPoseKit, a software toolkit for fast and robust animal pose estimation using deep learning ». In : *eLife* 8 (2019), e47994 (cf. p. 30, 37).

[Hei46] Fritz HEIDER. « Attitudes and cognitive organization ». In : *The Journal of psychology* 21.1 (1946), p. 107-112 (cf. p. 104, 110, 111).

[Hei58] Fritz HEIDER. *The psychology of interpersonal relations*. John Wiley & Sons Inc, 1958 (cf. p. 27, 104).

[Hen+09] SP HENZI, D LUSSEAU, T WEINGRILL et al. « Cyclicity in the structure of female baboon social networks ». In : *Behavioral Ecology and Sociobiology* 63.7 (2009), p. 1015-1021. ISSN : 0340-5443 (cf. p. 28, 111).

[HRS08] Cesar A HIDALGO et Carlos RODRÍGUEZ-SICKERT. « The dynamics of a mobile phone network ». In : *Physica A : Statistical Mechanics and its Applications* 387.12 (2008), p. 3017-3024 (cf. p. 68, 69).

[Hin76] R. A. HINDE. « Interactions, Relationships and Social Structure ». In : *Man* 11.1 (1976), p. 1-17. ISSN : 00251496. URL : http://www.jstor.org/stable/2800384 (cf. p. 27-29).

[HAW13] Elizabeth A HOBSON, Michael L AVERY et Timothy F WRIGHT. « An analytical framework for quantifying and testing patterns of temporal dynamics in social networks ». In : *Animal Behaviour* 85.1 (2013), p. 83-96 (cf. p. 29).

[Hol03] Petter HOLME. « Network dynamics of ongoing social relationships ». In : *EPL (Europhysics Letters)* 64.3 (2003), p. 427 (cf. p. 68).

[Hol13] Petter HOLME. « Epidemiologically optimal static networks from temporal network data ». In : *PLoS Comput Biol* 9.7 (2013), e1003142 (cf. p. 68).

[Hol15] Petter HOLME. « Modern temporal network theory : a colloquium ». In : *The European Physical Journal B* 88.9 (2015), p. 234 (cf. p. 29, 35, 68, 112).

[HS12] Petter HOLME et Jari SARAMÄKI. « Temporal networks ». In : *Physics reports* 519.3 (2012), p. 97-125 (cf. p. 29, 34, 35, 68).

[HLSL10] Julianne HOLT-LUNSTAD, Timothy B SMITH et J Bradley LAYTON. « Social relationships and mortality risk : a meta-analytic review ». In : *PLoS medicine* 7.7 (2010), e1000316 (cf. p. 69).

[HA85] Lawrence HUBERT et Phipps ARABIE. « Comparing partitions ». In : *Journal of classification* 2.1 (1985), p. 193-218 (cf. p. 58, 85).

[Hug+18] Lacey F. HUGHEY, Andrew M. HEIN, Ariana STRANDBURG-PESHKIN et al. « Challenges and solutions for studying collective animal behaviour in the wild ». In : *Philosophical Transactions of the Royal Society B : Biological Sciences* 373.1746 (2018), p. 20170005. DOI : 10.1098/rstb.2017.0005. eprint : https://royalsocietypublishing.org/doi/pdf/10.1098/rstb.2017.0005. URL : https://royalsocietypublishing.org/doi/abs/10.1098/rstb.2017.0005 (cf. p. 30, 37).

[Ila+13] Amiyaal ILANY, Adi BAROCAS, Lee KOREN et al. « Structural balance in the social networks of a wild mammal ». In : *Animal Behaviour* 85.6 (2013), p. 1397-1405 (cf. p. 77, 105, 111).

[Ise+11] Lorenzo ISELLA, Juliette STEHLÉ, Alain BARRAT et al. « What's in a crowd ? Analysis of face-to-face behavioral networks ». In : *Journal of theoretical biology* 271.1 (2011), p. 166-180 (cf. p. 29, 36, 41).

[Jia+16] Zhi-Qiang JIANG, Wen-Jie XIE, Ming-Xia LI et al. « Two-state Markov-chain Poisson nature of individual cellphone call statistics ». In : *Journal of Statistical Mechanics : Theory and Experiment* 2016.7 (2016), p. 073210 (cf. p. 80).

[JGN01] Emily M. JIN, Michelle GIRVAN et Micaleah NEWMAN. « Structure of growing social networks. » In : *Physical review. E, Statistical, nonlinear, and soft matter physics* 64 4 Pt 2 (2001), p. 046132 (cf. p. 31, 68, 69).

[KFS19] Peter KAPPELER, Claudia FICHTEL et Carel SCHAIK. « There Ought to Be Roots : Evolutionary Precursors of Social Norms and Conventions in Non-Human PrimatesEvolutionary Precursors of Social Norms and Conventions in Non-Human Primates ». In : juil. 2019, p. 65-82. ISBN : 9780190846466. DOI : 10.1093/oso/9780190846466.003.0003 (cf. p. 27).

[Kar+11] M. KARSAI, M. KIVELÄ, R. K. PAN et al. « Small but slow world : How network topology and burstiness slow down spreading ». In : *Physical Review E* 83.2 (2011). ISSN : 1550-2376. DOI : 10.1103/physreve.83.025102. URL : http://dx.doi.org/10.1103/PhysRevE.83.025102 (cf. p. 34).

[KP15] Mikko KIVELÄ et Mason A PORTER. « Estimating interevent time distributions from finite observation periods in communication networks ». In : *Physical Review E* 92.5 (2015), p. 052813 (cf. p. 68).

[KW06] G. KOSSINETS et D. J. WATTS. « Empirical analysis of an evolving social network ». In : *Science* 311 (2006), p. 88-90 (cf. p. 29, 34, 36).

[Kov+11] Lauri KOVANEN, Márton KARSAI, Kimmo KASKI et al. « Temporal motifs in time-dependent networks ». In : *Journal of Statistical Mechanics : Theory and Experiment* 2011.11 (2011), P11005 (cf. p. 103).

[KSK10] Lauri KOVANEN, Jari SARAMAKI et Kimmo KASKI. « Reciprocity of mobile phone calls ». In : *arXiv preprint arXiv :1002.0763* (2010) (cf. p. 74).

[Kra+15] Jens KRAUSE, Richard JAMES, Daniel FRANKS et al. *Animal Social Networks*. Oxford University Press, 2015. ISBN : 0191668281 (cf. p. 29, 30, 36).

[Kra+13] Jens KRAUSE, Stefan KRAUSE, Robert ARLINGHAUS et al. « Reality mining of animal social systems ». In : *Trends in Ecology & Evolution* 28.9 (2013), p. 541-551. ISSN : 0169-5347. DOI : https://doi.org/10.1016/j.tree.2013.06.002. URL : http://www.sciencedirect.com/science/article/pii/S0169534713001468 (cf. p. 37).

[Kri+12] Gautier KRINGS, Márton KARSAI, Sebastian BERNHARDSSON et al. « Effects of time window size and placement on the structure of an aggregated communication network ». In : *EPJ Data Science* 1.1 (2012), p. 4 (cf. p. 34, 35, 68).

[KGG05] Krzysztof KUŁAKOWSKI, PrzemisŁaw GAWRONSKI et Piotr GRONEK. « THE HEIDER BALANCE : A CONTINUOUS APPROACH ». In : *International Journal of Modern Physics C* 16.05 (2005), p. 707-716. ISSN : 0129-1831. DOI : 10.1142/S012918310500742X. URL : https://doi.org/10.1142/S012918310500742X (cf. p. 104, 105).

[Kur+14] Ralf H. J. M. KURVERS, Jens KRAUSE, Darren P. CROFT et al. « The evolutionary and ecological consequences of animal social networks : emerging issues ». In : *Trends in Ecology & Evolution* 29.6 (2014), p. 326-335. ISSN : 0169-5347. DOI : http://dx.doi.org/10.1016/j.tree.2014.04.002. URL : http://www.sciencedirect.com/science/article/pii/S0169534714000858 (cf. p. 29).

[Laz+09] David LAZER, Alex Sandy PENTLAND, Lada ADAMIC et al. « Life in the network : the coming age of computational social science ». In : *Science (New York, NY)* 323.5915 (2009), p. 721 (cf. p. 28, 36).

[LHK10] Jure LESKOVEC, Daniel HUTTENLOCHER et Jon KLEINBERG. « Signed Networks in Social Media ». In : *Proceedings of the SIGCHI Conference on Human Factors in Computing Systems*. CHI '10. Atlanta, Georgia, USA : ACM, 2010, p. 1361-1370. ISBN : 978-1-60558-929-9. DOI : 10.1145/1753326.1753532. URL : http://doi.acm.org/10.1145/1753326.1753532 (cf. p. 105).

[Lil+01] Fredrik LILJEROS, Christofer R. EDLING, Luís A. Nunes AMARAL et al. « The web of human sexual contacts ». In : *Nature* 411.6840 (2001), 907–908. ISSN : 1476-4687. DOI : 10.1038/35082140. URL : http://dx.doi.org/10.1038/35082140 (cf. p. 28).

[MC+18] A. A. MALDONADO-CHAPARRO, G. ALARCÓN-NIETO, J. A. KLAREVAS-IRBY et al. « Experimental disturbances reveal group-level costs of social instability ». In : *Proceedings of the Royal Society B : Biological Sciences* 285.1891 (2018), p. 20181577. DOI : 10.1098/rspb.2018.1577. eprint : https://royalsocietypublishing.org/doi/pdf/10.1098/rspb.2018.1577. URL : https://royalsocietypublishing.org/doi/abs/10.1098/rspb.2018.1577 (cf. p. 27).

[Mal+08] R Dean MALMGREN, Daniel B STOUFFER, Adilson E MOTTER et al. « A Poissonian explanation for heavy tails in e-mail communication ». In : *Proceedings of the National Academy of Sciences* 105.47 (2008), p. 18153-18158 (cf. p. 80).

[Man97] Brayan FJ MANLY. *Randomization, bootstrap and Monte Carlo methods in biology*. Rapp. tech. 1997 (cf. p. 55, 77).

[Mar+11] Seth A. MARVEL, Jon KLEINBERG, Robert D. KLEINBERG et al. « Continuous-time model of structural balance ». In : *Proceedings of the National Academy of Sciences* 108.5 (2011), p. 1771-1776. DOI : 10.1073/pnas.1013213108. URL : http://www.pnas.org/content/108/5/1771.abstract (cf. p. 104).

[MFB15] Rossana MASTRANDREA, Julie FOURNET et Alain BARRAT. « Contact patterns in a high school : a comparison between data collected using wearable sensors, contact diaries and friendship surveys ». In : *PloS one* 10.9 (2015), e0136497 (cf. p. 38, 41, 43, 49, 76, 96).

[MH19] Naoki MASUDA et Petter HOLME. « Detecting sequences of system states in temporal networks ». In : *Scientific reports* 9.1 (2019), p. 1-11 (cf. p. 30, 68, 81, 82, 88, 101).

[Mat+18] Alexander MATHIS, Pranav MAMIDANNA, Kevin M. CURY et al. « DeepLabCut : markerless pose estimation of user-defined body parts with deep learning ». In : *Nature Neuroscience* 21.9 (2018), p. 1281-1289. DOI : 10.1038/s41593-018-0209-y. URL : https://doi.org/10.1038/s41593-018-0209-y (cf. p. 30, 37).

[McC+11] Brenda MCCOWAN, Brianne A. BEISNER, John P. CAPITANIO et al. « Network Stability Is a Balancing Act of Personality, Power, and Conflict Dynamics in Rhesus Macaque Societies ». In : *PLOS ONE* 6.8 (août 2011), p. 1-8. DOI : 10.1371/journal.pone.0022350. URL : https://doi.org/10.1371/journal.pone.0022350 (cf. p. 28).

[MSLC01] Miller MCPHERSON, Lynn SMITH-LOVIN et James M COOK. « Birds of a feather : Homophily in social networks ». In : *Annual review of sociology* 27.1 (2001), p. 415-444 (cf. p. 27).

[Mil+19] Rachael M. MILWID, Terri L. O'SULLIVAN, Zvonimir POLJAK et al. « Validation of modified radio-frequency identification tag firmware, using an equine population case study ». In : *PLOS ONE* 14.1 (jan. 2019), p. 1-23. DOI : 10.1371/journal.pone.0210148. URL : https://doi.org/10.1371/journal.pone.0210148 (cf. p. 30, 35, 37).

[Mir+13a] Giovanna MIRITELLO, Rubén LARA, Manuel CEBRIAN et al. « Limited communication capacity unveils strategies for human interaction ». In : *Scientific reports* 3.1 (2013), p. 1-7 (cf. p. 69).

[MLM13] Giovanna MIRITELLO, Rubén LARA et Esteban MORO. « Time allocation in social networks : correlation between social structure and human communication dynamics ». In : *Temporal networks*. Springer, 2013, p. 175-190 (cf. p. 34).

[Mir+13b] Giovanna MIRITELLO, Esteban MORO, Rubén LARA et al. « Time as a limited resource : Communication strategy in mobile phone networks ». In : *Social Networks* 35.1 (2013), p. 89-95 (cf. p. 69).

[Moo02] James MOODY. « The Importance of Relationship Timing for Diffusion* ». In : *Social Forces* 81.1 (sept. 2002), p. 25-56. ISSN : 0037-7732. DOI : 10.1353/sof.2002.0056. eprint : https://academic.oup.com/sf/article-pdf/81/1/25/6519941/81-1-25.pdf. URL : https://doi.org/10.1353/sof.2002.0056 (cf. p. 34).

[Mor34] Jacob Levy MORENO. « Who shall survive ? : A new approach to the problem of human interrelations. » In : (1934) (cf. p. 28).

[Nav+17] Henry NAVARRO, Giovanna MIRITELLO, Arturo CANALES et al. « Temporal patterns behind the strength of persistent ties ». In : *EPJ Data Science* 6.1 (2017), p. 31 (cf. p. 68, 69).

[New01] M. E. J. NEWMAN. « The structure of scientific collaboration networks ». In : *Proceedings of the National Academy of Sciences* 98.2 (2001), p. 404-409. ISSN : 0027-8424. DOI : 10.1073/pnas.98.2.404. eprint : https://www.pnas.org/content/98/2/404.full.pdf. URL : https://www.pnas.org/content/98/2/404 (cf. p. 28).

[New04] M. E. J. NEWMAN. « Analysis of weighted networks ». In : *Physical Review E* 70.5 (2004). ISSN : 1550-2376. DOI : 10.1103/physreve.70.056131. URL : http://dx.doi.org/10.1103/PhysRevE.70.056131 (cf. p. 28, 33).

[New03] Mark EJ NEWMAN. « The structure and function of complex networks ». In : *SIAM review* 45.2 (2003), p. 167-256 (cf. p. 33).

[Nic+12] Vincenzo NICOSIA, John TANG, Mirco MUSOLESI et al. « Components in time-varying graphs ». In : *Chaos : An Interdisciplinary Journal of Nonlinear Science* 22.2 (2012), p. 023101. ISSN : 1089-7682. DOI : 10.1063/1.3697996. URL : http://dx.doi.org/10.1063/1.3697996 (cf. p. 34).

[O'B+19] Lisa R. O'BRYAN, Nicole ABAID, Shinnosuke NAKAYAMA et al. « Contact Calls Facilitate Group Contraction in Free-Ranging Goats (Capra aegagrus hircus) ». In : *Frontiers in Ecology and Evolution* 7 (2019), p. 73 (cf. p. 37).

[Onn+07a] J.-P. ONNELA, J. SARAMÄKI, J. HYVONEN et al. « Analysis of a large-scale weighted network of one-to-one human communication ». In : *New J. Phys* 9 (2007), p. 179 (cf. p. 29, 36).

[Onn+07b] J-P ONNELA, Jari SARAMÄKI, Jorkki HYVÖNEN et al. « Structure and tie strengths in mobile communication networks ». In : *Proceedings of the national academy of sciences* 104.18 (2007), p. 7332-7336 (cf. p. 68).

[Onn+05] Jukka-Pekka ONNELA, Jari SARAMÄKI, János KERTÉSZ et al. « Intensity and coherence of motifs in weighted complex networks ». In : *Physical Review E* 71.6 (2005), p. 065103 (cf. p. 103).

[Oze+20] Laura OZELLA, Joss LANGFORD, Laetitia GAUVIN et al. « The effect of age, environment and management on social contact patterns in sheep ». In : *Applied Animal Behaviour Science* (2020), p. 104964 (cf. p. 30, 41).

[PS11] Raj Kumar PAN et Jari SARAMÄKI. « Path lengths, correlations, and centrality in temporal networks ». In : *Physical Review E* 84.1 (2011). ISSN : 1550-2376. DOI : 10.1103/physreve.84.016105. URL : http://dx.doi.org/10.1103/PhysRevE.84.016105 (cf. p. 34).

[Pat+14] Annika PATZELT, Gisela H. KOPP, Ibrahima NDAO et al. « Male tolerance and male–male bonds in a multilevel primate society ». In : *Proceedings of the National Academy of Sciences* 111 (41) (2014), p. 14740-14745. DOI : 10.1073/pnas.1405811111. URL : http://www.pnas.org/content/early/2014/09/04/1405811111.abstract (cf. p. 30, 71).

[Ped+11] Fabian PEDREGOSA, Gaël VAROQUAUX, Alexandre GRAMFORT et al. « Scikit-learn : Machine learning in Python ». In : *Journal of machine learning research* 12.Oct (2011), p. 2825-2830 (cf. p. 58).

[Ped+20] Nicola PEDRESCHI, Christophe BERNARD, Wesley CLAWSON et al. « Dynamic core periphery structure of information sharing networks in entorhinal cortex and hippocampus ». In : *Network Neuroscience* Just Accepted (2020), p. 1-42 (cf. p. 101).

[PW+14] Noa PINTER-WOLLMAN, Elizabeth A. HOBSON, Jennifer E. SMITH et al. « The dynamics of animal social networks : analytical, conceptual, and theoretical advances ». In : *Behavioral Ecology* 25.2 (2014), p. 242-255. ISSN : 1045-2249. DOI : 10.1093/beheco/art047. URL : https://dx.doi.org/10.1093/beheco/art047 (cf. p. 30).

[Pso13] Ioannis PSORAKIS. « Probabilistic inference in ecological networks ; graph discovery, community detection and modelling dynamic sociality ». Thèse de doct. Oxford University, UK, 2013 (cf. p. 52, 68).

[Pso+12] Ioannis PSORAKIS, Stephen J ROBERTS, Iead REZEK et al. « Inferring social network structure in ecological systems from spatio-temporal data streams ». In : *Journal of the Royal Society Interface* 9.76 (2012), p. 3055-3066 (cf. p. 35, 52, 68).

[Rag+14] Vasanthan RAGHAVAN, Greg VER STEEG, Aram GALSTYAN et al. « Modeling temporal activity patterns in dynamic social networks ». In : *IEEE Transactions on Computational Social Systems* 1.1 (2014), p. 89-107 (cf. p. 80).

[Ran71] William M RAND. « Objective criteria for the evaluation of clustering methods ». In : *Journal of the American Statistical association* 66.336 (1971), p. 846-850 (cf. p. 58, 85).

[RB87] A Ramachandra RAO et Suraj BANDYOPADHYAY. « Measures of reciprocity in a social network ». In : *Sankhyā : The Indian Journal of Statistics, Series A* (1987), p. 141-188 (cf. p. 74).

[Rap53] Anatol RAPOPORT. « Spread of information through a population with socio-structural bias : I. Assumption of transitivity ». In : *The bulletin of mathematical biophysics* 15.4 (1953), p. 523-533. ISSN : 1522-9602. DOI : 10.1007/BF02476440. URL : https://doi.org/10.1007/BF02476440 (cf. p. 27, 104).

[RPB13] Bruno RIBEIRO, Nicola PERRA et Andrea BARONCHELLI. « Quantifying the effect of temporal resolution on time-varying networks ». In : *Scientific reports* 3 (2013), p. 3006 (cf. p. 57).

[RF+19] Francisco ROMERO-FERRERO, Mattia G. BERGOMI, Robert C. HINZ et al. « idtracker.ai : tracking all individuals in small or large collectives of unmarked animals ». In : *Nature Methods* 16.2 (2019), p. 179-182. DOI : 10.1038/s41592-018-0295-5. URL : https://doi.org/10.1038/s41592-018-0295-5 (cf. p. 30, 37).

[Ros+14] Martin ROSVALL, Alcides V ESQUIVEL, Andrea LANCICHINETTI et al. « Memory in network flows and its effects on spreading dynamics and community detection ». In : *Nature communications* 5.1 (2014), p. 1-13 (cf. p. 34).

[Rut+12] Christian RUTZ, Zackory T BURNS, Richard JAMES et al. « Automated mapping of social networks in wild birds ». In : *Current Biology* 22.17 (2012), R669-R671 (cf. p. 30, 35, 37).

[Rut+15] Christian RUTZ, Michael B MORRISSEY, Zackory T BURNS et al. « Calibrating animal-borne proximity loggers ». In : *Methods in Ecology and Evolution* 6.6 (2015), p. 656-667 (cf. p. 30, 35, 37).

[Ryd+12] Thomas B RYDER, Brent M HORTON, Mike van den TILLAART et al. « Proximity data-loggers increase the quantity and quality of social network data ». In : *Biology letters* 8.6 (2012), p. 917-920 (cf. p. 37).

[Sal+10] Marcel SALATHÉ, Maria KAZANDJIEVA, Jung Woo LEE et al. « A high-resolution human contact network for infectious disease transmission ». In : *Proceedings of the National Academy of Sciences* 107.51 (2010), p. 22020-22025 (cf. p. 29, 34, 36, 43).

[Sap83] Robert M SAPOLSKY. « Endocrine aspects of social instability in the olive baboon (Papio anubis) ». In : *American Journal of Primatology* 5.4 (1983), p. 365-379 (cf. p. 27).

[SM15] Jari SARAMÄKI et Esteban MORO. « From seconds to months : an overview of multi-scale dynamics of mobile telephone calls ». In : *The European Physical Journal B* 88.6 (2015), p. 164 (cf. p. 34, 67, 68, 71).

[Sch+10] Oliver SCHÜLKE, Jyotsna BHAGAVATULA, Linda VIGILANT et al. « Social bonds enhance reproductive success in male macaques ». In : *Current Biology* 20.24 (2010), p. 2207-2210 (cf. p. 27, 80).

[Hie] *scipy.cluster.hierarchy*. URL : https://docs.scipy.org/doc/scipy/reference/cluster.hierarchy.html (cf. p. 90).

[SSL16] Vedran SEKARA, Arkadiusz STOPCZYNSKI et Sune LEHMANN. « Fundamental structures of dynamic social networks ». In : *Proceedings of the national academy of sciences* 113.36 (2016), p. 9977-9982 (cf. p. 34).

[Sey77] Robert M. SEYFARTH. « A model of social grooming among adult female monkeys ». In : *Journal of Theoretical Biology* 65.4 (1977), p. 671-698. ISSN : 0022-5193. DOI : https://doi.org/10.1016/0022-5193(77)90015-7. URL : http://www.sciencedirect.com/science/article/pii/0022519377900157 (cf. p. 39, 47, 51).

[SO+02] Shai S SHEN-ORR, Ron MILO, Shmoolik MANGAN et al. « Network motifs in the transcriptional regulation network of Escherichia coli ». In : *Nature genetics* 31.1 (2002), p. 64-68 (cf. p. 103).

[SJ19] Daizaburo SHIZUKA et Allison E JOHNSON. « How demographic processes shape animal social networks ». In : *Behavioral Ecology* (juin 2019), arz083. ISSN : 1045-2249. DOI : 10.1093/beheco/arz083. eprint : http://oup.prod.sis.lan/beheco/advance-article-pdf/doi/10.1093/beheco/arz083/28785596/arz083.pdf. URL : https://doi.org/10.1093/beheco/arz083 (cf. p. 27).

[Sic+14] Claudia SICK, J. CARTER ALECIA, H. MARSHALL HARRY et al. « Evidence for varying social strategies across the day in chacma baboons ». In : *Biology Letters* 10.7 (2014), p. 20140249. DOI : 10.1098/rsbl.2014.0249. URL : https://doi.org/10.1098/rsbl.2014.0249 (cf. p. 28, 111).

[Sil07] Joan B SILK. « Social components of fitness in primate groups ». In : *Science* 317.5843 (2007), p. 1347-1351 (cf. p. 27, 69, 80).

[SAA03] Joan B. SILK, Susan C. ALBERTS et Jeanne ALTMANN. « Social Bonds of Female Baboons Enhance Infant Survival ». In : *Science* 302.5648 (2003), p. 1231. DOI : 10.1126/science.1088580. URL : http://science.sciencemag.org/content/302/5648/1231.abstract (cf. p. 27, 80).

[Sil+10] Joan B. SILK, Jacinta C. BEEHNER, Thore J. BERGMAN et al. « Female chacma baboons form strong, equitable, and enduring social bonds ». In : *Behavioral Ecology and Sociobiology* 64.11 (2010), p. 1733-1747. ISSN : 1432-0762. DOI : 10.1007/s00265-010-0986-0. URL : https://doi.org/10.1007/s00265-010-0986-0 (cf. p. 27, 28, 80, 111).

[Sil+09] Joan B. SILK, C. BEEHNER JACINTA, J. BERGMAN THORE et al. « The benefits of social capital : close social bonds among female baboons enhance offspring survival ». In : *Proceedings of the Royal Society B : Biological Sciences* 276.1670 (2009), p. 3099-3104. DOI : 10.1098/rspb.2009.0681. URL : https://doi.org/10.1098/rspb.2009.0681 (cf. p. 27, 80).

[Sil+15] Matthew J SILK, Andrew L JACKSON, Darren P CROFT et al. « The consequences of unidentifiable individuals for the analysis of an animal social network ». In : *Animal Behaviour* 104 (2015), p. 1-11 (cf. p. 36).

[Soc] *SocioPatterns website*. URL : http://www.sociopatterns.org/. (accessed : 01.09.2016) (cf. p. 39, 48).

[Son+10] Chaoming SONG, Tal KOREN, Pu WANG et al. « Modelling the scaling properties of human mobility ». In : *Nature Physics* 6.10 (2010), p. 818-823 (cf. p. 29).

[Squ+13] Tiziano SQUARTINI, Francesco PICCIOLO, Franco RUZZENENTI et al. « Reciprocity of weighted networks ». In : *Scientific reports* 3.1 (2013), p. 1-9 (cf. p. 74).

[SC+15] James JH ST CLAIR, Zackory T BURNS, Elaine M BETTANEY et al. « Experimental resource pulses influence social-network dynamics and the potential for information flow in tool-using crows ». In : *Nature Communications* 6 (2015), p. 7197 (cf. p. 30, 35, 37).

[SBPS13] Michele STARNINI, Andrea BARONCHELLI et Romualdo PASTOR-SATORRAS. « Modeling human dynamics of face-to-face interaction networks ». In : *Physical review letters* 110.16 (2013), p. 168701 (cf. p. 29).

[Ste+11] Juliette STEHLÉ, Nicolas VOIRIN, Alain BARRAT et al. « High-resolution measurements of face-to-face contact patterns in a primary school ». In : *PloS one* 6.8 (2011), e23176 (cf. p. 28, 41).

[Sto+14] Arkadiusz STOPCZYNSKI, Vedran SEKARA, Piotr SAPIEZYNSKI et al. « Measuring large-scale social networks with high resolution ». In : *PloS one* 9.4 (2014), e95978 (cf. p. 36).

[SP+15] Ariana STRANDBURG-PESHKIN, Damien R FARINE, Iain D COUZIN et al. « GROUP DECISIONS. Shared decision-making drives collective movement in wild baboons ». In : *Science (New York, N.Y.)* 348.6241 (juin 2015), p. 1358-1361. DOI : 10.1126/science.aaa5099. URL : https://www.ncbi.nlm.nih.gov/pubmed/26089514 (cf. p. 30, 34, 37).

[SM20] Kashin SUGISHITA et Naoki MASUDA. « Recurrence in the evolution of air transport networks ». In : *arXiv preprint arXiv :2005.14392* (2020) (cf. p. 30, 34, 81, 82, 101).

[SWL15] Xiaoqian SUN, Sebastian WANDELT et Florian LINKE. « Temporal evolution analysis of the European air transportation system : air navigation route network and airport network ». In : *Transportmetrica B : Transport Dynamics* 3.2 (2015), p. 153-168. DOI : 10.1080/21680566.2014.960504. eprint : https://doi.org/10.1080/21680566.2014.960504. URL : https://doi.org/10.1080/21680566.2014.960504 (cf. p. 34).

[SLT10] Michael SZELL, Renaud LAMBIOTTE et Stefan THURNER. « Multirelational Organization of Large-scale Social Networks in an Online World ». In : *Proceedings of the National Academy of Sciences* 107 (2010), p. 13636 (cf. p. 105, 108, 111).

[Tan+10] John TANG, Mirco MUSOLESI, Cecilia MASCOLO et al. « Analysing information flows and key mediators through temporal centrality metrics ». In : *Proceedings of the 3rd Workshop on Social Network Systems*. 2010, p. 1-6 (cf. p. 34).

[Thu18] Stefan THURNER. « Virtual social science ». In : *arXiv preprint arXiv :1811.08156* (2018) (cf. p. 104, 105).

[Tom+05] M. TOMASELLO, M. CARPENTER, J. CALL et al. « Understanding and sharing intentions : the origins of cultural cognition ». In : *Behavioral and Brain Sciences* 28.5 (2005), 675-91 ; discussion 691-735. ISSN : 0140-525X (Print). URL : http://www.ncbi.nlm.nih.gov/entrez/query.fcgi?cmd=Retrieve&db=PubMed&dopt=Citation&list_uids=16262930 (cf. p. 30).

[Tot+15] Damon JA TOTH, Molly LEECASTER, Warren BP PETTEY et al. « The role of heterogeneity in contact timing and duration in network models of influenza spread in schools ». In : *Journal of The Royal Society Interface* 12.108 (2015), p. 20150279 (cf. p. 36, 44).

[VTK13] Szabolcs VAJNA, Bálint TÓTH et János KERTÉSZ. « Modelling bursty time series ». In : *New Journal of Physics* 15.10 (2013), p. 103023 (cf. p. 80).

[Ves+16] Christian L VESTERGAARD, Eugenio VALDANO, Mathieu GÉNOIS et al. « Impact of spatially constrained sampling of temporal contact networks on the evaluation of the epidemic risk ». In : *European Journal of Applied Mathematics* 27.6 (2016), p. 941-957 (cf. p. 41, 50, 141).

[WF94] Stanley WASSERMAN et Katherine FAUST. *Social network analysis : Methods and applications*. T. 8. Cambridge university press, 1994 (cf. p. 74, 104).

[WW19] Quinn M.R. WEBBER et Eric Vander WAL. « Trends and perspectives on the use of animal social network analysis in behavioural ecology : a bibliometric approach ». In : *Animal Behaviour* 149 (2019), p. 77 -87. ISSN : 0003-3472. DOI : https://doi.org/10.1016/j.anbehav.2019.01.010. URL : http://www.sciencedirect.com/science/article/pii/S0003347219300119 (cf. p. 29).

[Wey+08] Tina WEY, Daniel T BLUMSTEIN, Weiwei SHEN et al. « Social network analysis of animal behaviour : a promising tool for the study of sociality ». In : *Animal behaviour* 75.2 (2008), p. 333-344 (cf. p. 29).

[Whi08] H. WHITEHEAD. *Analyzing animal societies : quantitative methods for vertebrate social analysis*. University of Chicago Press, 2008. ISBN : 0226895238 (cf. p. 29, 64, 77, 111).

[WB88] Andrew WHITEN et Richard W BYRNE. « Tactical deception in primates ». In : *Behavioral and brain sciences* 11.02 (1988), p. 233-244. ISSN : 1469-1825 (cf. p. 30).

[WA+19] Jared K WILSON-AGGARWAL, Laura OZELLA, Michele TIZZONI et al. « High-resolution contact networks of free-ranging domestic dogs Canis familiaris and implications for transmission of infection ». In : *PLoS neglected tropical diseases* 13.7 (2019), e0007565 (cf. p. 30, 35, 37, 41, 43).

[Zha+11] Kun ZHAO, Juliette STEHLÉ, Ginestra BIANCONI et al. « Social network dynamics of face-to-face interactions ». In : *Physical review E* 83.5 (2011), p. 056109 (cf. p. 29).

[ZP19] Xinzhe ZUO et Mason A PORTER. « Models of continuous-time networks with tie decay, diffusion, and convection ». In : *arXiv preprint arXiv :1906.09394* (2019) (cf. p. 68, 78).

# ANNEXES

# A. Detection of discrete states : Other timescales

Figure A.1 shows matrices of global cosine similarity between network snapshots computed for all couple of times, using a 5-hours time resolution, taking some values of the parameter $\alpha$ of different order of magnitude ((a), (b), (c) correspond to $\alpha$ equal to 0.0001, 0.001 and 0.01 respectively) and for the two types of aggregation ((d), (e)), i.e. with a fix 5-h time-window and an increasing time-window, that is, aggregating on the [0,t] period. The perturbation consisted in the switch of two adult males id for $\Delta t$=3 days, from July $1^{st}$ to July $4^{th}$ 2019. The 2 individuals were involved overall in the 34% of the total interactions. The matrices show qualitatively that the detection of the perturbed period depends on the value of the parameter $\alpha$ and on the type of aggregation. In particular, the cases of very low values of $\alpha$ (0.0001) and of the increasing time-window result in a very flat and stable dynamics (all the pairs of time frames are extremely similar). For higher values of $\alpha$ and for the case of fixed time-window aggregation we observe that the dynamics of the network starts to emerge. Not only the simulated perturbation is distinguishable, but also several different sub-structures of the network dynamics. In the case of the fixed time-window this pattern appears very noisy. Panel (f) shows the values of the average silhouette index resulting from the hierarchical clustering analysis, setting the number of clusters equal to 3, only for the networks computed with our framework, for different values of $\alpha$. Silhouette values relative to the two aggregated approaches are not shown here because in neither case the network was able to detect the simulated perturbation. The plot compares the ability of different representations to detect the perturbation. Our framework appears to detect the perturbation for several values of $\alpha$ (min. = 0.18 for $\alpha = 0.2$; max=0.45 for $\alpha = 0.005$).

Figure A.2 (analogue to the Figure 4.6), shows the matrices of global cosine similarities between perturbed network snapshots, using a time resolution of 3 hours, for different network representations. The simulated perturbation consisted in reshuffling the identities of the 25% most active individuals, i.e. individuals associated to the highest numbers of interactions, for the entire second day of data collection (2013-12-03). Overall, the individuals were involved in 68% of the interactions occurred during the entire period of interest. Panels (a), (b), (c) concern the networks computed with the continuous-time framework, using $\alpha$ equal to 0.0001, 0.01 and 0.1, respectively. Panels (d) and (e) concern the two types of aggregated networks, namely with increasing time-window [0,t] and with fixed time-window. For low values of alpha ($\alpha = 0.0001$ in panel (a) and $\alpha = 0.01$ in panel (b)) the matrices show that network weights evolution is

"delayed" with respect to the perturbation of the system, revealing that the value of the parameter may be not the most adequate to describe the system dynamics. Contrarily, for $\alpha = 0.1$), the change points are well and promptly detected. We can distinguish in fact the transition of the systems from the non-perturbed to perturbed state (switch of individuals identities) and the second transition in which individuals are re-assigned with their original identities. Figure A.2(f) shows the average silhouette plot for each network representation, referring to clusters configurations obtained using the hierarchical clustering algorithm. The panel reveals that the clustering algorithm compute a correct partition of the network snapshots for three different representations of the network, namely the aggregated network with a fixed time window of 3 hours, and the model representation for 2 values of the parameter $\alpha$. Among these, our model performs a better detection of the perturbation (avg. silhouette = 0.35 for $\alpha = 0.05$; 0.30 for $\alpha = 0.1$) with respect to the fixed time-window aggregation (avg. silhouette = 0.26).

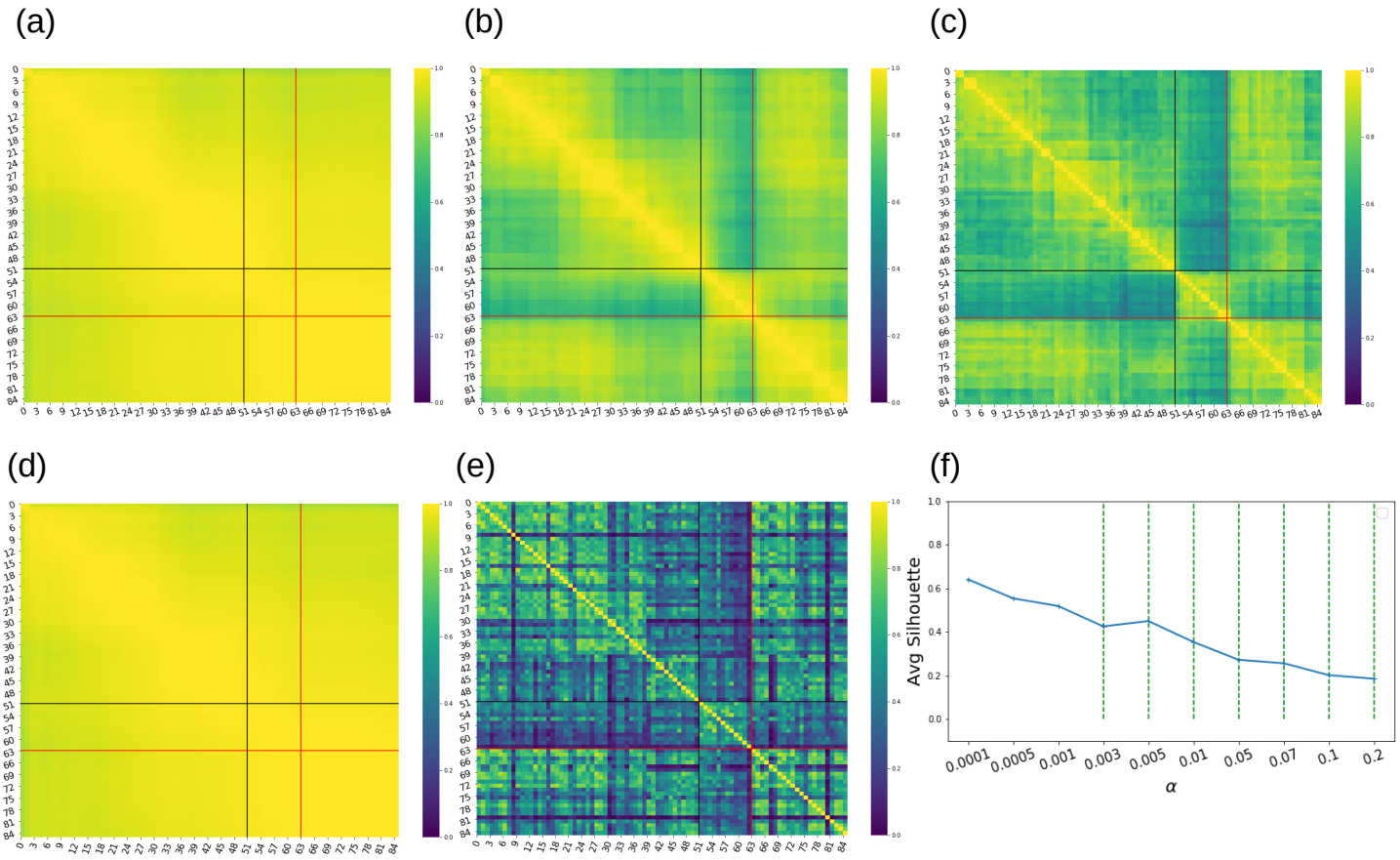


FIGURE A.1. : **Comparison between various network representations, with 5-hours time resolution, in response to a simulated perturbation on baboons contact data (exchange of two nodes' id in the network for $\Delta t$ = 3 days and $t_0$ = 2019-07-01)** The entries of the matrices in (a), (b), (c), (d), (e) represent the values of global cosine similarity between all possible couple of network snapshots relative to different times (t,t') for several temporal network representations. In particular, (a), (b), (c) are the representations obtained with our framework, using different values of the parameter $\alpha$ (0.0001, 0.001 and 0.01, respectively) ; panels (d), (e) concern the two aggregated representations, using an increasing time windows [0,t], and a fixed 5-hours time window, respectively. Black and red lines correspond to the time of the beginning and of the end perturbation, respectively. (f) : Average silhouette values over all data points, resulting from the hierarchical clustering analysis applied to the matrices, with the number of clusters $C = 3$. The value measures the ability of our framework to detect perturbations, for different values of $\alpha$, and for the two aggregated representations. Green vertical dashed lines correspond to the values of $\alpha$ for which the perturbation is well detected, i.e. the clustering algorithm classified the snapshots corresponding to $\Delta t$ as a single (perturbed) state on its own (successful detection for $\alpha \in [0.003, 0.2]$ ). For the other values of $\alpha$, the clustering algorithm failed to identify the perturbation as a separate state, therefore even in the values of the silhouette may be high, they refer to "incorrect" partitions. For $\alpha = 0.003$ and 0.005, our framework yield thus a quantitatively better detection of the perturbation than the aggregated network.

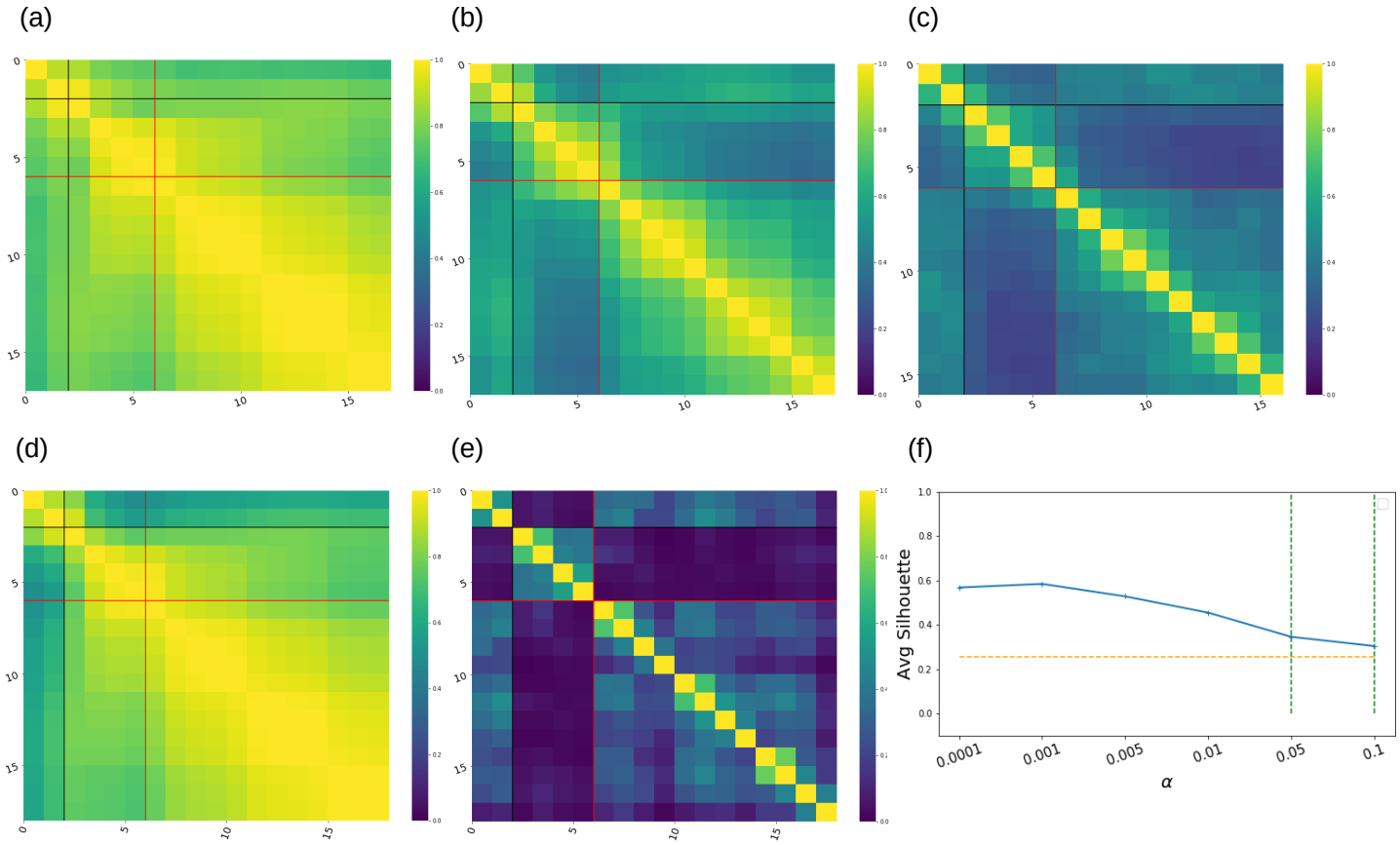


FIGURE A.2. : **Comparison between various network representations, with 3-hours time resolution, in response to a simulated perturbation on students contact data.** The entries of the matrices in (a), (b), (c), (d), (e) represent the values of global cosine similarity between all couples of network snapshots (t,t') for several temporal network representations, using a time resolution of 3 hours. The simulated perturbation consisted in reshuffling the identities of the 82 (25%) most active individuals (i.e. involved in highest numbers of interactions) for the entire $2^{nd}$ day of data collection 2013-12-03 (in this case, $\Delta t = 4$ snapshots of 3 hours, covering a time period from 8am to 17pm). Panels (a), (b), (c) concern the representations obtained with our framework, using different values of the parameter $\alpha$ (0.0001, 0.01 and 0.1, respectively) ; panels (d), (e) concern the two aggregated representations, using an increasing time windows [0,t], and a fixed time window of 3h. Black and red lines correspond to the time of the beginning and of the end perturbation, respectively. (f) : Average silhouette values over all data points, resulting from the hierarchical clustering analysis applied to the matrices, with the number of clusters $C = 3$. Green dashed lines correspond to the values of $\alpha$ for which the perturbation is well detected, while for all other values of $\alpha$ the silhouette, even if higher, the cluster algorithm that failed to detect the perturbation (network snapshots were incorrectly grouped). The orange horizontal dashed line corresponds to the silhouette relative to the aggregated network with the fixed time window. The silhouette relative to the aggregated representation with increasing time windows is not showed here, since it failed to detect the perturbation.

# B. Robustness of sensors system : lack of data due to failure of a reader

In section 3.3.2 we showed the advantages of wearable sensors devices in collecting a large amount of data with relatively little costs and inferring reliable social patterns and network structure already at short timescales. Despite this advantage, wearable sensors, like any automatic device, are inevitably subject to the risk of data loss (see VESTERGAARD, VALDANO, GÉNOIS et al. 2016) and thus to sampling effects. On the one hand, covering all the population is unrealistic in most of the cases (FOURNET et BARRAT 2014; GÉNOIS, VESTERGAARD, CATTUTO et al. 2015) (in our case for example, we could infer a social network only involving the 13 individuals who wore collars), and on the other hand, possibilities of technical failures have to be taken into account (CATTUTO, BROECK, BARRAT et al. 2010).

In order to test the robustness of the results obtained from the wearable sensor data with respect to sampling issues, we have simulated the failure of a reader. This corresponds to removing from the data set the contacts that were registered only by that reader. Note that a number of contacts are registered by more than one reader, so that these contacts would still be present in the resampled data set after the simulation of the failure. As we have three readers (called f2, f3 and f4), we simulate successively the failure of each of these readers.

Figure B.1 shows the effect of the failure of a single reader in terms of the amount of "lost" contacts, i.e., of contacts present in the whole data set but not in the data set with a reader failure simulated. The average amounts of lost contacts over all the period of study are 44%, 7% and 10% for the failure of readers f2, f3 and f4 respectively.

Despite these potentially large data losses, Figure B.2(a) and Figure B.2(b) show that both the distributions of the durations of contacts and of link weights for the incomplete data sets are extremely robust with respect to the absence of a reader. Most importantly, FigureB.3 shows that the link weights of the networks built from the incomplete data are extremely correlated with those of the network obtained from the whole dataset. The networks remain fully connected (no link is missing in the incomplete data) and the Pearson correlation coefficient between the lists of weights (sampled vs. whole data set for each reader failure) is $\sim 0.99$ in all cases. Finally, the cosine similarity values between the networks built from the sampled data and from the complete data are almost 1 ($> 0.99$ for all the sampling cases and both cosine similarity measures). Overall, networks resulting from incomplete data proved to be

highly similar to that resulting from the whole dataset, according to several metrics. We can conclude that the system is extremely robust with respect to a data sampling due to a reader failure issue.

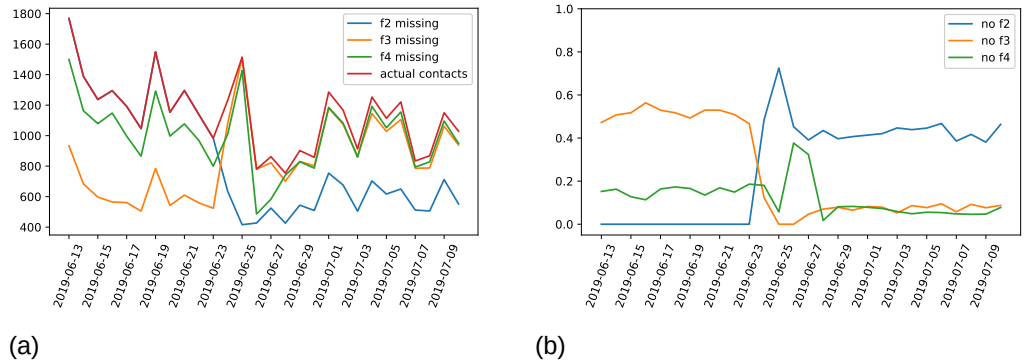


FIGURE B.1. : **Amount of lost contacts in case of reader failure.** (a) : Number of contacts registered each day in total, and in case of failure of one single reader. For the first ten days the curve relative to the reader f2 overlaps with the total amount of contacts because the reader had not yet been installed. (b) : Fraction of lost contacts in the three cases for each day of data collection.

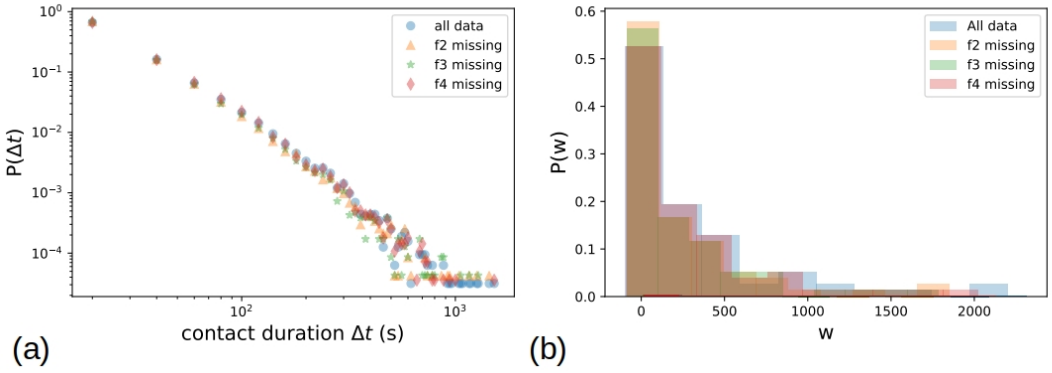


FIGURE B.2. : **Distributions of durations of contacts and weights for sampled data sets.** (a) Distributions of contact durations for sampled data sets in which a single reader failure is simulated, compared with the distributions obtained from the whole data set. (b) Distribution of network weights for sampled data sets in which data from one reader has been removed, compared with the distributions obtained from the whole data set.

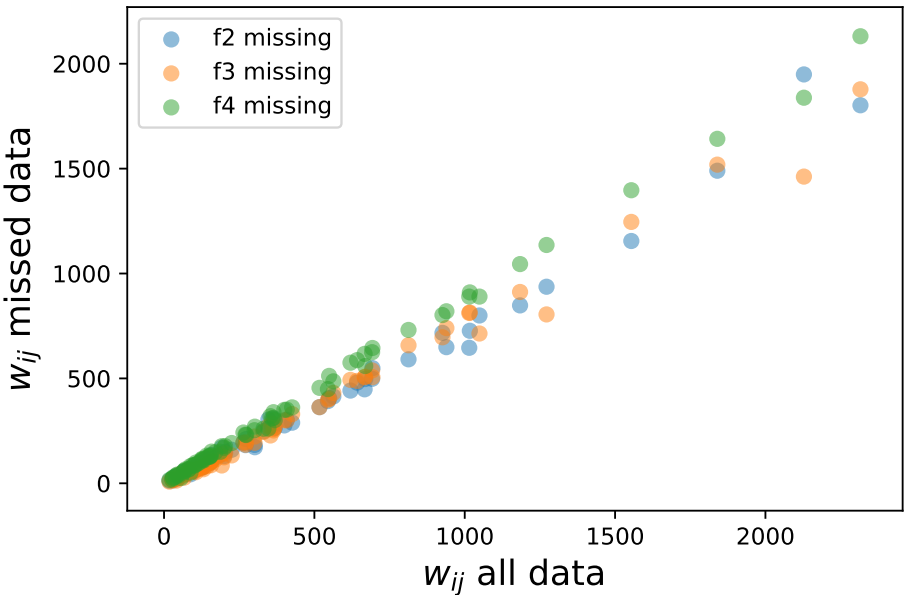


FIGURE B.3. : **Weights of the contact network aggregated on the whole observation period, for the whole data set vs. for a data set with simulated missing data.**